ISTANBUL TECHNICAL UNIVERSITY ★ GRADUATE SCHOOL

A REMEDY FOR MAJOR COSMOLOGICAL TENSIONS: DARK ENERGY WITH AN OSCILLATING INERTIAL MASS DENSITY

M.Sc. THESIS

Cihad KIBRIS

Department of Physics Engineering

Physics Engineering Programme

DECEMBER 2022

ISTANBUL TECHNICAL UNIVERSITY ★ GRADUATE SCHOOL

A REMEDY FOR MAJOR COSMOLOGICAL TENSIONS: DARK ENERGY WITH AN OSCILLATING INERTIAL MASS DENSITY

M.Sc. THESIS

Cihad KIBRIS
(509181122)

Department of Physics Engineering

Physics Engineering Programme

Thesis Advisor: Assoc. Prof. Dr. Özgür AKARSU

DECEMBER 2022

İSTANBUL TEKNİK ÜNİVERSİTESİ ★ LİSANSÜSTÜ EĞİTİM ENSTİTÜSÜ

BAŞLICA KOZMOLOJİK GERİLİMLER İÇİN TEK BİR REÇETE: SALINIMLI EYLEMSİZLİK KÜTLE YOĞUNLUĞUNA SAHİP KARANLIK ENERJİ

YÜKSEK LİSANS TEZİ

Cihad KIBRIS
(509181122)

Fizik Mühendisliği Anabilim Dalı

Fizik Mühendisliği Programı

Tez Danışmanı: Doç. Dr. Özgür AKARSU

ARALIK 2022

Cihad KIBRIS, a M.Sc. student of ITU Graduate School student ID 509181122, successfully defended the thesis entitled “A REMEDY FOR MAJOR COSMOLOGICAL TENSIONS: DARK ENERGY WITH AN OSCILLATING INERTIAL MASS DENSITY”, which he prepared after fulfilling the requirements specified in the associated legislations, before the jury whose signatures are below.

Thesis Advisor :	**Assoc. Prof. Dr. Özgür AKARSU** Istanbul Technical University	....
Jury Members :	**Prof. Dr. A. Savaş ARAPOĞLU** Istanbul Technical University	....
	Assoc. Prof. Dr. Ayşe Nihan KATIRCI Doğuş University	....

Date of Submission : 20 December 2022
Date of Defense : 26 December 2022

To my family,

FOREWORD

First of all, I would like to express my heartfelt gratitude to my advisor Assoc. Prof. Özgür Akarsu. Without his invaluable support, input and guidance throughout my studies, the realization of this work would not be possible.

Also I would like to thank my family for supporting me in any circumstances. Their unconditional love and encouragement were really helpful in finalizing this process.

December 2022 Cihad KIBRIS

TABLE OF CONTENTS

Page

ABBREVIATIONS

ΛCDM	: Lambda Cold Dark Matter
Λ_sCDM	: Sign-Switching Lambda Cold Dark Matter
***w*CDM**	: *w* Cold Dark Matter
BAO	: Baryon Acoustic Oscillations
CMB	: Cosmic Microwave Background
DE	: Dark Energy
gDE	: Graduated Dark Energy
simple-gDE	: Simple Graduated Dark Energy
EDE	: Early Dark Energy
EoS	: Equation of State
EMT	: Energy-Momentum Tensor
RW	: Robertson Walker
FRW	: Friedmann Robertson Walker
GR	: General Relativity
QFT	: Quantum Field Theory
const.	: Constant
Mpc	: Megaparsec
km	: Kilometer
s	: Second
TRGB	: Tip of the Red Giant Branch
SH0ES	: Supernova H0 for the Equation of State
BOSS	: Baryon Oscillation Spectroscopic Survey
eBOSS	: Extended Baryon Oscillation Spectroscopic Survey
DR11	: Data Release 11
CPL	: Chevallier-Polarski-Linder
SNIa	: Supernova Type Ia
LSS	: Large Scale Structure
Ly-α	: Lyman-α
WEC	: Weak Energy Condition
PLK	: Planck
H	: Cosmic Chronometers
SN	: Supernova
sgn	: Signum
KiDS	: KiloDegree Survey
SDSS	: Sloan Digital Sky Survey
BBN	: Big Bang Nucleosynthesis
eV	: Electronvolt
JWST	: James Webb Space Telescope
CL	: Confidence Level
MC	: Markov Chain
MGS	: Main Galaxy Sample
6dFGS	: Six-Degree Field Galaxy Survey

SYMBOLS

Λ	: Cosmological constant
Λ_{s}	: Sign-Switching cosmological constant
w	: Equation of state parameter
ρ	: Energy density
p	: Pressure
ϱ	: Inertial mass density
$G_{\mu\nu}$	: Einstein tensor
a	: Scale factor
z	: Cosmological redshift
$g_{\mu\nu}$	: Metric tensor
H	: Hubble parameter
H_0	: Hubble constant
h	: Dimensionless reduced Hubble constant
$T_{\mu\nu}$	: Energy-momentum tensor
G	: Newton's constant
R	: Ricci Scalar
u^{μ}	: Four-velocity
∇	: Covariant derivative
D_{μ}	: Fully orthogonally projected covariant derivative
c	: Speed of light
ω_{b}	: Dimensionless present-day density of baryons
ω_{c}	: Dimensionless present-day density of cold dark matter
ω_{r}	: Dimensionless present-day density of radiation
ω_{γ}	: Dimensionless present-day density of photons
θ_{*}	: The ratio of the sound horizon to the angular diameter distance at last scattering
t	: Cosmic (proper) time
Ω	: Density parameter
$h_{\mu\nu}$	: Projection Tensor
δ_{m}	: Matter density contrast
δ	: Fractional deviation from the ΛCDM's Hubble parameter
c_{s}^2	: Adiabatic speed of sound squared
$\mathcal{H}$	: Enthalpy

$\mathcal{L}$	: Lagrangian
N_{eff}	: Effective number of neutrino species
σ_8	: Root mean square mass fluctuation amplitude in spheres of size 8 Mpc/h.
S_8	: Combined growth parameter.
θ_*	: Angular scale at recombination
r_*	: The comoving sound horizon at recombination
$D_{\text{M}}(z_*)$	: The comoving angular diameter distance to the surface of last scattering
σ	: Standard deviation
λ	: Graduated dark energy model parameter
γ	: Graduated dark energy model parameter
M_{B}	: Supernova absolute magnitude
ϕ	: Scalar field
Ψ	: Combined graduated dark energy parameter
$z_\dagger$	: Sign-switching redshift
ψ	: Wavelet
$\Psi(z_*)$	: Integral of wavelet over the interval $[0, z_*]$
Σ	: Maximally symmetric, homogeneous and isotropic spacelike hypersurface
γ_{ij}	: Metric components of maximally symmetric 3D metric
Θ	: Scalar of volume expansion rate
$\bar{\Lambda}$	: Oscillating dark energy model parameter
Q_1	: Oscillating dark energy model amplitude parameter
Q_2	: Oscillating dark energy model frequency parameter
φ	: Oscillating dark energy phase
Ci	: Cosine integral function
Si	: Sine integral function
$\bar{\xi}_1$	: Combined oscillating dark energy model parameter
$\bar{\xi}_2$	: Combined oscillating dark energy model parameter
m_ν	: Neutrino mass
q	: Deceleration parameter
V	: Scalar field potential

LIST OF FIGURES

Page

A REMEDY FOR MAJOR COSMOLOGICAL TENSIONS: DARK ENERGY WITH AN OSCILLATING INERTIAL MASS DENSITY

SUMMARY

The preponderance of observational evidence indicates that a vast portion of the energy density of the Universe today comes in dark matter and enigmatic dark energy (DE). The standard cosmological model, namely, the so-called Lambda Cold Dark Matter model (ΛCDM), resting on this dark sector as well as a small fraction of baryons has been remarkably successful in elucidating the bulk of Universe we inhabit. Though, astronomical observations improving in precision over the course of years are increasingly exposing that ΛCDM is significantly discrepant with various datasets. The direct and local measurements of the present-day expansion rate yielding $H_0 = 73.04 \pm 1.04\ \mathrm{km\,s^{-1}\,Mpc^{-1}}$ are at more than 5σ tension (the Hubble H_0 tension) with the one $H_0 = 67.36 \pm 0.54\ \mathrm{km\,s^{-1}\,Mpc^{-1}}$ inferred within the ΛCDM based on matter-baryon densities and the spacing between acoustic peaks of the CMB. The H_0 tension effectively propagates to the supernovae absolute magnitude M_B through the distance modulus $\mu(z_i, H(z)) = m_{B,i} - M_{B,i}$ where $m_{B,i}$ is the measured apparent magnitude of the supernovae observed at the redshift z_i, and creates a 3.4σ tension with the results calibrated by the CMB sound horizon scale. Another discrepancy regarding the expansion rate $H(z)$ within the best fit ΛCDM is the $\sim 1.5\sigma$ tension between low (Galaxy BAO) and high redshift (Lyman-α at $z \approx 2.33$) BAO data. It first emerged as a preference for smaller $H(z)$ and accompanying negative DE densities for $1.7 \lesssim z \lesssim 2.34$, being at 2.5σ tension with ΛCDM. In addition, ΛCDM predicts a larger weighted amplitude of matter fluctuations S_8 in comparison with what the independent large scale structure dynamical low-redshift probes suggest, thereby running into 2 to 3σ tension. Given the long-standing theoretical issues such as the cosmological constant and coincidence problems related to the Λ, all these enumerated challenges and more inevitably motivate many to seek for a more complete framework either as modified theories of gravity or as minimal extensions beyond ΛCDM in the context of General Relativity (GR). In this sense, an approach that constitutes an example of the latter attempts focuses on inertial mass density $\varrho = \rho + p$ parametrizations. The graduated dark energy (gDE) model proposed in Akarsu *et al.* [Phys. Rev. D 101, 063528 (2020)], whose inertial mass density ϱ measures the minimum dynamical deviation $\varrho \propto \rho^{\lambda}$ from the assumption of null QFT vacuum energy $\varrho_\Lambda = 0$ is one that exhibits nontrivial properties. It turns out that smaller and smaller negative values of the parameter λ corresponds to a constant negative DE density that changes its sign from negative to positive in the past. Such a dynamical behavior would imply that $H(z)$ suppressed by the presence of a negative source at high redshifts results in an enhanced $H(z)$ at lower redshifts as the comoving angular

diameter distance $D_M(z)$ to the surface of last scattering $D_M(z_*) = c\int_0^{z_*} H^{-1}(z)\mathrm{d}z$ is very stringently and almost model-independently constrained by the CMB for any given pre-recombination physics and should be kept unaltered. This means that if the redshift at which the sign-flip in the DE density occurs is slightly below the anomalous Ly-α at effective redshift $z \approx 2.34$, it is quite conceivable that a dynamical DE possessing negative energy density mitigates both the H_0 and Ly-α discrepancies. The observational analysis of the gDE strongly favors a scenario in which the sign change of the gDE density is so swift it is practically identical to the cosmological constant phenomenologically flipping its sign much like the step function, except that $\Lambda < 0$ in the past. It arises as a limiting case $\lambda \to -\infty$ of the gDE such that $\rho_{\rm gDE}(a) \to \rho_{\rm gDE,0}\mathrm{sgn}[f(a)]$ where sgn is the signum function. This limit has been comprehensively studied under the name of the $\Lambda_{\rm s}$CDM model in Akarsu *et al*. [Phys. Rev. D 104, 123512 (2021)] where the late-time accelerated expansion is driven by $\Lambda_s \equiv \Lambda_{s0}\mathrm{sgn}[z - z_\dagger]$ with $z_\dagger$ being the switching redshift rather than the usual Λ. The confrontation with the data sets encompassing CMB, Pantheon SNIa with and without SH0ES M_B priors and BAO, shows that $\Lambda_{\rm s}$CDM simultaneously ameliorates six of the present significant tensions, namely H_0, M_B, S_8, Ly-α, t_0 and ω_b tensions. However, these simultaneous improvements in consistency with the high-precision data are observed to be impeded by the Galaxy BAO data which act to push smaller $z_\dagger$ enabling better agreement up to higher values. So one plausible solution without compromising on the achievements of the model would be the inclusion of a wiggly type non-monotonicity at low redshifts on top of the sign-switch conjecture. In actual, the necessity of these wiggles is underpinned by the notion that any smooth deformation $\psi_i(z)$ from the ΛCDM Hubble radius $H^{-1}(z)$ brought about by a viable cosmological model that accords with the early and late Universe account of ΛCDM must be given by admissible wavelets or in other words must have an oscillatory form. Following this suggestion and notion, in this dissertation a new parametrization $\varrho_{\rm DE}\ (a) = Q_1 \sin[Q_2(a-1)+\varphi]$ of the inertial mass density of vacuum energy has been proposed with the aim of accommodating the supposed wiggles and bettering the fit to the Galaxy BAO data in the late Universe. This is, in essence, equivalent to Fourier expanding the inertial mass density to first order with respect to the scale factor a. As a first step, the tools and physical features of the model containing the new DE source $\rho_{\rm DE}(a)$ were derived from the principles of GR. The oscillating nature of the parametrization of inertial mass density of vacuum manifested itself in the form of the special cosine integral function Ci(a) in the DE density $\rho_{\rm DE}(a)$. Ci(a) led to unique characteristics that play crucial roles in the expansion dynamics of the Universe through the Friedmann equation. To explore it to a greater extent, a preliminary investigation of the free parameters ($\bar{\Lambda}$, Q_2 and φ) and their influence on this dynamics along with the model capabilities was carried out. In the investigation, the early Universe description of ΛCDM is preserved. For the ranges $0.7 \lesssim \bar{\Lambda} \lesssim 1.3$ and $13 \lesssim Q_2 \lesssim 15$, it was found out that it is possible to obtain fits that agree excellently with a number of data points such as the local TRGB, SH0ES H_0 measurements and full BAO set in the case of $H(z/(1+z)$ and $c\ln(1+z)/D_M$. Subsequently, for certain values of the model parameters $\bar{\Lambda}$, Q_2 and φ, the corresponding DE density $\rho_{\rm DE}(z)$ is observed to demonstrate ever-decaying oscillations at low redshifts preceded by the familiar sign-switching behavior at high redshifts. These wiggles are reflected in the late expansion rate $H(z)$ due to slowly dominating DE density and cause a dip and a bump in $H(z)/(1+z)$ that respectively yield a much better fit to the Ly-α

and Galaxy BAO data than both ΛCDM and $\Lambda_{\rm s}$CDM. As for the H_0 values, although the reconciliation of the most recent the SH0ES measurement demanded relatively high-amplitude oscillations that slightly exacerbate the fit to the Galaxy BAO data in $c\ln(1+z)/D_M$, it appeared likely to attain a value that falls within the error margins of both the SH0ES and BAO data at the same time. Furthermore, a sign-switch phenomenon in the DE density $\rho_{\rm DE}(z)$ similar to that of the gDE or $\Lambda_{\rm s}$CDM models emerged due to Ci(a). It differs from that of $\Lambda_{\rm s}$CDM in that $\rho_{\rm DE}(z)/\rho_{\rm cr,0}$ starts out negative, albeit with no lower bound, in the remote past and dynamically switches its sign at about redshifts typically much greater (e.g. $z\sim 40$) than reasonable $z_\dagger$ values (e.g. $z_\dagger\sim 2$) and then settles into $\rho_{\rm DE}(z)/\rho_{\rm cr,0}\sim 0.64$. Despite these differences, it can be said that the sinusoidal parametrization of $\varrho_{\rm DE}$ fulfils the initial expectations. Additionally, it has been realized that the DE equation of state parameter(EoS) $w_{\rm DE}(z)$ that inherits the wiggles from the inertial mass density displays a very similar pattern found in model-independent reconstructions of dark energy EoS parameter. The same situation holds for the deceleration parameter $q(z)$, which lends extra confidence in prospect of success of the parametrization. Finally the oscillatory DE source was checked whether or not it is compatible with the notion of wavelets. Numerical calculations at the end of the thesis validated that the sinusoidal parametrization of $\varrho_{\rm DE}$ is indeed compatible with it. With all of these in mind, it can be deduced that the oscillating DE arising from $\varrho_{\rm DE}\,(a) = Q_1\sin[Q_2(a-1)+\varphi]$ seems to have the potential to reproduce the successes of $\Lambda_{\rm s}$CDM and even improve its shortcomings concerning the Galaxy BAO data.

BAŞLICA KOZMOLOJİK GERİLİMLER İÇİN TEK BİR REÇETE: SALINIMLI EYLEMSİZLİK KÜTLE YOĞUNLUĞUNA SAHİP KARANLIK ENERJİ

ÖZET

Gözlemsel kanıtların büyük çoğunluğu günümüz evreninin enerji yoğunluğunun yüksek oranda karanlık madde ve hala gizemini korumakta olan karanlık enerjiden oluştuğuna işaret etmektedir. Evrenin bu karanlık kesimini ve görece az miktarda baryonları temel alan Lambda-Soğuk Karanlık Madde (ΛCDM) modeli olarak da bilinen standart kozmolojik model, içinde bulunduğumuz evreni açıklamakta oldukça başarılı olduğu bilinen bir modeldir. Ne var ki, astronomik gözlemlerin zaman içerisinde gelişen hassasiyeti, ΛCDM modelinin aslında birçok veri setiyle önemli ölçüde uyumsuzluk gösterdiğini giderek artan bir şekilde ortaya koymaktadır. Evrenin doğrudan ve yerel ölçümlerden elde edilen günümüz genişleme hızı $H_0 = 73.04 \pm 1.04\ \mathrm{km\,s^{-1}\,Mpc^{-1}}$, ΛCDM kapsamında, madde-baryon yoğunluğu ve kozmik mikrodalga ardalan ışınımında (CMB) gözlemlenen ses tepelerinin arasındaki uzaklık baz alınarak çıkarsanan genişleme hızı olan $H_0 = 67.36 \pm 0.54\ \mathrm{km\,s^{-1}\,Mpc^{-1}}$ ile 5σ güven aralığında bir gerilim gösterir. Hubble gerilimi olarak da bilinen bu problem uzaklık modülü $\mu(z_i, H(z)) = m_{B,i} - M_{B,i}$ aracılığıyla süpernova salt parlaklığı M_B'ye kadar uzanır ve CMB ses ufku kullanılarak ayarlanan M_B değerleriyle 3.4σ güven aralığında bir uyumsuzluk oluşturur; burada $m_{B,i}$ süpernovaların görünür parlaklığın ve z_i kırmızıya kaymasıdır. ΛCDM modeli çerçevesinde genişleme hızı $H(z)$'ye ilişkin bir diğer problem ise düşük kırmızıya kayma (Gökada BAO verisi) ve yüksek kırmızıya kayma ($z \approx 2.33$'deki Ly-α verisi) değerlerinde yapılan Baryon Ses Salınımları (BAO) ölçümlerinden elde edilen genişleme hızları arasındaki 1.5σ güven aralığındaki gerilimdir. Bu gerilim, en başta daha düşük $H(z)$ değerlerini ve $1.7 \lesssim z \lesssim 2.34$ aralığında buna eşlik eden negatif karanlık enerji yoğunluklarını yeğleyen ve ΛCDM'deki karanlık enerji yoğunluğu değeriyle 2.5σ güven aralığında bir uyumsuzluk oluşturan gözlemsel veri olarak ortaya çıkmıştır. Ayrıca, küçük kırmızıya kaymalarda büyük ölçekli yapıları gözlemleyen dinamik kozmolojik sondalara kıyasla, ΛCDM modeli daha büyük bir ağırlıklı madde salınım genliği S_8 öngörür ki bu da 2-3σ güven aralığında bir uyumsuzluk oluşturur. Kozmolojik sabit Λ'ya ilişkin, kozmolojik sabit problemi ve denk geliş problemleri gibi uzun süredir var olan kuramsal bazı sorunlar da gözönünde bulundurulduğunda, bütün bu sayılan gerilimler kaçınılmaz bir şekilde daha eksiksiz bir kuramsal model arayışının güdüsünü oluşturmuştur. Bu arayış çoğu zaman ya değiştirilmiş genelçekim kuramları ya da genel görelilik çerçevesinde ΛCDM modeline en az değişiklikle yapılan eklemeler şeklindedir. Bu anlamda, bu eklemelerin bir örneğini teşkil eden bir yaklaşım da eylemsizlik kütle yoğunluğu parametrizasyonları üzerine odaklanır. Eylemsizlik kütle yoğunluğu ϱ, Kuantum Alan Teorisi (QFT) vakum enerjisinin sıfır eylemsizlik kütle yoğunluğuna

sahip olması varsayımından olabilecek en küçük dinamik sapmayı $\varrho \propto \rho^{\lambda}$ dikkate alan kademeli karanlık enerji (graduated dark energy, gDE), dikkate değer davranışlar sergileyen bu parametrizasyonlardan biridir. λ parametresinin çok büyük negatif değerlerinde, gDE, sabit bir eksi enerji yoğunluğuna sahip olan ve geçmişte işaretini eksiden artıya çeviren bir kaynağa karşılık gelir. Böyle bir dinamik kaynak şu anlama gelir; yüksek kırmızıya kayma değerlerinde negatif enerji varlığı tarafından baskılanan Hubble parametresi $H(z)$ düşük kırmızıya kaymalarda arttırılmış bir genişleme hızına yol açar. Bunun nedeni son saçılma yüzeyine olan eşhareketli açısal mesafenin $D_M(z_*) = c\int_0^{z_*} H^{-1}(z)\mathrm{d}z$ açısal akustik ölçek θ_* aracılığıyla neredeyse modelden bağımsız olarak CMB tarafından çok iyi derecede kısıtlanmış olması ve bunun değişmesinin beklenmemesi gerektiğidir. Yani, gDE yoğunluğunun işaret değişiminin gerçekleştiği kırmızıya kayma değeri Ly-α $z = 2.34$ değerinden bir miktar küçükse, eksili enerjiye sahip dinamik bir kaynak olarak hem H_0 hem de Ly-α gerilimlerini ortadan kaldırabilmektedir. Gözlemsel incelemeler, yoğunluktaki bu işaret değiştirmenin çok hızlı olması dolayısıyla, gDE'nin esasında fenomenolojik olarak geçmişte eksili olup işaret değiştiren kozmolojik sabite eşdeğer olduğu durumu çok güçlü bir şekilde yeğlemektedir. Bu durum gDE'nin $\lambda \to -\infty$ sınır durumundan kaynaklanır ve adım fonksiyonu davranışı, yani $\rho_{\mathrm{gDE}}(a) \to \rho_{\mathrm{gDE},0}\mathrm{sgn}[f(a)]$, ile betimlenebilir. Bu sınır durum ise işaret değiştiren kozmolojik sabit modeli Λ_{s}CDM adı altında ayrıntılı olarak çalışılmıştır. Burada $\Lambda_s \equiv \Lambda_{\mathrm{s}0}\mathrm{sgn}[z - z_\dagger]$ artılı kozmolojik sabit Λ'nın yerini alır ve $z_\dagger$'da işaret değiştirir. CMB, Pantheon SNIa ve tam BAO gibi veri kümelerini içeren daha geniş bir gözlemsel incelemede Λ_{s}CDM'nin aynı anda H_0, M_B, S_8, Ly-α, t_0 and ω_b gibi başlıca altı tane gerilimi iyileştirdiği görülmüştür. Bununla beraber, aynı anda gerçekleşen bu iyileşmelere bir engelin, daha iyi sonuçlar veren küçük $z_\dagger$ değerlerinin Gökada BAO verisi tarafından daha yüksek değerler almaya zorlanması olduğu anlaşılmıştır. Halihazırdaki bu kazanımlardan taviz vermeden atılabilecek bir sonraki adım ise, işaret değiştirme fikrinin üzerine, küçük kırmızıya kayma değerlerinde genişleme hızında dalgalı davranışa izin vermek olacaktır. Esasında, sözü geçen dalgalanmaların gerekliliği şuradan da temellendirilebilir: ΛCDM'in Hubble yarıçapı $H^{-1}(z)$'nin üzerine bir kozmolojik model tarafından getirilen sürekli bir değişiklik $\psi_i(z)$'ler, eğer model ΛCDM'in erken ve geç evren betimlemesiyle tutarlıysa, kabul edilebilir dalgacıklar (admissible wavelets) olarak verilmek zorundadır, diğer bir deyişle, salınım yapan bir biçime sahip olmalıdır. Bu tezde ise, geç evrende söz konusu dalgacıkları elde etmek ve bu sayede Gökada BAO verilerini daha iyi temsil etmek amacıyla, karanlık enerjinin $\varrho_{\mathrm{DE}}\ (a) = Q_1 \sin[Q_2(a-1) + \varphi]$ eylemsizlik kütle yoğunluğu parametrizasyonu öne sürülmüştür. Bu parametrizasyon aynı zamanda eylemsiz kütle yoğunluğunu ölçek faktörü a cinsinden birinci derecede Fourier serisine açmaya karşılık gelir. Yani karanlık enerjinin, dolayısıyla da evrenin evrimini yerel olarak belirli noktalar komşuluğunda yakınsamak yerine, bütün tarihini birinci dereceden hassasiyetle anlatmaya olanak verir. Bu doğrultuda tezin ilk kısmında gerekli araçlar ve yeni bir karanlık enerji kaynağını içeren modelin fiziksel özellikleri genel görelilik çerçevesinde türetilmiştir. Süreklilik denkleminin çözülmesiyle, eylemsiz kütle yoğunluğunun salınımlı doğasının kendisini enerji yoğunluğu $\rho_{\mathrm{DE}}(a)$'da kosinüs integral fonksiyonu $\mathrm{Ci}(Q_2a)$ biçiminde ortaya çıkardığı, $\mathrm{Ci}(Q_2a)$ fonksiyonunun da Friedmann denklemi vasıtasıyla evrenin genişleme dinamiğinde çok önemli bir rol oynayan özgün karakteristiklere yol açtığı görülmüştür. Sonrasında modelin yeterliliklerinin yanı sıra, modelin serbest parametreleri olan $\bar{\Lambda}$, Q_2 ve φ ve bunların evrenin genişleme dinamiği üzerindeki etkilerinin bir önaraştırması yapılmıştır. Önaraştırmada ΛCDM'in erken evreni iyi açıkladığı kabul edilip, bu erken evren betimlemesine dokunulmamıştır. $0.7 \lesssim \bar{\Lambda} \lesssim 1.3$ ve $13 \lesssim Q_2 \lesssim 15$ değer aralıklarında, $H(z/(1+z)$ ve $c\ln(1+z)/D_M$ durumlarında, yerel TRGB, SH0ES H_0 ölçümleri ve tam BAO kümesini içeren veri noktalarıyla çok iyi uyum gösteren eğriler elde edilmesinin mümkün olduğu görülmüştür. Devamında modelin serbest parametreleri $\bar{\Lambda}$ ve φ'nin bazı değerleri alması durumunda, karanlık enerjinin enerji yoğunluğu $\rho_{\mathrm{DE}}(z)$'nin düşük kırmızıya kaymalarda giderek sönümlenen salınımlar, bunun öncesinde, yani büyük kırmızıya kaymalarda ise bir işaret değiştirme davranışı yaptığı gösterilmiştir. Günümüze yaklaştıkça geç evrende karanlık enerjinin baskın hale gelmesiyle birlikte, düşük kırmızıya kaymalardaki salınıcı davranış doğal olarak genişleme oranı $H(z)$'de dalgalanmalar şeklinde belirmiş ve bu dalgalanmaların $H(z)/(1+z)$ grafiğinde Ly-α değeri ile uyumlu bir çukur ve Gökada BAO verisiyle hem ΛCDM hem Λ_{s}CDM'in olduğundan çok daha uyumlu bir tepe oluşturduğu görülmüştür. Bu anlamda Gökada BAO verileri diğer veri kümeleri için bir sorun olmaktan çıkar. H_0 gerilimine gelince, her ne kadar en güncel SH0ES ölçümlerinin modelle daha iyi uyuşması yüksek genlikli salınımların varlığını gerektirip diğer yandan $c\ln(1+z)/D_M$ grafiğinde Gökada BAO verisiyle olan uyumu kötüleştirse de, veri noktalarının yanılgı payları dahilinde her iki durumla da tutarlılık içerisinde olan parametre kombinasyonlarının olası olduğu görülmüştür. Ek olarak, ortaya çıkan gDE'dekine benzer işaret değiştirme davranışı enerji yoğunluğunda barındırılan $\mathrm{Ci}(Q_2 a)$ fonksiyonundan ileri gelmektedir. Ancak aralarında birtakım farklılıklar vardır: Karanlık enerjinin yoğunluğu $\mathrm{Ci}(Q_2 a \approx 0.6165) = 0$ noktasında eksiliye dönüp geçmişe gittikçe daha da eksilileşmektedir. Bu da yoğunluğun alabileceği eksili değerler için gDE'nin aksine bir en küçük alt sınırın olmadığı anlamına gelmektedir. Dahası, modelin verilerle uyumlu olarak gösterdiği işaret değiştirmelerin kırmızıya kayma değerlerinin ($z \sim 40$), Λ_{s}CDM'de gözlemsel analizden elde edilen tipik işaret değiştirme kırmızıya kaymalarından ($z_{\dagger} \sim 2$) çok daha büyük olduğu görülmektedir. Ne var ki, bu farklılıklara karşın, eylemsizlik kütle yoğunluğunun sinüzoidal parametrizasyonunun ilk aşamada beklentileri karşıladığı söylenebilir. Ayrıca yoğunluktaki salınımların bir sonucu olarak, karanlık enerji durum denklemi $w_{\mathrm{DE}}(z)$'nin de azalan kırmızıya kayma değerleriyle frekansı giderek artan salınımlar yaptığı ve bunların da herhangi bir modelden bağımsız şekilde gözlemlerden hareketle oluşturulan karanlık enerji durum denklemi eğrileriyle $0 \lesssim z \lesssim 2$ aralığında kabaca örtüştüğü görülmüştür. Aynı durumun yavaşlama parametresi $q(z)$ için de geçerli olduğu görülmüştür; bu da parametrizasyonun başarılı olma ihtimali konusunda daha da güven vermektedir. Tezin son kısmında ise modelin geç evrende neden olduğu dalgalanmaların kozmoloji bağlamındaki dalgacık (wavelet) kavramıyla tutarlılık içerisinde olup olmadığı test edilmiş ve yapılan sayısal hesaplamalarla karanlık enerjinin eylemsizlik kütle yoğunluğunun sinuzoidal parametrizasyonunun dalgacıklar için verilen koşullarla tutarlı olduğu doğrulanmıştır. Bütün bunlar göz önünde bulundurulacak olursa, $\varrho_{\mathrm{DE}}\,(a) = Q_1 \sin[Q_2(a-1)+\varphi]$'nin bir sonucu olarak ortaya çıkan salınımlı karanlık enerji modelinin Λ_{s}CDM'in başarılarını yenilemekle kalmayıp onun Gökada BAO verisine ilişkin sorunlarını çözerek daha yüksek kozmolojik gerilimleri çözebilen tek bir reçete sunmaya güçlü bir aday olduğunu söyleyebiliriz.

1. INTRODUCTION

It has been revealed through Supernova Type Ia surveys [1, 2] of the last two decades that the Universe has recently entered a stage of accelerated expansion, which, with the advancement and diversification of our astronomical probes, was also verified in the ensuing years by other independent observations such as the cosmic microwave background (CMB) [3–5] and the baryon acoustic oscillations (BAO) [6–9]. The simplest and arguably the most natural candidate driving this late-time acceleration is the cosmological constant Λ [10–12] comprising an essential component of what has come to be recognized today as the standard model of cosmology, namely, the Lambda Cold Dark Matter (ΛCDM) model [13–15]. Predictions of the standard model agree exquisitely well with the most of the observed properties of the Universe, ranging from the abundances of light elements set in the first few minutes [16–21] to the formation of large scale structures (LSS) [22] and their statistical distribution throughout space based on the minute temperature fluctuations imprinted in the CMB [3–5]. Its success and explanatory power notwithstanding, as the precision of data sets keeps increasing, it is becoming more and more evident that the ΛCDM in fact suffers a number of serious low and high redshift tensions that have been turned out be persistent in the model in the past couple of years [23–31]. Among them is the most prominent the Hubble constant H_0 tension of more than about 5σ [32–35], which is the conspicuous discrepancy between the value of $H_0 = 73.04 \pm 1.04\ \mathrm{km\,s^{-1}\,Mpc^{-1}}$ [36] obtained from the local, model-independent measurements, namely, the Cepheid-calibrated distance ladder method [37–39] that exploits the luminosity distance-redshift relation, and the value $H_0 = 67.36 \pm 0.54\ \mathrm{km\,s^{-1}\,Mpc^{-1}}$ inferred from the stringent constraints placed on the positions and relative heights of the acoustic peaks by the CMB-Planck satellite, assuming the ΛCDM [5].

Other significant challenges plaguing the standard model in connection with the Λ involve the infamous cosmological constant problem [14, 40–42] as well as the coincidence problem [10–12, 40, 41, 43] concerning the highly unlikely yet comparable present-day energy densities of dark energy $\rho_{\mathrm{DE},0}$ and matter $\rho_{\mathrm{m},0}$, or put it another way, the problem of "why the observed acceleration is happening today out of the virtually infinite possible time scales in the history of the Universe". This is particularly intriguing considering the fact that ρ_{DE} and ρ_{m} scale much differently with the expansion of the Universe, that is $\rho_{\mathrm{DE}} = \mathrm{const}$ and $\rho_{\mathrm{m}} \propto a^{-3}$ with a being the scale factor. A wealth of literature has been produced over the course of years by many who are in search for viable alternative cosmological models or minimal extensions of the standard model that could potentially provide satisfactory resolutions to these issues and more without disrupting hitherto successful account of the Universe [23, 31, 35]. Generically, the two most common approaches adopted in this context entail either treating general relativity (GR) as the correct theory of gravitation and introducing more general, brand-new dark fluids to the cosmic inventory (occasionally with non-minimal interactions between them) rather than one with constant equation of state (EoS) parameter $w = -1$ or contriving modifications in the gravitational theory such as $f(R)$ and scalar-tensor theories, Gauss-Bonnet gravity, Braneworld models coming with extra set of degrees of freedom that can generate the desired cosmological features [12, 44–46]. A renowned example of the former is quintessence models described by a minimally coupled canonical scalar field possessing an energy density that increases with the redshift [45, 47, 48]. Quintessence has remained as a popular subject of study as a candidate for dark energy and the solution to the current discrepancies for years. Unfortunately, it has been shown that quintessence models with EoS $-1 < w < -1/3$ are incapable of resolving for instance the H_0 tension as a late time modification to the expansion rate $H(z)$ since the required expansionary behavior is slightly phantom $w < -1$ [49–52]. Surprisingly, even the phantom models, made up of scalar fields with negative kinetic term and quintom models accommodating both phantom and canonical fields, cannot fully resolve the tension, but only yield limited alleviation [49–53]. Furthermore, the fact that Lyman-α (Ly-α) BAO measurements at $z \sim 2.34$ first presented in the DR11 release by the BOSS collaboration provide circumstantial evidence for nonmonotonic evolution of $H(z)$ as well as the preference for negative dark energy densities renders dynamical dark energy models more appealing and promising than ever [54, 55]. For instance, as we will also see in Chapter 2, this kind of dynamical behavior was discussed in Ref. [56] in the case of what is called *graduated dark energy* (gDE), stemming from the elevation of the null inertial mass density ϱ of the usual vacuum energy of the quantum field theory (QFT), i.e., $\varrho \equiv \rho + p = 0$ to a more general function of $\varrho \equiv \rho + p \propto \rho^{\lambda}$ quantifying the minimal dynamical deviation from the constant Λ, where λ is the ratio of two odd integers, along with its sign-switching cosmological constant (Λ_s) limit, which leads to the Λ_sCDM model [57]. Likewise, the authors conclude that the data analysis strongly signals a nonmonotonicity at $z \sim 2.3$ involving a clear detection of a sign-switching phenomenon in the dark energy (DE) density, which ultimately addresses a broad range of discrepancies such as H_0, Ly-α, M_B, S_8 and so on. They also reported the necessity of wiggles in the Hubble parameter $H(z)$ as the Galaxy BAO data did not behave well with the Λ_sCDM model [56–59].

Another frequently espoused approach giving rise to interesting dynamical cosmological consequences is to abandon the assumption of the constant dark energy EoS, $w_{\rm DE} = $ const. In this regard, numerous phenomenological parametrizations of dark energy have been investigated [60–73], mostly motivated by the aforementioned observational signatures and the recent model-independent reconstructions that hint at a time-varying dark energy $w_{\rm DE}(a)$ rather than a (cosmological) constant with more than 3σ [74–78]. One of the earliest and well-known parametrizations of this sort is the so-called Chevallier-Polarski-Linder (CPL) parametrization where the EoS is given by a relation linearly dependent on a (essentially first order Taylor expansion), that is $w_{\rm DE}(a) = w_0 - w_a(1-a)$ with w_0 and w_a being two real free parameters. It is a sensitive-to-data (SNIa) and well-behaved form for the early universe, $a \sim 0$ hence $w_{\rm DE} \approx w_0 - w_a$, and present time $a \sim 1$ hence $w_{\rm DE} \approx w_0$ reducing to the same old constant EoS [79, 80]. The CPL parametrization is often utilized for observational analyses in the literature [49, 67, 81] for its choice of parametrization in a in contrast to the earlier redshift z parametrizations, e.g., $w_{\rm DE}(z) = w_0 - w_1 z$ (first order Taylor expansion in z), has the advantages that it does not lead to observational pathologies unlike its redshift counterpart and covers most of the observationally accessible epochs of the Universe [80,82]. Nevertheless, it blows up in the far future $w_{\rm DE} \to \infty$ as $a \to \infty$; thus, various other parametric forms have been discussed with a view to avoiding the divergence issue [71, 83–85]. It is also possible to include higher order terms of expansion but at this point, downside of introducing more free parameters is that not only the model becomes more and more prone to the overfitting but also the parameters become more degenerate [86]. Accordingly, more data/calibrators become necessary to break the degeneracy and constrain the parameter space. Besides the polynomial parametrizations, an idea worthy of investigation is the possible nonmonotonicity in the evolution of $w_{\rm DE}(a)$ that could cause the dark energy density to cross even below the phantom divide [83, 87–89]. A particular family of functions that are able to pull off the feat is the one displaying oscillatory properties or the ubiquitous sinusoidal functions, which, as we will see, constitute the crux of our discussion in this thesis. Such a behavior might have the prospect of providing solutions to some naturalness and fine-tuning problems. As a matter of fact, dark energy models with an oscillating dark energy EoS parameter, i.e., $w_{\rm DE} \propto \cos(a,z,t)$ first proposed in the literature can be attributed to the effort of solving the cosmic coincidence problem [90–93]. The gist of the argument is that an oscillating form of dark energy would cause the Universe to accelerate and decelerate successively, nullifying the purported specialness of the present-day accelerated expansion period in the standard model. Aside from purely phenomenological attempts, though being quite non-trivial to achieve, it is a theoretical possibility to be able to attain oscillating EoS within the framework of the field theory with an appropriate potential $V(\phi)$. For instance, the pseudo-Nambu-Goldstone Boson (PNGB) field characterized by the Lagrangian $\mathcal{L} = \frac{1}{2} g^{\mu\nu}\partial_\mu\phi\partial_\nu\phi - M^4[\cos(\phi/f)+1]$, where M is the explicit global symmetry breaking scale and f is the spontaneous global symmetry breaking scale, can result in wiggles, hence a nonmonotonic evolution in the EoS, depending on how deep the field rolls down the potential [94–96]. If the field has not already rolled through the minimum potential, it yields a monotonically evolving EoS parameter that can reduce to the CPL case [91]. Consequently, note that an oscillating potential does not necessarily give rise to an oscillating EoS parameter.

While the idea of parametrizing dark energy directly through EoS offers diverse cosmological scenarios, a deeper approach towards the nature of dark energy should be centered around more fundamental physical quantities such as the DE energy density $\rho_{\rm DE}$ and the inertial mass density defined as $\varrho_{\rm DE} \equiv \rho_{\rm DE} + p_{\rm DE}$. Indeed there have been some efforts to parametrize the dark energy density $\rho_{\rm DE}$ in this direction [97–102]. Nevertheless, arguably, the inertial mass density $\varrho_{\rm DE}$ can be viewed to be more fundamental than both the energy density $\rho_{\rm DE}$ and $w_{\rm DE}$ on the grounds that it enters energy and momentum conservation equations as the factor of proportionality as we shall see in Chapter 3. Consequently, it determines the nature of matter and its properties pertaining to energy and momentum. For instance, the condition that $\varrho < 0$ tells us the density of the fluid increases as the Universe expands. This also means the fluid is forced to flow in the direction opposite to the pressure gradient exerted, violating what is known as the weak energy condition (WEC) [103, 104]. So one can maintain that the energy density or EoS alone does not impart information on the behavior and nature of matter to the extent the inertial mass density does. Moreover, while one can always find a corresponding $w_{\rm DE}$ for any given dynamical $\varrho_{\rm DE}$, simplest parametrizations of $\varrho_{\rm DE}$ could give rise to very nontrivial and nonmonotonic behaviors of $w_{\rm DE}$ that are unlikely to be introduced by hand if $w_{\rm DE}$ were to be parametrized directly or to be obtained via some straightforward scalar field dynamics. It therefore stands as a reasonable choice to parametrize the inertial mass density $\varrho_{\rm DE}$.

All things considered, we are motivated to decide the functional form of the inertial mass density to be $\varrho_{\rm DE}\,(a)\;\propto \sin(a)$ based on the following arguments: **(1)** First and foremost ϱ is a very fundamental and comprehensive quantity characterizing the energy-momentum content (not just the energy content) of a system, given the fact that pressure gravitates in the theory of relativity. This becomes less obscure if one thinks of ϱ as being *enthalpy* per unit volume. $\varrho = \rho + p = \mathcal{H}/V$ which also helps us define the *specific enthalpy*, $\mathcal{H}/N = (\rho + p)/n$, that is the enthalpy associated to a single particle. **(2)** Recent model-independent reconstructions of dark energy $w_{\rm DE}$ and density $\rho_{\rm DE}$ point toward a dynamical dark energy with wiggly EoS $w_{\rm DE}$ [76–78]. **(3)** As we just discussed it is reported that the Galaxy BAO data necessitate a wiggly behavior in the expansion rate and suppress the amelioration of the other tensions in the gDE and $\Lambda_{\rm s}$CDM models [57,59]. **(4)** It has the potential to alleviate or even solve the significant tensions like H_0, M_B as well as S_8 and so on simultaneously. **(5)** The recent realization that deviations from the Hubble radius of the ΛCDM respecting the early and late time physics of it must be given in the form of oscillatory functions [105]. **(6)** The challenging reconciliation of the Ly-α BAO measurements of BOSS collaboration with the ΛCDM expansion rate at $z \approx 2.3$, suggesting a negative dark energy density $\rho_{\rm DE}$ that is about 1.5σ different from the unity value of ΛCDM, which is in turn implying a dynamical dark energy density that could even switch its sign from negative to positive [54, 106]. **(7)** Over suitable intervals, the average value of a sinusoidal function is zero. In our case this corresponds to $\langle\varrho_{\rm DE}\rangle \approx 0$, recovering the null inertial mass density of usual vacuum energy of the QFT, $\varrho = 0$, representing considerably non-trivial and drastic deviations from the ΛCDM in relatively short periods, but recovering it in adequately prolonged time-scales. **(8)** Oscillating dark energy models are able to lead to results consistent with observations. **(9)** Oscillating cosmological models are apt candidates for the solution to coincidence problem. **(10)** Last but not least, the parametrization is done with respect to the scale factor a because we prefer to keep what presents cosmological interest to us finite in an interval $[0,1]$ over which a is well-defined. This amounts to shifting the oscillations tending to infinity to the far future, which is vice-versa in the case of parametrizing in z (though the z case appears interesting to investigate). Additionally, the scale factor a appearing in the FRW solution of GR is arguably the most natural and fundamental variable affecting the energy-momentum content of an expanding universe. Redshift z in this sense can be thought of as being somewhat secondary to the scale factor a as it emerges as a physical consequence of expansion encoded by a therefore serves to link the theory with observations.

In this thesis, we will first give a summary of the well-studied parametrizations of the inertial mass density as well as their detailed observational analyses in Chapter 2: the simple-graduated dark energy and the graduated dark energy. Then we will keep on with the particular limit of the graduated dark energy where it can be described by what is named as the sign-switching cosmological constant. Subsequently we will close Chapter 2 by a profound mathematical consequence regarding the requirement of wiggles in the post-recombination Universe. In Chapter 3, we will introduce our model in which we parametrize the inertial mass density by upgrading it to a sinusoidal function and investigate the free parameters of the model in addition to its cosmological implications. Lastly we will carry out a consistency-check with the conditions given at the end of Chapter 3.

2. INERTIAL MASS DENSITY PARAMETRIZATIONS IN LITERATURE

In this chapter, we briefly discuss implications of inertial mass density parametrizations (as a summary of Refs. [56–59]) together with their accompanying observational analyses.

2.1 Simple-Graduated Dark Energy

One of the simplest extensions of the base ΛCDM can be achieved through the consideration of a more supple concept of inertial mass density ϱ that can assume non-zero values unlike that of the usual vacuum energy of the QFT, which is null $\varrho = 0$. For example, in the simplest case, if we consider ϱ given by a constant named as the simple-gDE [58],

$$\varrho_{\rm ci} = \text{const} < 0 \tag{2.1}$$

whose corresponding energy density (and its redshift dependency) is described by,

$$\rho_{\rm ci} = \rho_{\rm ci0} + 3\ \varrho_{\rm ci}\ \ln(1+z), \tag{2.2}$$

where $\rho_{\rm ci0} > 0$ in accordance with the observational data. It satisfies the EoS parameter,

$$w_{\rm ci} = -1 + \frac{1+w_{\rm ci0}}{1+3(1+w_{\rm ci0})\ln(1+z)} \tag{2.3}$$

from which it can be noticed that the source approximates the Λ when $z \gg 0$ and its energy density $\rho_{\rm ci}$ resembles usual phantom sources ($w < -1$), except that at some point in the past $\rho_{\rm ci}$ turns minus as the term $3\ \varrho_{\rm ci}\ \ln(1+z)$ becomes more and more negative and eventually dominates the energy density. This crossing takes place at the redshift;

$$z_* = -1 + e^{-\rho_{\rm ci0}/3\varrho_{\rm ci}}. \tag{2.4}$$

Furthermore, the base ΛCDM can be extended by the inclusion of the spatial curvature (its corresponding density parameter is given by parameter Ω_k) in the Friedmann equation. Notably, the constant positive curvature $\Omega_{k,0} < 0$ offers an interesting case since together with the cosmological constant Λ it can be amalgamated into a composite effective source $f_{\rm eff}(z) \equiv \Omega_\Lambda + \Omega_{k,0}(1+z)^2$. The Λ is compansated by the curvature term with the increasing redshift thus the effective source behaves like a fluid with the negative energy density and EoS parameter $w = -1/3$ beyond certain redshift. As promising as it may seem to be a candidate for the possible need of a negative energy density source, it has the drawback of being at odds with spatially flat Universe $\Omega_{k,0} \approx 0$, given the BAO, SNIa and cosmic chronometers observations [107–109].

One can further elaborate the above scenario combining the source having constant negative ϱ rather than the Λ with the spatial curvature Ω_k. Now the energy density of this effective source is then,

$$\rho_{k\rm ci} = \rho_{\rm ci,0}[1 + 3(1 + w_{\rm ci,0})\ln(1+z)] + \rho_{k0}(1+z)^2 \tag{2.5}$$

which likewise crosses below zero as well at different redshifts depending on the value of $w_{\rm ci,0}$. It is shown by the above equation that the for example if we take the redshift $z_* = e - 1$ at which $\rho_{k\rm ci}$ becomes negative, we require $\rho_{k\rm ci}(z_*) = 0$ giving the relation,

$$\Omega_{k,0} = \frac{2.1 w_{\rm ci,0} + 2.8}{3 w_{\rm ci,0} - 3.39}. \tag{2.6}$$

Equation (2.6) implies if the Universe is spatially flat $\Omega_{k,0} = 0$, then $w_{\rm ci,0} = -1.33$. If the Universe is currently assumed to be dominated by the Λ, that is $w_{\rm ci,0} = -1$, then we have $\Omega_{k,0} = -0.11$, both of which represent substantial departures from the observational constraints on the $w_{\rm ci,0}$ and $\Omega_{k,0}$. However, it is possible to circumvent this problem by simultaneoulsy relaxing the values of $w_{\rm ci,0}$ and $\Omega_{k,0}$, yet still remain within the bounds of observations. That is to say, it is possible to have $w_{\rm ci,0} = -1.1$ and $\Omega_{k,0} = -0.07$. This trade-off between $w_{\rm ci,0}$ and $\Omega_{k,0}$ can be shown better in Fig. 2.1 below [58] . Any two values lying on the red line satisfy Equation (2.6).

In the detailed observational analysis, the two models, i.e., the simple-gDE arising from the constancy of the inertial mass density and the other containing simple-gDE+the spatial curvature which are denoted by DE and oDE, are confronted with the most recent data at the time and compared with the ΛCDM and its simplest extension $o\Lambda$CDM involving the curvature. The main datasets used in the analysis are the Planck CMB data (PLK) [5], supernova type Ia (SN), Galaxy BAO consensus, Lyman-α BAO from BOSS DR14, the SDSS Main Galaxy Sample (MGS) and the Six-Degree Field Galaxy Survey (6dFGS) [110–115], and cosmic chronometers

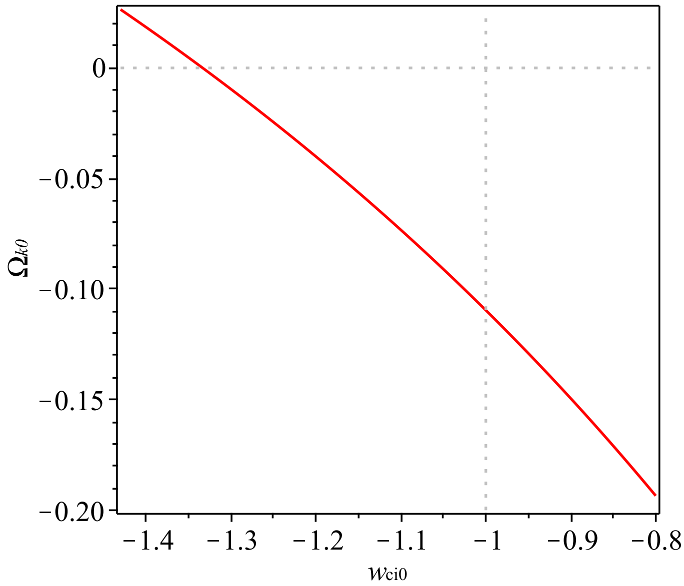

Figure 2.1 : The trade-off between $\Omega_{k,0}$ and $w_{ci,0}$ plotted for the redshift $z_* = e-1 \approx 1.7$. The intersection point of the two dotted lines specifies the where the ΛCDM lies. The figure is retrieved from Ref. [57]

(H) [116] as well as the BBN prior on the baryons [117]. The analysis is comprised of two sections, the first of which presents the fact that when the entire joint dataset BAO+SN+H+PLK is taken into account, no statistically meaningful evidence in favor of the extended models (DE, oDE and $o\Lambda$CDM) has been found, meaning that the tensions prevalent in the ΛCDM persist. On the other hand, in the second part the results change a great deal and the extensions exhibit interesting cosmological features if the CMB data is excluded from the analysis.

Above all, subject to the BAO+SN+H set, the simple-gDE falls short of the initial anticipations by giving poorer $H_0 = 67.06 \pm 2.02\ \mathrm{km\,s^{-1}\,Mpc^{-1}}$ than the ΛCDM value $H_0 = 68.27 \pm 0.88\ \mathrm{km\,s^{-1}\,Mpc^{-1}}$ as the data suggests $\varrho_{\rm ci} = (3.46 \pm 4.76) \times 10^{-31}\mathrm{g\,cm^{-3}}$ whose mean value is in contrast with the case of the original interest $\varrho_{\rm ci} < 0$. This implies that $w_{\rm ci0}$ lies in the quintessence region, i.e., $-1 < w_{\rm ci,0} = -0.937 \pm 0.0084 < -1/3$, which indeed yields lower H_0 values. If the spatial curvature is allowed on top of $\varrho_{\rm ci}$ corresponding to oDE model, only a partial improvement in H_0, i.e., $H_0 = 68.84 \pm 2.60\ \mathrm{km\,s^{-1}\,Mpc^{-1}}$, can be achieved since the effect of $\varrho_{\rm ci}$ is now offset by the positive spatial curvature even though the data prefers even higher $\varrho_{\rm ci} = (7.65 \pm 5.72) \times 10^{-31}\mathrm{g\,cm^{-3}}$ with $w_{\rm ci0} = -0.872 \pm 0.097$ than the one in the DE model. This intricate state of affairs is summarized in Fig. 2.2 [58]. In addition, $H(z)/(1+z)$ of both extensions DE and oDE fit better to the Ly-α BAO at $z \approx 2.34$

merely because the Ly-α data point enters the bounds of the new, enlarged probability distribution permitted by the dataset. Overall, of all the models, the oDE model agrees the best with BAO+SN+H dataset but the Bayesian evidence provides a compelling evidence for the ΛCDM in comparison with the extended models.

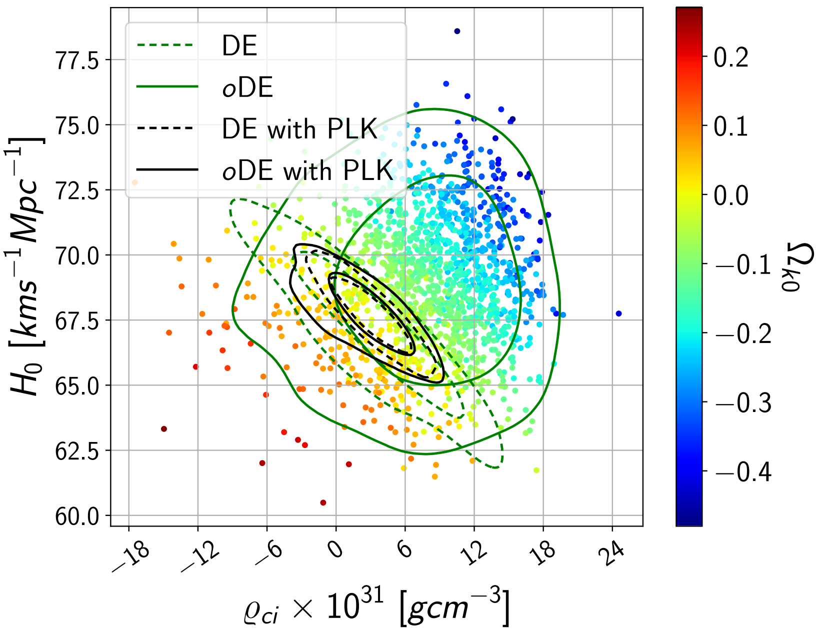

Figure 2.2 : The relationship among $\varrho_{\rm ci}$, $\Omega_{k,0}$ and H_0 with and without the Planck data. High H_0 values(represented by the blue dots) are scattered within a region that corresponds to $\varrho_{\rm ci} > 0$, which is in contrast with Equation (2.1). The figure is from Ref. [57]

.

When the CMB data is added to analysis, that is the case of BAO+SN+H+PLK, the previous constraints(of BAO+SN+H) on the oΛCDM are not affected much, however, surprisingly oDE model, which initially preferred a closed universe, now suggests a spatially flat universe with $\Omega_{k,0} = -0.0001 \pm 0.0019$ more precisely than the oΛCDM model with $\Omega_{k,0} = 0.0012 \pm 0.0018$ does. Consistently, the Bayesian evidence disfavor oΛCDM and oDE that in fact fits better than the ΛCDM to the BAO+SN+H+PLK dataset along with DE model. This significant suggestion of the spatial flatness or the lack of positive spatial curvature kills the possibility of lifting H_0 to the values consistent with the local measurements even if the diminished $\varrho_{\rm ci} = (2.85 \pm 2.58) \times 10^{-31}\,{\rm g\,cm^{-3}}$ (still positive though close to being null) tends to slightly increase it. Last but not least, the effective energy densities of the models (oΛCDM and oDE) containing spatial curvature cross below zero at redshifts which the data shows to be too big to lead to augmented H_0 values, even for the lowest constraints placed on z_*.

To recapitulate, neither BAO+SN+H nor BAO+SN+H+PLK provides evidence that these extended models are able to qualify as a replacement for the ΛCDM to resolve or alleviate the H_0 tension as well as the high-redshift challenges such as Ly-α BAO. Both datasets favor non-phantom ϱ, i.e., $\varrho_{\rm ci} > 0$, which is the opposite of what was expected to solve the H_0 problem, suggest no significant departure from the expansion history of the ΛCDM till the present time, yet based on the sign of $\varrho_{\rm ci}$, predicts a future evolution a far cry from that of the standard model [58].

2.2 Graduated Dark Energy and Sign-Switching Cosmological Constant

A slightly more complicated generalization of the inertial mass density ϱ of the usual vacuum energy of QFT, which is dubbed *graduated dark energy* [56], is realized by promoting it to a power function of the energy density ρ measuring the minimal dynamical deviation from the constant Λ assumption.

$$\varrho = \gamma\rho_0 \left(\frac{\rho}{\rho_0}\right)^{\lambda}, \tag{2.7}$$

where γ and λ are two real-valued parameters and ρ_0 is the present day energy density, which is $\rho_0 > 0$ as suggested by the observations. It is straightforward to check that the case $\gamma = 0$ reduces to the ΛCDM, $\lambda = 1$ generates a dark energy with $w = \text{const}$ known as the wCDM models and $\lambda = 0$ reduces to the simple-gDE that we have discussed in the previous section. The energy density of the gDE is obtained from the continuity equation,

$$\int \rho^{-\lambda} \mathrm{d}\rho = -3\gamma\rho_0^{1-\lambda} \int \frac{\mathrm{d}a}{a}, \tag{2.8}$$

and finally the scale factor dependence of the gDE energy density is given by,

$$\rho(a) = \rho_0[1 + 3\gamma(\lambda - 1)\ln a]^{\frac{1}{1-\lambda}} \tag{2.9}$$

satisfying the EoS parameter,

$$w = -1 + \frac{\gamma}{1 + 3\gamma(\lambda - 1)\ln a}. \tag{2.10}$$

As $a \to 0$ and $a \to \infty$ that is in the distant past and future $w \approx -1$. For a particular combination of the free parameters γ and λ the energy density switches its sign at some redshift z_*. This switching occurs at the future or past redshift depending on the factor $\gamma(\lambda - 1)$,

$$z_* = e^{1/3\gamma(\lambda-1)} - 1. \tag{2.11}$$

If $\gamma(\lambda - 1) > 0$ then z_* is some time in the past $z > 0$ and if $\gamma(\lambda - 1) < 0$ then it is in the future $-1 < z_* < 0$. If one proceeds with the former case, that is $\gamma(\lambda - 1) > 0$ with $\lambda < 1$ and $\gamma < 0$, it appears that for large negative values of λ, which is given as the ratio of two odd integers, the DE density turns into a source that dynamically flips its sign in the past. Note that as the λ gets larger and larger negative values, $\rho(z)$

increasingly becomes like the step-function. In the limit of $\lambda \to -\infty$, the model can be interpreted as the cosmological constant Λ phenomenologically changing its sign from $\Lambda < 0$ into $\Lambda > 0$ at relatively recent times. We will give a more detailed description of this limit in the next section.

To gain a better intuition about the way the model parameters operate, assume for example $z_* = e - 1 \approx 1.7$. From the above relation (2.11), we find that $3\gamma = 1/(\lambda - 1)$. If we take $w_0 = -1.03$, i.e., the prediction by the Planck release [5], then from $w_0 = \gamma - 1$ we have $\gamma = -0.03$, which yields $\lambda = -10.11$, meeting both $\lambda \ll 0$ and $\gamma < 0$. Taking $\gamma = -0.03$ and $\lambda = -10.11$ according to Ref. [56], the energy density evolves as in Fig. 2.3,

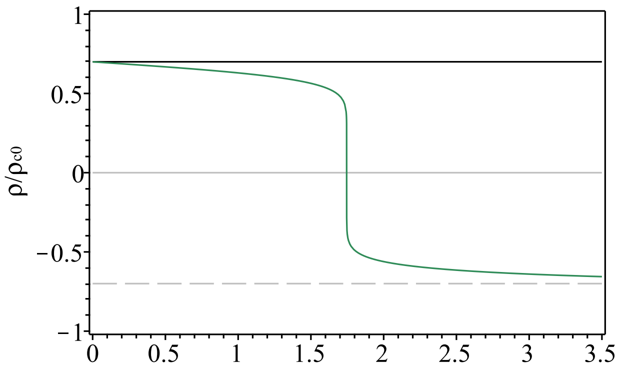

Figure 2.3 : The evolution of $\rho_{\mathrm{gDE}}/\rho_{\mathrm{cr},0}$ with respect to the redshift z with $z_* \approx 1.7$. The figure is retrieved from Ref. [56].

where $\rho_{\mathrm{gDE}}(z)/\rho_{\mathrm{cr},0}$ slowly increases as the Universe expands and about $z_* \approx 1.7$ makes a very sharp transition and settles to $\rho_{\mathrm{gDE},0}/\rho_{\mathrm{cr},0}$ which is the negative of the initial value with which it has started out. Correspondingly, the effective w is singular at the relevant redshift, possessing a pole in Fig. 2.4.

The gDE model has been confronted with the observational data encompassing the Planck (PLK), which is considered as a "BAO experiment" at $z_* = 1090$ that measures the sound horizon angular scale $[D_M(z = 1090)/r_d]$ in the early Universe (this consideration ignores the distinction between r_* and the BAO scale r_d however it turns out the approximation holds up to 0.1σ in the ΛCDM), high-precision Baryon Acoustic Oscillations (BAO) [55], supernova Type Ia (SN) and cosmic chronometers (H) [116].

For $-4 < \lambda \leq 0$, the model displays no statistically significant superiority over the ΛCDM. Nonetheless, for $\lambda \leq -4$, as λ gets larger and larger negative values and

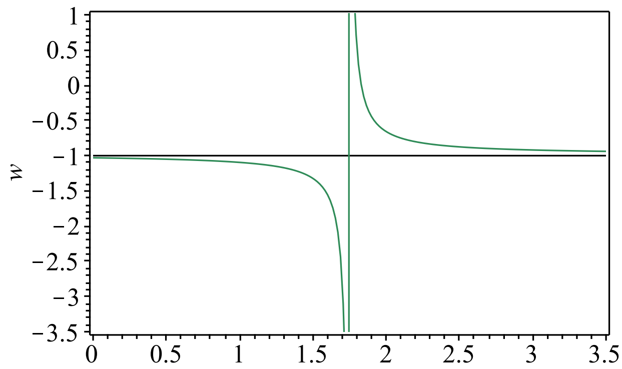

Figure 2.4 : The gDE EoS parameter $w_{\mathrm{gDE}}(z)$ vs z. At the time z_* when the gDE passes below zero, it has a vanishing energy density, causing a pole in its EoS parameter. The figure is taken from Ref. [56].

when it is free, γ begins exhibiting a posterior probability distribution whose peak (maximum) is decisively becoming more and more distinct and positioned away from the one containing the ΛCDM model ($\gamma = 0$), resulting in a great betterment of the fit. It has been observed in Fig. 2.5 that the peak persists in a very stable position in λ-Ψ space corresponding to $\Psi \equiv -3\gamma(\lambda-1) = -0.86$ [56]. Note that the quantity Ψ is what determines when the event of sign-switching (or equivalently the pole in the EoS parameter) occurs, which the data definitively suggests to be at $z_* \approx 2.32$.

In Fig. 2.6 [56] is given the probability distribution of the scaled gDE density $\rho_{\mathrm{gDE}}(z)/\rho_{\mathrm{cr},0}$. The pinkish regions, which are the areas of higher probability, show that for $0 < z < z_*$, the gDE best-fit value (black dashed line) can be described by a positive Λ (solid black line) to a very good approximation. Likewise, the same thing is also true for $z > z_*$, except that it converges to the negative cosmological constant $-\Lambda$. This is because the transition timescale of the gDE energy density is controlled by the parameter λ and when it is large negative-valued as preferred by the data or when it is free, the switching happens very rapidly, which forces the gDE energy density to evolve in a way that renders it increasingly difficult to demarcate it from the constant Λ behavior for $z > z_*$ and $z < z_*$. It is therefore tempting to conclude that the limit of $\lambda \to -\infty$ in which the gDE transforms into a simpler model where the sign of the Λ makes a swift spontaneous change deserves a special attention, which we will discuss in the next section.

In addition, the new dynamical nature of gDE helps ameliorate some significant tensions. For instance the H_0 values predicted by the gDE with the parameters that are

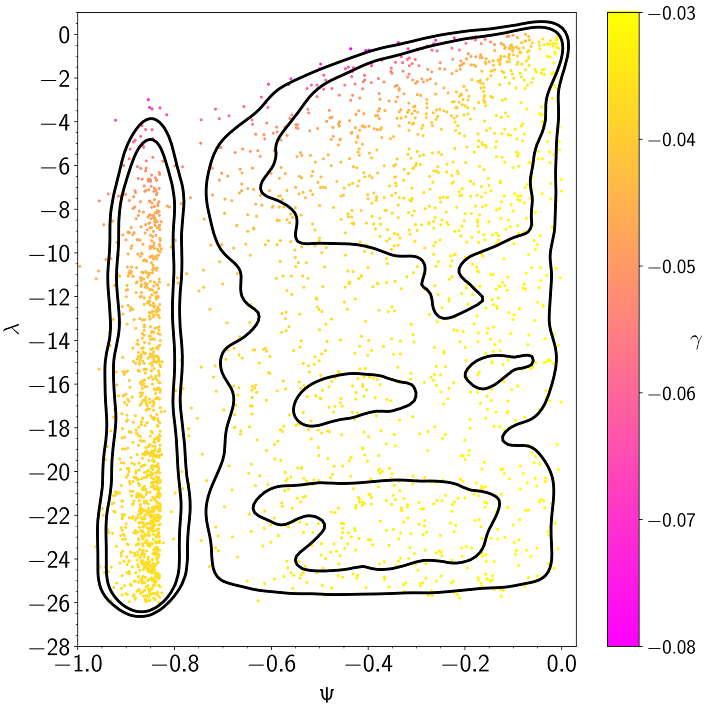

Figure 2.5 : The distribution splits into two separate regions: at the left, the very orderly and sharp distribution including the new stable peak at $\Psi \sim -0.86$ is shown and at the right there is the wide, less stable patch that also harbors the ΛCDM or $\Psi \sim 0$, reflecting the bimodal characteristic of the parameters. The figure is from Ref. [56].

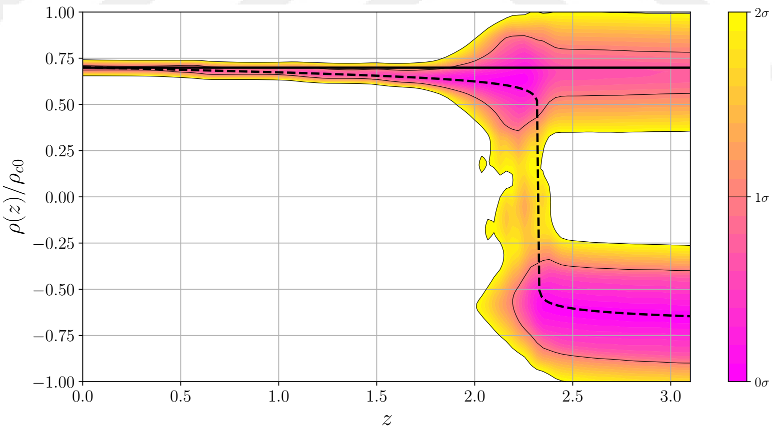

Figure 2.6 : The evolution of $\rho_{\rm gDE}(z)/\rho_{\rm cr,0}$ with z. The swift transition in the energy density about $z \sim 2.34$ enables one to describe its behavior by the step-function. The figure is retrieved from Ref. [56].

favored by the stable peak position at $\Psi \sim -0.86$ agrees with the Tip of the Red Giant Branch-calibrated (TRGB) supernovae measurements of H_0 [118] much better than the ΛCDM living at the position $\Psi \sim 0$ does. This is well illustrated in the Fig 2.7 [56]

Besides the H_0 tension, the gDE can assist $H_{\rm gDE}(z > 2.32)$ in assuming smaller values compared to the $H_{\Lambda\rm CDM}(z > 2.32)$ thanks to the sudden decline in its energy density. As the expansion rate is directly related to the the total energy density of the Universe,

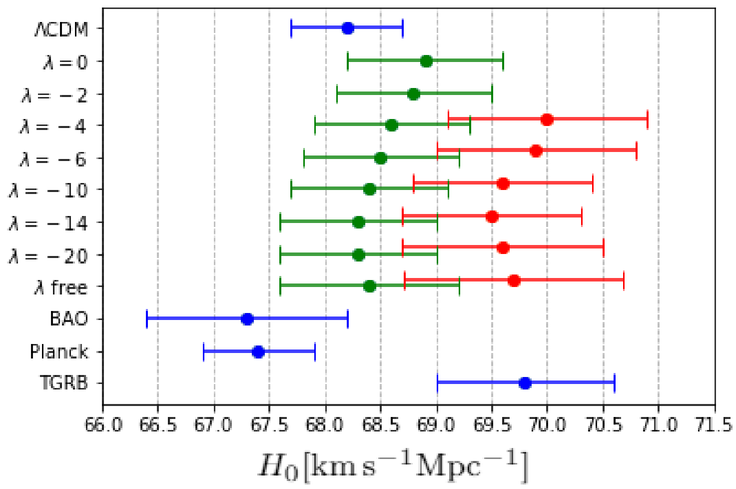

Figure 2.7 : The red error bars of 1σ confidence level (CL) show the improvement in H_0 with respect to the ΛCDM model and other less stable combinations of the free parameters λ and γ, that is $\Psi < -0.86$. The H_0 values (red error bars) are in excellent agreement with the local TRGB measurements that gives $H_0 = 69.8 \pm 0.8\ \mathrm{km\,s^{-1}\,Mpc^{-1}}$. (The fig. is taken from Ref. [56])

$H_{\mathrm{gDE}}(z > 2.32)$ correspondingly gets smaller values, allowing $H(z)$ to pass through the Ly-α BAO ($z = 2.34$) data point [8, 54] hence resolving the tension. How this decline is reflected in $H(z)$ can be seen in Fig. 2.8 very nicely.

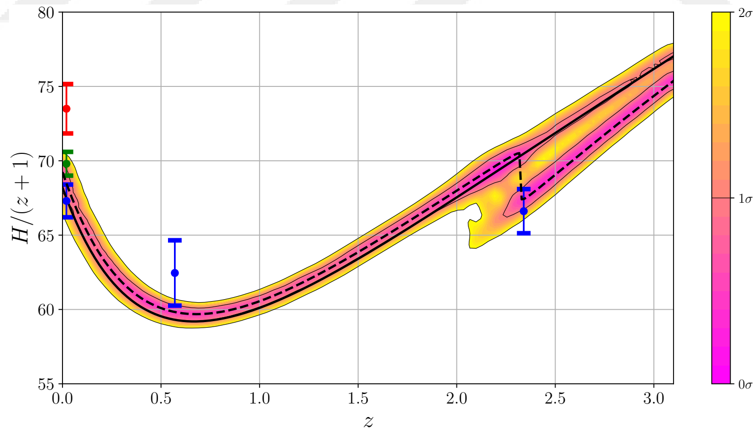

Figure 2.8 : $H(z)/(1+z)$ according the best fit gDE value (the dashed line). It simultaneously resolves the Ly-α and H_0 discrepancies. (The fig. taken from Ref. [56])

All of these improvements in the fit and the data repeatedly favoring $\Psi \sim -0.86$ for large enough negative values of λ constitute a significant observational piece of evidence that the Universe might have spontaneously transitioned from AdS to dS vacua at $z \sim 2.32$ or thereabouts. That this transition might hold intriguing implications from the perspective of the string theory where dS vacua are difficult to come by [56].

2.3 Λ_sCDM: Sign-Switching Cosmological Constant

In the previous section we saw that as λ gets larger in negative values, namely in the limit of $\lambda \to -\infty$, $\rho_{\rm gDE}(a)$ produces the behavior of the step function as nicely indicated by the likelihood analysis in Fig. 2.6. Therefore guided by the observations, the so-called minimum dynamical deviation can be described by the step function quite accurately,

$$\frac{\rho_{\rm gDE}(a)}{\rho_{\rm cr,0}} \to \Omega_{\rm gDE,0}\,{\rm sgn}[1-\Psi\ln a], \tag{2.12}$$

where sgn[x] is the familiar signum function that outputs -1, 0, 1 for $x<0$, $x=0$ and $x>0$, meaning that a_* is the scale factor $\rho_{\rm gDE}(a)$ passes below zero at, then for $a<a_*$, gDE$(a) \to -\Lambda$ and for $a>a_*$, $\rho_{\rm gDE}(a) \to \Lambda$, which, phenomenologically can be thought of as being equivalent to a model where Λ spontaneously switches sign at some a_* and triggers the acceleration of the late-time expansion of the Universe. In fact, the sign-switching cosmological constant represents a theoretically appealing regime for it offers an important means of avoiding the physical constraints the gDE fails to obey. To elaborate, the adiabatic sound speed $c_s^2 = {\rm d}p/{\rm d}\rho$ respects the condition $0<c_s^2<1$ whose upper limit marks the boundary between causal and non-causal behavior of matter. Violation of the upper limit means that the fluid supports the propagation of signals faster than the speed of light, contravening the chief tenet of the theory of relativity. Take the gDE with $c_s^2 = -1+\gamma\lambda\left(\frac{\rho}{\rho_0}\right)^{\lambda-1} \gg 1$ for $0<\rho\ll\rho_0$ much greater than the upper limit. On the other hand, an effective source originating from geometric considerations would not be subject to the aforementioned constraints [56]. For instance the cosmological constant can also be interpreted as the curvature of empty space; therefore, it is not only observationally plausible but also theoretically appealing to view the gDE emerging as an effective source approximating the cosmological constant that spontaneously flippes its sign. This limit of the gDE has been branded as the *sign-switching cosmological constant* [57] and it is described by

$$\Lambda_{\rm s} \equiv \Lambda_{\rm s0}{\rm sgn}[z-z_\dagger], \tag{2.13}$$

where $z_\dagger$ denotes the redshift of the so-called sign-switching and the model replaces the Λ of ΛCDM with $\Lambda_{\rm s}$ to give birth to $\Lambda_{\rm s}$CDM.

A comprehensive observational study involving datasets such as the full *Planck* CMB data [5], the full BAO set [106] and Pantheon SNIa [119] reveals that the sign-switching cosmological constant simultaneously relaxes, if not fully resolve, a wide range of discrepancies majority of other alternative models out there cannot without exacerbating at least one of them. These discrepancies encompass H_0 and the associated M_B tensions, Ly-α, S_8, t_0 and ω_b tensions [57, 59]. To exemplify, when the joint CMB+BAO dataset is considered, the model yields $H_0 = 68.82 \pm 0.55\ \mathrm{km\,s^{-1}\,Mpc^{-1}}$, which is in a good agreement with the TRGB measurements [118]. What is more is that it has been argued that remedying the H_0 tension is in essence nearly the same as resolving the SNIa absolute magnitude (M_B) tension due to the equivalency between Λ_sCDM and ΛCDM for $z < z_\dagger$ and the way they are incorporated into the methods of local H_0 measurements and the relevant cosmography. Greater H_0 values attained by the Λ_sCDM correspond to smaller M_B values. For example, for $z_\dagger = 1.6$, Λ_sCDM yields $M_B \approx -19.25$ mag. This agrees very well with the $M_B^{R20} = -19.244 \pm 0.037$ mag calibrated via Cepheids [120] based on Pantheon SNIa data [119], which is in 3.4σ tension with the $M_B^{Planck2018} = -19.401 \pm 0.027$ mag calibrated via the sound horizon scale (based on parametric free inverse distance ladder) [121]. One of the other discrepancies addressed by the Λ_sCDM is the growth tension, also known as the S_8 tension [31]. It refers to the mismatch between the growth rates suggested by the *Planck*/ΛCDM and dynamical probes such as weak lensing [122, 123], cluster counts [124, 125] and redshift-space distortion [126, 127]. The combined growth parameter is defined as $S_8 \equiv \sigma_8\sqrt{\Omega_\mathrm{m}/0.3}$ where σ_8 is the amplitude of matter root-mean-square fluctuations enclosed within the radius of $8h^{-1}$Mpc today. *Planck*/ΛCDM in the context of GR suggests $S_8 = 0.834 \pm 0.016$ [5], on the other hand, for example the KiloDegree Survey(KiDS-1000) finds $S_8 = 0.766^{+0.018}_{-0.015}$ (cosmic shear+galaxy-galaxy lensing) [128] being at about 3σ tension. Including only the CMB data in the analysis, Λ_sCDM gives a relaxed value of $S_8 = 0.8071 \pm 0.0210$ despite the increased $\sigma_8 = 0.8223 \pm 0.0098$ with respect to $\sigma_8 = 0.8117 \pm 0.0076$ in the ΛCDM. This is because of the suppressed $\Omega_{\mathrm{m},0} = 0.2900 \pm 0.0160$ within the Λ_sCDM compared to the ΛCDM value of $\Omega_{\mathrm{m},0} = 0.3162 \pm 0.0084$. Additionally, as we mentioned before, first noticed in the BOSS DR11 as 2.5σ discrepancy in the ΛCDM, now being at a mild 1.5σ after the eBOSS

SDSS-DR16, Ly-α measurement at $z \approx 2.33$ has been troublesome to reconcile with the theory as the data favors negative DE densities at that redshift [54, 106, 129]. In this direction, it has been shown that the sign-switch conjecture of the gDE hence Λ_sCDM resolves the Ly-α tension at $z \approx 2.33$ as well. On the other hand, in the case of full BAO set containing the Galaxy BAO data at effective redshifts $z_{\rm eff} = 0.15, 0.38, 0.51, 0.70, 0.85$ [106], the fact that the Galaxy BAO data prefer higher $z_\dagger$ values precludes the Λ_sCDM from efficiently mitigating the other discrepancies. This can be seen from the Fig 2.9 [57].

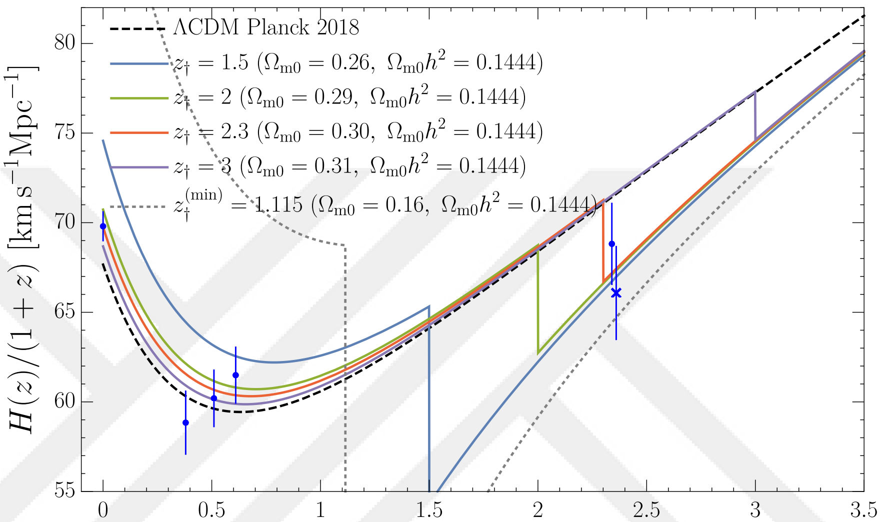

Figure 2.9 : As $z_\dagger$ gets values smaller than about 2.2, higher and higher tension with the data points at $z_{\rm eff} = 0.38, 0.51$ arises. This implies that the lower limit for the sign-switching redshift $z_\dagger$ is set by the Galaxy BAO data while the upper limit $z_{\rm eff} \approx 2.33$ is determined by the Ly-α data since if the sign-switching takes place at higher redshifts, the reconciliation with the data point is immediately lost. (The figure is retrieved from Ref. [58].)

That is to say, the $M_B \approx -19.25$ obtained for $z_\dagger = 1.6$ is not allowed when the full BAO is introduced to the analysis. As $z_\dagger$ is forced to assume higher values than $z_\dagger = 1.6$, the corresponding M_B values decline, building up the so-called tension. Therefore it seems to be case that the Galaxy BAO data tend to offset the relaxations of the significant discrepancies achieved by the Λ_sCDM model. As a result, it has been argued in Refs. [57, 59] that for the model both to be in agreement with the full BAO set [106] and to retain its success in bringing discrepant high-redshift values to more compatible ranges at the same time, a wiggly behavior in the late-time evolution of $H(z)$ that would fit better to the Galaxy BAO might be necessary. In the next section we will now see that there is actually much more to the idea of wiggles than just this.

2.4 The Inevitable Manifestation of Wiggles in the Late Universe

In addition to the observational precursors, further conviction on the requirement of wiggles in the late Universe has come from a deeper mathematical realization. It has been shown that smooth deviations from the Hubble radius $H^{-1}(z)$ of the ΛCDM respecting the early and late time physics of it must be given in the form of oscillatory (but not necessarily periodic) functions [105]. To justify this assertion, let us start giving the comoving angular diameter distance $D_M(z_*)$ to the surface of last scattering

$$D_M(z_*) = c\int_0^{z_*} \frac{\mathrm{d}z}{H(z)}, \tag{2.14}$$

where z_* the redshift at decoupling. A well-known fact is that given the pre-recombination physics (which is described by the ΛCDM in this case), the constraint placed by the near model-independent determination of the angular acoustic scale on $D_M(z_*)$ is very stringent [4, 5]. Therefore alternative models that claim to be consistent with the pre-recombination physics of the ΛCDM at least at the background level are expected to keep $D_M(z_*)$ unchanged. This translates to

$$\int_0^{z_*} \frac{\mathrm{d}z}{H_{\Lambda\mathrm{CDM}}(z)} \approx \int_0^{z_*} \frac{\mathrm{d}z}{H(z)}, \tag{2.15}$$

where $H(z)$ is the Hubble parameter of any given model whose departure $\psi(z)$ from the ΛCDM is quantified by its Hubble radius $\psi(z) = H^{-1}(z) - H^{-1}_{\Lambda\mathrm{CDM}}(z)$. Notice it is immediate from the fact that the description of the early Universe ($z \geq z_*$) is given by the ΛCDM that $\psi(z \geq z_*) = 0$ (1st condition) so that $H(z) = H_{\Lambda\mathrm{CDM}}(z)$. Altogether Equation (2.15) implies,

$$D_M(z_*) = c\int_0^{z_*} \frac{\mathrm{d}z}{H(z)} = c\int_0^{z_*} \frac{\mathrm{d}z}{H_{\Lambda\mathrm{CDM}}(z)} + c\int_0^{z_*} \psi(z)\mathrm{d}z \tag{2.16}$$

which then imposes the 2nd condition,

$$\Psi(z_*) \equiv \int_0^{z_*} \psi(z)\mathrm{d}z = 0. \tag{2.17}$$

If one further requires that the standard model explains the late Universe successfully [5, 106, 123], imposing the 3rd condition

$$\psi(z = 0) = 0, \tag{2.18}$$

along with the 1st $\psi(z \geq z_*) = 0$ and the 2nd condition (2.17), then these three conditions are satisfied by a special group of oscillatory functions known as *wavelets* [130, 131]. It is because, provided that $\psi(z) \neq 0$ everywhere in the interval $(0, z_*)$, in order for the integral to vanish, for every negative value of $\psi(z)$, there must be the corresponding positive value, which suggests an oscillating type of behavior. The condition (2.17) is known as the *admissibility condition* for wavelets [130]. Moreover another mathematical underpinning is provided by what is known as the *Rolle's theorem*, which, adapted to our case, states that if at the boundaries $\Psi(z = 0) = 0$, $\Psi(z_*) = 0$ and $\Psi(z)$ is continuous on $[0, z_*]$ and differentiable on $(0, z_*)$, then at least one redshift z_p exists in the history of the Universe for which the following holds,

$$\left.\frac{\mathrm{d}\Psi}{\mathrm{d}z}\right|_{z=z_p} = \psi(z_p) = 0, \tag{2.19}$$

which unambiguously shows that the smooth deformations $\psi(z)$ introduced by any cosmological model on top of $H^{-1}_{\Lambda\mathrm{CDM}}(z)$ must be in the form of functions of oscillatory but not necessarily periodic kind, viz., wavelets, so long as the above conditions are exactly or approximately met. Fig. 2.10 [105] exemplifies some typical wavelets with their relevant parameters varied, such as the Haar wavelet given by,

$$\psi_H = \bar{\alpha}\psi_h\left[\bar{\beta}(z - \bar{z}_\dagger) + \frac{1}{2}\right], \tag{2.20}$$

and Hermitian wavelets, for example $\psi_{G3}(z)$ described by,

$$\psi_{G3}(z) = -8\beta^2\left[\beta(z - z_\dagger)^3 - \frac{3}{2}(z - z_\dagger)\right]\psi_{G0}(z), \tag{2.21}$$

which is generated by taking the n-th order derivative such that $\psi_{Gn}(z) = \frac{\mathrm{d}^n\psi_{G0}(z)}{\mathrm{d}z^n}$ (where $n = 3$ hence $G3$ in this particular case) of a Gaussian distribution $\psi_{G0}(z)$ of the form of,

$$\psi_{G0}(z) = -\frac{\alpha}{2\beta}e^{-\beta(z - z_\dagger)^2}. \tag{2.22}$$

For $n = 4$, it generates,

$$\psi_{G4}(z) = 16\beta^2\left[\beta^2(z - z_\dagger)^4 - 3\beta(z - z_\dagger)^2 + \frac{3}{4}\right]\psi_{G0}(z). \tag{2.23}$$

It turns out that wavelets are very efficient in granting a model nonmonotonic behavior, making the model far more flexible against the observational data. This becomes the the most transparent when we look at the evolution of the Hubble parameter

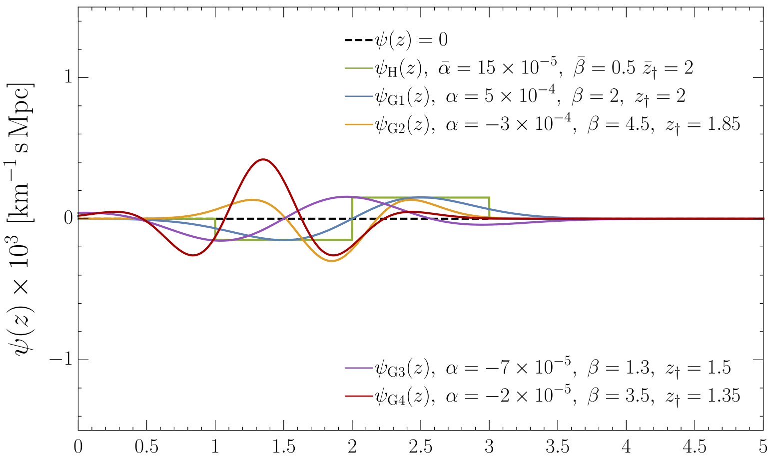

Figure 2.10 : Scaled wavelets vs z on the top of the Hubble radius. Notice the generic property of having a vanishing integral over a finite interval as well as the nonperiodic, localized oscillations. The figure is retrieved from Ref. [104].

in the presence of wavelets in Fig. 2.11 [105]. It is conceivable that thanks to a simplest non-periodic wiggle in the late-Universe, reconciliation of the entire BAO data set [106] can be accomplished by a hypothetical model having a mechanism with exactly or approximately similar to the wavelet-type behavior. At this spot, it is crucial to recall that the supposed oscillations need not be perodic and localized or decay well within some small redshift interval. Instead, they might have varying periods and can be spreaded over much of the history of the Universe into the past or future.

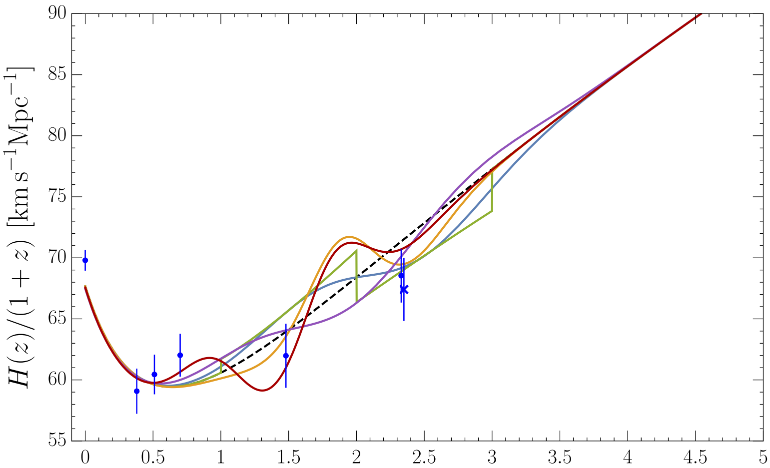

Figure 2.11 : The influence of wavelet deformations in Fig. 2.10 on the expansion rate vs z. The data points include the BOSS DR12 consensus Galaxy at $z_{\rm eff} = 0.38, 0.51$, eBOSS DR16 LRG at $z_{\rm eff} = 0.70$ with eBOSS DR16 Quasar, Ly-α-Ly-α, and Ly-α-Quasar at $z_{\rm eff} = 1.48,\ 2.33$ and 2.33 respectively.The figure is from Ref. [104].

Furthermore, the oscillations present in the Hubble radius can have different origins to descend from. That is to say it is possible to track their origins for example down to the dark energy density $\rho_{\mathrm{DE}}(z)$ or to the gravitational coupling strength $G_{\mathrm{eff}}(z)$. We can justify the former possibility by defining the fractional deviation,

$$\delta(z) = \frac{H_{\mathrm{DE}}(z) - H_{\Lambda\mathrm{CDM}}(z)}{H_{\Lambda\mathrm{CDM}}(z)}, \tag{2.24}$$

which for small enough deviations $|\delta(z)| \ll 1$ can be written as,

$$\delta(z) \approx -\psi(z) H_{\Lambda\mathrm{CDM}}(z). \tag{2.25}$$

Neglecting the radiation, the Friedmann equation(in geometrized units)

$$3H^2(z) = \rho_{\mathrm{m},0}(1+z)^3 + \rho_{\mathrm{DE},0} f(z) \tag{2.26}$$

allows us to write,

$$\Delta\rho_{\mathrm{DE}}(z) \approx 6\delta(z) H^2_{\Lambda\mathrm{CDM}}(z), \tag{2.27}$$

where we have made the definition of the deviation from the effective energy density of the cosmological constant

$$\Delta\rho_{\mathrm{DE}}(z) \equiv \rho_{\mathrm{DE},0} f(z) - \rho_{\Lambda}. \tag{2.28}$$

We see from Equation (2.27) that any oscillation present in $H_{DE}(z)$ might arise as a direct outcome of the deviation from the constant energy density of the usual vacuum energy, that is $\Delta\rho_{\mathrm{DE}}(z) \propto \psi(z)$.

All in all, one can conclude that the mathematical framework of wavelets in the cosmological context, coupled with the observational signatures from the troublesome anomaly between Galaxy BAO and Ly-α BAO data consolidates the idea of a wiggly, or in other words sought-after nonmonotonic, behavior of $H(z)$ stemming from the DE energy density in the time period $0 < z < z_*$ [55–57, 59, 106, 114]. This is exactly what we are going to explore in the subsequent section since our oscillatory parametrization indeed reflects the deviation from the null vacuum or constant EoS $w_\Lambda = -1$ assumption.

3. OSCILLATORY DARK ENERGY

The simple-gDE is as its name suggests the simplest ever deviation from the null inertial mass density of the usual vacuum [58]. It was described by a constant, non-dynamical inertial mass density. The extensive observational analysis revealed that even its co-operation with the spatial curvature could not lead to considerable relaxation of the existent cosmological tensions. So the next step was to consider a minimum dynamical deviation achieved by the gDE, which leads to the Λ_sCDM model as a limiting case [56,57,59]. In the observational test to which they have been put, they performed very well, addressing an array of tensions of various degree of significance. In spite of the remarkable achievements, their shortcoming was that they lacked the required flexibility to conform to Galaxy and Ly-α BAO data simultaneously. This, armed with the mathematical consequences just discussed [105], then implied that wiggles in $H(z)$ appear inevitable in order for the model to perform even better. In line with this argument, the next step we take in this section is to attempt to implement a cosmological scenario in which both sign-switch concept and non-monotonicity in the form of oscillations (wiggles) in the energy density, of which the previous models are bereft, legitimately co-exist.

3.1 Model: Oscillating Inertial Mass Density

We first start with the fact that the Universe, on sufficiently large scales, is well described by the Robertson-Walker (RW) spacetime;

$$\mathrm{d}s^2 = -\mathrm{d}t^2 + a^2(t)\mathrm{d}\Sigma^2, \tag{3.1}$$

where $a(t)$ is the scale factor of the Universe with t being the cosmic time and $\mathrm{d}\Sigma^2$ is the maximally symmetric metric of three-dimensional homogeneous and isotropic spacelike slices (hypersurfaces) at each instant of cosmic time, which is in reduced-circumference polar coordinates given by

$$\mathrm{d}\Sigma^2 = \gamma_{ij}(x)\mathrm{d}x^i\mathrm{d}x^j = \frac{\mathrm{d}r^2}{1-kr^2} + r^2\mathrm{d}\Omega^2. \tag{3.2}$$

Here $\mathrm{d}\Omega^2 = \mathrm{d}\theta^2 + \sin^2\theta\,\mathrm{d}\phi^2$ and $k = +1, 0, -1$ are the three possible constant (in space) curvatures of the spatial metric $\mathrm{d}\Sigma^2$ corresponding to a spatially closed, flat and open universes respectively [132, 133]. To the precision the most contemporary observations are able to measure, the Universe appears to be devoid of spatial curvature, i.e., $\Omega_{k,0} \approx 0$ [107–109]. Thus, in the rest of the dissertation we will assume that we inhabit a spatially flat universe with $k = 0$ unless otherwise specified, meaning that we at same time stay in concert with the canonical inflationary scenarios [134–136]. We continue with writing the metric of spacetime $g_{\mu\nu}$ in terms of its parallel and perpendicular components as follows,

$$g_{\mu\nu} = h_{\mu\nu} - u_\mu u_\nu \tag{3.3}$$

where $h_{\mu\nu}$ is the projection tensor and the four-velocity u_μ is the unique unit timelike field that is tangent to the worldlines of comoving observers and satisfies the relations $u_\mu u^\mu = -1$ and $\nabla_\nu u^\mu u_\mu = 0$. The general form of the energy momentum tensor (EMT) describing the flow of a perfect fluid within the RW spacetime is then $T_{\mu\nu} = (\rho + p)u_\mu u_\nu + pg_{\mu\nu}$ in which the energy density ρ with respect to u_μ and the isotropic pressure p of the fluid in the rest frame of observers comoving with the fluid are given by $\rho = T_{\mu\nu}u^\mu u^\nu$ and $p = h^{\mu\nu}(T_{\mu\nu}/3)$ respectively. It is well known in classical general relativity (GR), via the field equations $G_{\mu\nu} = -T_{\mu\nu}$, that the twice-contracted Bianchi identity guarantees that the EMT is divergence-free, that is $\nabla_\mu T^{\mu\nu} = 0$. Within the 1+3 covariant decomposition approach, one can split spacetime into its parallel and orthogonal components relative to u_μ and obtain the corresponding energy (the continuity) and momentum (the Euler) conservation equations from this divergence-free property of the EMT (See Appendix A):

$$\dot{\rho} + \Theta(\rho + p) = 0 \tag{3.4}$$

and

$$\mathrm{D}^\mu p + (\rho + p)\dot{u}^\mu = 0, \tag{3.5}$$

where $\Theta = \mathrm{D}^\mu u_\mu$ is the scalar of volume expansion rate in the case of no cosmic shear and vorticity, i.e., pure expansion and the projected spatial derivative D_μ is given by $\mathrm{D}_\nu u_\mu = \nabla_\nu u_\mu + \dot{u}_\mu u_\nu$ [103, 104, 132]. The overdot represents derivative with respect to the proper time t measured by the clocks of the fundamental observers, that is, the comoving time. In Equation (3.5), the gradient of pressure $\mathrm{D}^{\mu} p$ gives rise to the four acceleration $\dot{u}_{\mu}$ in the same sense as in the Newton's 2nd law. This implies that inertial content of matter is not determined by energy density alone, but rather by a combination of energy density and pressure, which we recognize as the *inertial mass density*, $\varrho \equiv \rho + p$. For the conventional vacuum energy (of QFT), or for the effective energy density of a cosmological constant when it is absorbed into the EMT, the inertial mass density is null, i.e., $\rho + p = 0$; and Equation (3.5) is often paid relatively little attention. However, there appears a plethora of uncharted cosmological implications if we give up on the notion of the null inertial mass density of the conventional vacuum and promote it to a special function of the scale factor a of the Universe. Based on the arguments given in the Introduction section, we introduce the inertial mass density ϱ of the vacuum energy assigned to a periodic, oscillating function of the scale factor a of the form of

$$\varrho_{\mathrm{DE}}(a) = Q_1 \sin[Q_2(a-1)+\varphi]. \tag{3.6}$$

Note that this choice is also tantamount to Fourier-expanding $\varrho_{\mathrm{DE}}(a)$ to the first order, enabling us to study its variations along the entire history of the Universe rather than in the neighborhood of some specific point. Here Q_1 and Q_2 are real constants, $\varphi = n\pi$ is the phase given in radians, and n is a real number that can take on values in the range $0 \leq n \leq 2$ for which the above parametrization is periodic. Q_1 and Q_2 serve to modulate the amplitude and frequency of the oscillation respectively. As $a \to 1$, provided that one sets the phase shift $\varphi = 0$, the inertial mass density approximately becomes null $\varrho_{\mathrm{DE}} \equiv \rho_{\mathrm{DE}} + p_{\mathrm{DE}} = 0$, so the cosmological constant behavior of the usual vacuum can be recovered today, which can also be verified by checking $\left.\frac{\mathrm{d}\rho_{\mathrm{DE}}(a)}{\mathrm{d}a}\right|_{a=1}$. Conversely, one can get rid of φ, one of the free parameters of the model by stipulating/demanding that the model, under investigation converges to the standard ΛCDM model at low redshifts $z \sim 0$; nevertheless, for the sake of not losing generality we proceed keeping the phase shift. Assuming that each source is locally and individually conserved, i.e., there is no mutual non-minimal interaction between the components, we solve the continuity equation to obtain the dark energy density ρ_{DE};

$$\dot{\rho}_{\mathrm{DE}} + 3HQ_1 \sin[Q_2(a-1)+\varphi] = 0, \tag{3.7}$$

where $H = \dot{a}/a$ is the Hubble parameter. From the integration

$$\rho_{\rm DE} = -\int \frac{3Q_1 \sin[Q_2(a'-1)+\varphi]}{a'} {\rm d}a', \tag{3.8}$$

we arrive at a very particular and non-trivial source of an oscillating kind;

$$\rho_{\rm DE}(a) = \tilde{\Lambda} - 3Q_1\left[\cos(\varphi - Q_2){\rm Si}(Q_2 a) + \sin(\varphi - Q_2){\rm Ci}(Q_2 a)\right], \tag{3.9}$$

where ${\rm Ci}(a)$ is the special cosine integral function with γ being the Euler-Mascheroni constant and ${\rm Si}(a)$ is the special sine integral function,

$${\rm Ci}(a) = \gamma + \ln a + \int_0^a \frac{\cos\tau - 1}{\tau}{\rm d}\tau, \qquad {\rm Si}(a) = \int_0^a \frac{\sin\tau}{\tau}{\rm d}\tau. \tag{3.10}$$

Here $\tilde{\Lambda}$ is an integration constant so that when there is no oscillation, $Q_1 = 0$, the 2nd and 3rd terms in Equation (3.9) drop and then the dark energy density reduces to a simple constant $\tilde{\Lambda}$. Any non-zero value of Q_1 represents the deviation from the constant nature of the vacuum energy such that $\rho_{\rm DE}(a) = \tilde{\Lambda} + f(a)$ where $f(a)$ can be regarded as higher order corrections/extensions to the effective dark energy density.

On an important note, the integral functions ${\rm Ci}(x)$ and ${\rm Si}(x)$, in the way they are, are difficult to intuit and deal with analytically. Therefore it is often more convenient to invoke some series approximations suitable to particular cases. In the early Universe, that is when the argument is small, $x \sim 0$ ($Q_2 a \sim 0$ for our source) one can exploit the convergent series expansions,

$${\rm Si}(x) = \sum_{n=0}^{\infty} \frac{(-1)^n x^{2n+1}}{(2n+1)(2n+1)!} = x - \frac{x^3}{3!\cdot 3} + \frac{x^5}{5!\cdot 5} - \frac{x^7}{7!\cdot 7} \pm \cdots \tag{3.11}$$

and

$${\rm Ci}(x) = \gamma + \ln x + \sum_{n=1}^{\infty} \frac{(-1)^n x^{2n}}{2n(2n)!} = \gamma + \ln x - \frac{x^2}{2!\cdot 2} + \frac{x^4}{4!\cdot 4} \mp \cdots, \tag{3.12}$$

where γ is the same Euler-Mascheroni constant just introduced above. Though the series may require more and more higher order terms depending on the amount of precision needed. In the cases in which one is interested in the features of the distant future of the Universe, that is when the argument is large $x \gg 1$ ($Q_2 a \gg 1$ for our source) the following series, which are divergent and asymptotic, may be useful for computational purposes,

$${\rm Si}(x) \approx \frac{\pi}{2} - \frac{\cos x}{x}\left(1 - \frac{2!}{x^2} + \frac{4!}{x^4} - \frac{6!}{x^6}\cdots\right) - \frac{\sin x}{x}\left(\frac{1}{x} - \frac{3!}{x^3} + \frac{5!}{x^5} - \frac{7!}{x^7}\cdots\right) \tag{3.13}$$

and

$$\mathrm{Ci}(x) \approx \frac{\sin x}{x}\left(1-\frac{2!}{x^2}+\frac{4!}{x^4}-\frac{6!}{x^6}\cdots\right)-\frac{\cos x}{x}\left(\frac{1}{x}-\frac{3!}{x^3}+\frac{5!}{x^5}-\frac{7!}{x^7}\cdots\right). \qquad (3.14)$$

For example, if we keep the terms up to the second order in (3.14),

$$\mathrm{Ci}(x) \approx \frac{\sin x}{x}\left(1-\frac{2!}{x^2}\right)-\frac{\cos x}{x}. \qquad (3.15)$$

At $x = 2.2$, the function (3.15) approximates $\mathrm{Ci}(x)$ with the relative error of 1.74% and it rapidly diverges for values smaller than $x \sim 2.2$.

Besides, we work with the scale factor $a_0 = 1$ normalized to today and the subscript 0 represents the present day values of the associated physical quantities throughout the dissertation. Accordingly, the present-day value of the energy density is,

$$\rho_0 = \tilde{\Lambda} - 3Q_1\left[\cos(\varphi - Q_2)\mathrm{Si}(Q_2) + \sin(\varphi - Q_2)\mathrm{Ci}(Q_2)\right], \qquad (3.16)$$

which enables us to write more compactly,

$$\rho_{\mathrm{DE}}(a) = \rho_0[\bar{\Lambda} + \bar{\xi}_1\mathrm{Si}(Q_2 a) + \bar{\xi}_2\mathrm{Ci}(Q_2 a)] \qquad (3.17)$$

$\bar{\xi}_1$ and $\bar{\xi}_2$ are the new combined constants into which the free parameters $\bar{\Lambda}$, Q_2 and some factor of the phase difference φ are packed in order to avoid the cumbersome way of writing. Also the bars at their tops remind us of the normalization by the present-day energy density as in $\bar{\Lambda} = \tilde{\Lambda}/\rho_0$ and $\bar{\xi}_{1,2} = \xi_{1,2}/\rho_0$. The caveat here is that $\tilde{\Lambda}$ is not necessarily the positive cosmological constant in this way of renaming. Instead, the dimensionless $\bar{\Lambda}$ can be thought of as being composed of two parts $\bar{\Lambda} = 1 + C$ where some arbitrary constant difference C from unity measures the deviation from the usual cosmological constant Λ. $\bar{\xi}_1$ and $\bar{\xi}_2$ are given by,

$$\bar{\xi}_1 = \frac{(1-\bar{\Lambda})\cos(\varphi - Q_2)}{\cos(\varphi - Q_2)\mathrm{Si}(Q_2) + \sin(\varphi - Q_2)\mathrm{Ci}(Q_2)}, \qquad (3.18)$$

and

$$\bar{\xi}_2 = \frac{(1-\bar{\Lambda})\sin(\varphi - Q_2)}{\cos(\varphi - Q_2)\mathrm{Si}(Q_2) + \sin(\varphi - Q_2)\mathrm{Ci}(Q_2)}. \qquad (3.19)$$

We notice from Equations (3.15) and (3.17) that the oscillatory behavior of ϱ_{DE} propagates to the dark energy density ρ_{DE}; however, the two types of oscillations are quite different from each other by nature: the former has a constant amplitude while the latter has a decaying one. Besides that, as we will see later, ρ_{DE} does not start oscillating up until some critical scale factor a_c value from the past through the present day. It is important to point out that the amplitudes of the oscillations are determined by different constants. In ϱ_DE, the amplitude depends merely on Q_1, whereas in ρ_DE, the amplitudes $\bar{\xi}_1$ and $\bar{\xi}_2$, of the oscillation inherited from ϱ_DE are joint effects of $\bar{\Lambda}$, frequency Q_2 and phase difference φ. In the latter case, Q_1 does not appear since it is embedded into $\tilde{\Lambda}$. Furthermore, if the material content of the Universe is modeled by perfect fluids with barotropic EoS, viz., $p(\rho)$, we can extract the relevant time-dependent dark energy EoS parameter from,

$$\frac{\mathrm{d}\rho_\mathrm{DE}}{\mathrm{d}a}+\frac{3}{a}(1+w_\mathrm{DE})\rho_\mathrm{DE}=0. \tag{3.20}$$

And, for our oscillating dynamical dark energy, we find an evolving EoS dependent on the scale factor a as follows;

$$w_\mathrm{DE}(a)=-1-\frac{\bar{\xi}_1\sin(Q_2a)+\bar{\xi}_2\cos(Q_2a)}{3[\bar{\Lambda}+\bar{\xi}_1\mathrm{Si}(Q_2a)+\bar{\xi}_2\mathrm{Ci}(Q_2a)]}. \tag{3.21}$$

When $z\gg 0$, that is $a\sim 0$, $\mathrm{Si}(Q_2a)\sim 0$, $\rho_\mathrm{DE}(a)\approx\tilde{\Lambda}+\xi_2\ln a$, the oscillatory behavior of the inertial mass density reduces to that of the simple-gDE [58] which is described by some constant inertial mass density, $\varrho_\mathrm{ci}=\mathrm{const}$, where $\rho_\mathrm{DE}(a)=\rho_\mathrm{ci0}-3\,\varrho_\mathrm{ci}\ln a$ (so $\xi_2\approx -3\,\varrho_\mathrm{ci}$) as we discussed in the previous section. In this regime where we get no oscillation, the EoS parameter (3.21) simplifies to

$$w_\mathrm{DE}(a)\approx -1+\frac{1}{3(\bar{\Lambda}/\bar{\xi}_2+\ln a)}. \tag{3.22}$$

In the past, taking the limit of Equation (3.21) (or (3.22)) gives

$$\lim_{a\to 0}w_\mathrm{DE}(a)=-1. \tag{3.23}$$

It means that irrespective of the model parameters, as we go back to the very distant past, the oscillating dark energy becomes more and more indistinguishable from the cosmological constant Λ.

The total energy budget of a spatially flat RW universe is given by the sum $\rho_\mathrm{tot}=\sum_i\rho_i$ containing pressureless matter $\rho_\mathrm{m}(z)\propto(1+z)^3$, radiation $\rho_\mathrm{r}(z)\propto(1+z)^4$ and our novel oscillating dark energy $\rho_\mathrm{DE}(z)$. Altogether they set the expansion dynamics governed by the Friedman equation,

$$\frac{\dot{a}^2}{a^2}=\frac{8\pi G}{3}\sum_i\rho_i, \tag{3.24}$$

which can be re-written in terms of the present-day density parameters by way of the definition for the i-th fluid $\Omega_{i,0} = \rho_{i,0}/\rho_{\mathrm{cr},0}$ where $\rho_{\mathrm{cr},0} = 3H_0^2/8\pi G$ and in a flat universe we have $\sum_i \Omega_{i,0} = 1$,

$$\frac{H^2}{H_0^2} = \Omega_{\mathrm{m},0}(1+z)^3 + \Omega_{\mathrm{r},0}(1+z)^4 + \Omega_{\mathrm{DE},0}\left[\bar{\Lambda} + \bar{\xi}_1 \mathrm{Si}\left(\frac{Q_2}{1+z}\right) + \bar{\xi}_2 \mathrm{Ci}\left(\frac{Q_2}{1+z}\right)\right]. \tag{3.25}$$

We here switched from the scale factor a to the cosmological redshift z dependence in order for the equation to be observationally meaningful via the transformation $1+z = \frac{1}{a}$. As usual energy densities of matter and radiation increase much faster than that of the dynamical dark energy as we go to the past. During the sufficiently early epochs the Universe is predominantly filled with matter and radiation; therefore, the wiggly nature of dark energy does not influence the expansion rate $H(z)$ which in turn approximates the expansion of the ΛCDM. As a matter of fact, in what follows we will do a more rigorous job by fixing the angular scale so as to elicit information on how the free parameters affect the Hubble expansion and what values they can attain to paint a picture compatible with the latest observations as well as the fresh realization that the wiggles are inevitable on the provisos given at the end of the second section [105].

3.2 Preliminary Investigation

In this section we will estimate a number of free parameters of the model that could yield improved fits to some anomalous data points, e.g., Ly-α BAO at $z \approx 2.34$ and Galaxy BAO measurements [112,114,115], and extract a value for the Hubble constant H_0 in better agreement with the direct, local methods [36, 118] while preserving the accurate depiction of the early Universe at the background level. Consequently, to retain the concordance with the already-existing data sets, it is plausible to proceed with the presumption that the pre-recombination universe is described by the ΛCDM, primarily based on its successful predictions pertaining to the Big Bang Nucleosynthesis (BBN) [16–21] and the density/temperature fluctuations observed in the CMB [3, 5]. Therefore, we assume no significant alteration is made to the early expansion history of the standard model all the way from BBN epoch up to the time of decoupling. Leaving the pre-recombination Universe untouched implies that the sound horizon scale r_*, which depends solely on the pre-recombination physics, remains unaltered as well,

$$r_* = \int_{z_*}^{\infty} \frac{c_s(z)}{H_{\Lambda\mathrm{CDM}}(z)} \mathrm{d}z, \tag{3.26}$$

where $z_* \sim 1090$ is the last scattering redshift for which the optical depth to Thomson scattering reaches unity and $c_s(z)$ is the speed of sound in the photon-baryon plasma determined by its baryon-to-photon ratio,

$$c_s(z) = \frac{c}{\sqrt{3\left(1 + \frac{\omega_{\mathrm{b}}}{\omega_\gamma}\frac{1}{(1+z)}\right)}}, \tag{3.27}$$

where we defined the dimensionless baryon and photon densities $\omega_{\mathrm{b}} \equiv \Omega_{\mathrm{b},0}h^2$ and $\omega_\gamma \equiv \Omega_{\gamma,0}h^2$ respectively using the definition of the reduced Hubble constant $h = H_0/100\ \mathrm{km\,s^{-1}\,Mpc^{-1}}$. Some early-time resolutions to the Hubble tension such as Early Dark Energy (EDE) [137–142] and dark radiation [143, 144] attempt to increase H_0 by modifying the early expansion rate $H(z)$, at $z \sim 3000$, therefore they end up altering the sound horizon, which is a very precisely calculated quantity within the ΛCDM. For example as can be seen from Equation (3.26), EDE reduces r_* through the insertion of an additionally postulated dark energy source that acts as a cosmological constant in the very distant past and gets unfrozen/dynamical around the matter-radiation equality. It slightly boosts the early expansion rate $H(z > z_*)$ to yield a higher H_0 value and dilutes away fast enough right before the recombination so that the post-recombination Universe stays unaffected. This sort of scenarios is known to be realized, for instance, by slowly-rolling scalar fields and oscillating scalar fields with an axion potential (PNGB) [139, 145–147]. Nevertheless, the improvement in H_0 comes at the expense of worsening the present tensions like the LSS and S_8 [148–150] and, or even worse creating a new tension with BAO data [151] as well as yielding poorer fits to BBN than that of the ΛCDM [152]. In addition, EDE models typically suffer from a particular kind of coincidence problem as there is no specific reason why the purported leap in the fractional contribution of EDE to the total cosmic energy budget should begin happening and come to a halt exactly in a relatively short and designated period of time. Contrary to the early-time modifications [137–144], our parametrization serves as a late-time modification fixing the comoving angular distance $D_M(z_*)$ to last scattering surface. We perform the fixing by means of the angular scale θ_* that can be measured with a precision as small as 0.03% in a near model-independent fashion from the location of the first acoustic peak present in the

CMB anisotropy power spectra [4,5]. To elaborate, this robust measurement of angular spacing θ_* along with the calculated r_* used as a standard ruler help to define the comoving angular diameter distance $D_M(z_*) = r_*/\theta_*$, which is also the distance at which a present day observer lies to the surface of last scattering,

$$D_M(z_*) = c\int_0^{z_*} \frac{\mathrm{d}z}{H(z)}. \tag{3.28}$$

We can rewrite the above expression as follows;

$$\frac{r_*}{\theta_*} = \int_0^{z_*} \frac{c\,\mathrm{d}z}{\sqrt{\omega_\mathrm{m}(1+z)^3+\omega_\mathrm{r}(1+z)^4+(h^2-\omega_\mathrm{m}-\omega_\mathrm{r})f_\mathrm{DE}(z)}}, \tag{3.29}$$

where we have defined $f_\mathrm{DE}(z)$ as

$$f_\mathrm{DE}(z) = \bar{\Lambda} + \bar{\xi}_1 \mathrm{Si}\left(\frac{Q_2}{1+z}\right) + \bar{\xi}_2 \mathrm{Ci}\left(\frac{Q_2}{1+z}\right) \tag{3.30}$$

encoding the time-evolution of our oscillatory dark energy source. To ensure that pre-recombination physics is the same as in the standard ΛCDM model, we pick its two base parameters (θ_*, ω_m) $\omega_\mathrm{m} = \omega_\mathrm{b} + \omega_\mathrm{c} = 0.1430 \pm 0.0011$, where ω_b and ω_c are baryon and cold dark matter densities that can be very precisely determined by the relative heights of the acoustic peaks, the angular spacing $100\theta_* = 1.04110 \pm 0.00031$ and as a derived parameter the resultant sound horizon as $r_* = 144.43 \pm 0.26$ Mpc from the Planck 2018-TT,TE,EE+lowE+lensing best fit mean values [5]. The density of photons ρ_γ is deduced by the measurement CMB monopole temperature determined to be the precise $T_{\mathrm{CMB},0} = 2.7255 \pm 0.0006$ [153],

$$\rho_\gamma = \frac{\pi^2}{15} T_\mathrm{CMB}^4. \tag{3.31}$$

In accordance with the standard model of particle physics, we take the radiation density $\omega_\mathrm{r} = 2.469 \times 10^{-5}(1 + 0.2271 N_\mathrm{eff})$ where $N_\mathrm{eff} = 3.04$ is the number of effective neutrino species with minimum allowed mass $\sum m_\nu = 0.06$ eV. Now given the set of the parameters $\bar{\Lambda}$ and Q_2, the integral (3.29) can be solved numerically for H_0 so that the entire expansion history of the universe $H(z)$ can be reconstructed for all redshifts.

First of all, we observe that the supposed wiggles due to ρ_DE(z) do not become manifest in $H(z)$ up until the frequency factor Q_2 reaches values greater than $Q_2 \sim 8$. In Fig. 3.1 we notice about $Q_2 \sim 13$ a bump conducive to a remarkable agreement

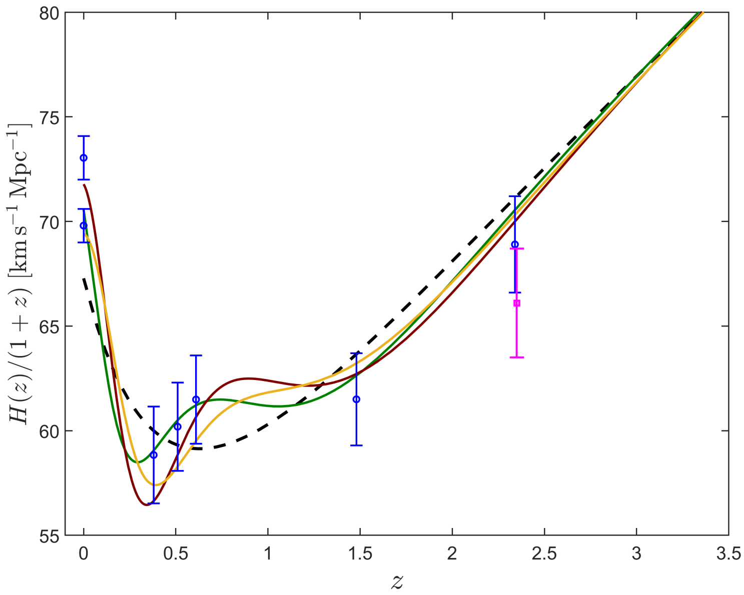

Figure 3.1 : Plot of $H(z)/(1+z)$ versus z in which a set of parameter values with better fits to the observational values $H_0 = 69.8 \pm 0.8$ km s^{-1} Mpc^{-1} of the TRGB and $H_0 = 73.04 \pm 1.04$ km s^{-1} Mpc^{-1} from the SH0ES is presented. The black dashed curve represents the standard ΛCDM, while the green curve is the oscillating dark energy with $\bar{\Lambda} = 0.777$, $Q_2 = 13.8$, $n = 0.88$ and $H_0 = 70.57$ km s^{-1} Mpc^{-1}, the claret red is the one with $\bar{\Lambda} = 1.1437$, $Q_2 = 14.5$, $n = 0.14$ and $H_0 = 71.78$ km s^{-1} Mpc^{-1} and lastly the yellow is $\bar{\Lambda} = 1.162$, $Q_2 = 14.9$, $n = 0.27$ and $H_0 = 69.41$ km s^{-1} Mpc^{-1}.

with the consensus Galaxy BAO data from the SDSS BOSS DR12 [112] at $z_{\rm eff} = 0.38, 0.51, 0.61$ emerges around $0.4 < z < 1.5$. And the increase in $\bar{\Lambda}$ acts to make the amplitude of the wiggles more salient. For all the three Hubble functionals, the nonmonotonicity due to wiggles in the dark energy density becomes more and more discernible as the Universe expands. Their diminished values of $H(1.25 \lesssim z \lesssim 3.5)$ fit better to the Ly-α BAO from the SDSS-eBOSS DR14 [114, 115] at $z_{\rm eff} = 2.34$ (correlation), $z_{\rm eff} = 2.35$ (cross-correlation) than the base ΛCDM. This deficit in $H(z)$ is then compensated by the so-called subsequent bump at lower redshifts $0.4 \lesssim z \lesssim 1.25$, which again provides the needed wiggles hence a better fitting behavior to the Galaxy BAO data [112] at the same time. By the same mechanism, we attain an enhancement in H_0, which can be seen in Fig. 3.1 and Fig. 3.2. Despite the dip at $z \sim 0.3$, that is in Fig. 3.1 green and yellow curves with $H_0 = 70.57$ km s^{-1} Mpc^{-1} and $H_0 = 69.41$ km s^{-1} Mpc^{-1} match the TRGB measurements $H_0 = 69.8 \pm 0.8$ km s^{-1} Mpc^{-1} and the claret red with $H_0 = 71.78$ km s^{-1} Mpc^{-1} match the SH0ES result $H_0 = 73.04 \pm 1.04$ km s^{-1} Mpc^{-1} within its error margin.

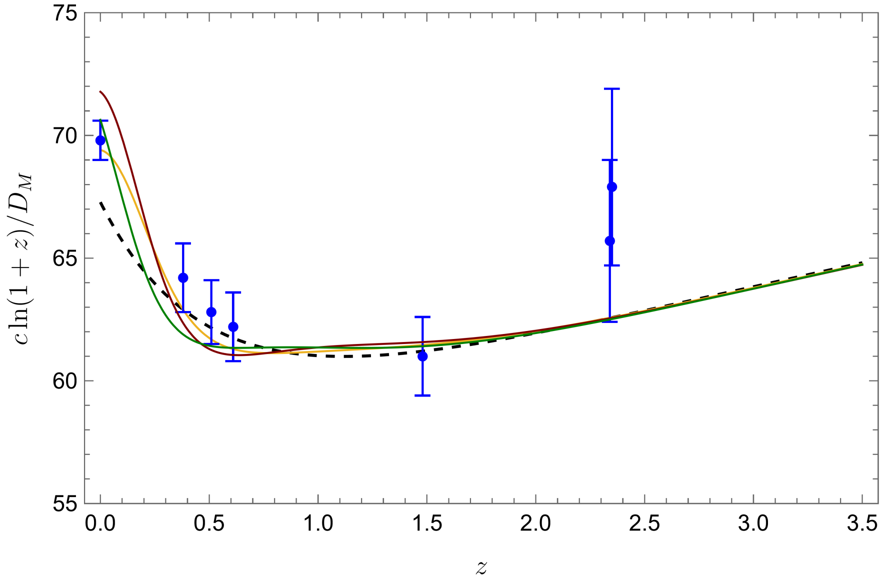

Figure 3.2 : The comoving angular diameter distance $D_M(z)$ scaled by $c\ln(1+z)$ vs z. The BAO data points are given at the effective redshifts $z_{\rm eff} = 0.38$, 0.51, 0.61 (Galaxy/BAO), 1.48 (Quasar), 2.34 (Lyα-Lyα), 2.35 (Lyα-Quasar). The better the fit to the Galaxy BAO in Fig. 3.1, the worse it gets in D_M case yet compromise is possible e.g. the yellow curve.

While the agreement with the data in Fig. 3.1 is outstanding, it is also equally crucial not to lose the coherence between the datasets. Namely, in Fig. 3.2, we see that all cases show almost no difference from the ΛCDM for $z > 2$ so they fit equally well to the Ly-α with no betterment. However, as the dust density diminishes faster than the DE, the DE gradually dominates the Universe and D_M begins exhibiting wiggles for $z \lesssim 2$, albeit less pronounced than in the case of $H(z)/(1+z)$. Although the green curve with $\bar{\Lambda} = 0.777$, $Q_2 = 13.8$, $n = 0.88$ and $H_0 = 70.57$ km s^{-1} Mpc^{-1} fits better to the Galaxy/BAO set in Fig. 3.1 than the the red and yellow curve, in the case of $c\ln(1+z)/D_M$ it yields the worst fit especially to the data point at $z = 0.38$. On the other hand, the yellow curve with $\bar{\Lambda} = 1.162$, $Q_2 = 14.9$, $n = 0.27$ and $H_0 = 69.41$ km s^{-1} Mpc^{-1} still remains within the error margins in Fig. 3.2.

As a result at this point it is worth noting that wavy deformations emerging as a result of the oscillating DE density during the late time expansion of the Universe brings forth a rather effective way to reconcile various data sets that are otherwise difficult to do so within the framework of the standard model and other competing models.

Moreover, if we take a closer look at the time-evolution of the DE energy density in Fig. 3.3, we notice that the parameter combinations under investigation give rise to negative DE densities beyond a certain redshift into the past. This is one of the outcomes of the unique behaviors of the special cosine integral function $\mathrm{Ci}[Q_2/(1+z)]$ present in $f_{\mathrm{DE}}(z)$. As $z \to \infty$, $\mathrm{Si}[Q_2/(1+z)] \to 0$ and $\mathrm{Ci}[Q_2/(1+z)] \to -\infty$ so $\rho_{\mathrm{DE}}(z)$ decreases indefinitely and monotonically, eventually becoming negative. In order to see this more clearly, recall that for small arguments $\mathrm{Ci}[Q_2/(1+z)]$ can be approximated by the convergent series expansions (3.11) and (3.12). Then the DE density $\rho_{\mathrm{DE}}(z)$ can be written in terms of the series,

$$\begin{aligned}\rho_{\mathrm{DE}}(z) = \rho_{\mathrm{DE},0}\Bigg(\bar{\Lambda} + \bar{\xi}_1\Bigg[\left(\frac{Q_2}{1+z}\right) - \frac{1}{3!\cdot 3}\left(\frac{Q_2}{1+z}\right)^3 \\ + \frac{1}{5!\cdot 5}\left(\frac{Q_2}{1+z}\right)^5 - \frac{1}{7!\cdot 7}\left(\frac{Q_2}{1+z}\right)^7 \pm \cdots\Bigg] \\ + \bar{\xi}_1\left[\gamma + \ln\left(\frac{Q_2}{1+z}\right) + \frac{1}{2!\cdot 2}\left(\frac{Q_2}{1+z}\right)^2 + \frac{1}{4!\cdot 4}\left(\frac{Q_2}{1+z}\right)^4 \mp \cdots\right]\Bigg).\end{aligned} \tag{3.32}$$

In the sufficiently remote past, that is $Q_2/(1+z) \ll 1$, we can employ the small argument approximation and omit the terms greater than the linear order to get,

$$\rho_{\mathrm{DE}}(z) \approx \rho_{\mathrm{DE},0}\left(\bar{\Lambda} + \bar{\xi}_1\left(\frac{Q_2}{1+z}\right) + \bar{\xi}_2\left[\gamma + \ln\left(\frac{Q_2}{1+z}\right)\right]\right). \tag{3.33}$$

With the increasing redshift, the terms $\bar{\Lambda}$ and $\bar{\xi}_1[Q_2/(1+z]$ in Equation (3.33) are dynamically screened by the logarithmic term carrying over from $\mathrm{Ci}[Q_2/(1+z)]$ so long as $\bar{\xi}_2 > 0$ and $\rho_{\mathrm{DE},0} > 0$ and the DE density $\rho_{\mathrm{DE}}(z)$ attains negative values at some critical redshift z_c. Reversing the history, $\rho_{\mathrm{DE}}(z)$ starts out as negative $\rho_{\mathrm{DE}}(z) < 0$ before the critical redshift $z > z_c$, and changes its sign at $\rho_{\mathrm{DE}}(z = z_c) = 0$ to positive $\rho_{\mathrm{DE}}(z) > 0$ when $z < z_c$. The critical redshift z_c can be calculated by,

$$\bar{\Lambda} + \bar{\xi}_1 \mathrm{Si}\left(\frac{Q_2}{1+z_c}\right) + \bar{\xi}_2 \mathrm{Ci}\left(\frac{Q_2}{1+z_c}\right) = 0. \tag{3.34}$$

Equation (3.34) cannot be solved analytically because of the implicit special integral functions. So the redshift at which this sign-flip takes place can be found by solving for z_c numerically, for which with the parameters we got we obtain $z_{c,\mathrm{green}} = 36.6$ ($\bar{\Lambda} = 0.777$, $Q_2 = 13.8$, $n = 0.88$), $z_{c,\mathrm{red}} = 37.15$ ($\bar{\Lambda} = 1.1437$, $Q_2 = 14.5$, $n = 0.14$) and $z_{c,\mathrm{yellow}} = 46.02$ ($\bar{\Lambda} = 1.1162$, $Q_2 = 14.9$, $n = 0.27$) as can also be noticed from Fig. 3.3.

These redshift values are too high in contrast to the gDE sign switching redshift $z \sim 2.32$ [56] and to the range $1.6 \lesssim z \lesssim 3.5$ in which the possible negative DE density is favored/implied by the BAO data [54, 55]. Although when this crossing occurs in

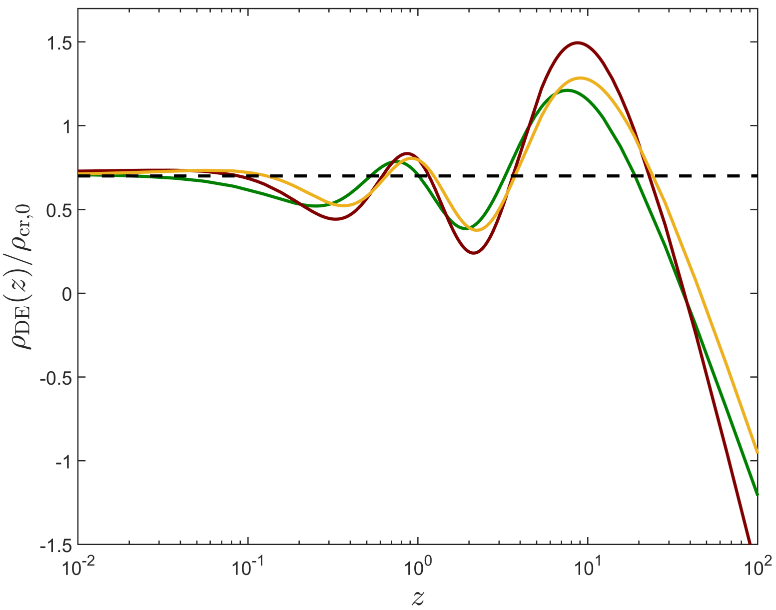

Figure 3.3 : The dashed line intersects the vertical axis at 0.7. In the limit of $z \to \infty$, $\mathrm{Si}[Q_2/(1+z)] \to 0$ and $\mathrm{Ci}[Q_2/(1+z)] \to -\infty$. $\bar{\xi}_2 > 0$ the for all cases, hence $\rho_{\rm DE}(z) \to -\infty$ as $z \to \infty$, yet $\Omega_{\rm DE} \to 0$. There are also some combinations of the parameters giving non-negative energy densities, that is when $\bar{\xi}_2 < 0$.

Fig. 3.3 hinges on all of the model parameters, principally it has to do with the behavior of the cosine integral $\mathrm{Ci}(x)$. The higher the values of Q_2, the larger the crossing redshift gets. For instance, take $Q_2 = 10$ and $Q_2 = 15$. Because $\mathrm{Ci}(x \approx 0.6165) = 0$ we have $[10/(1+z_{\rm c})] \approx 0.6165$ and $[15/(1+z_{\rm c})] \approx 0.6165$, which gives $z_{\rm c} \sim 15.2$ and $z_{\rm c} \sim 23.3$ respectively. It means that $z_{\rm c}$ receives a push to higher redshift values from the increase in Q_2. Accordingly, notice the positive correlation between Q_2 and $z_{\rm c}$ for the green, red, and yellow curves in Fig. 3.3. The higher the frequency of oscillations, the earlier the DE density switches its sign. On the other hand, it is conceivable that there might be unexplored regions of the parameter space where the amplitude of wiggles in DE allows for the alleged negativity in the DE density at $z \sim 1.6$ and beyond especially considering the dip coinciding with the aforementioned range in Fig. 3.4.

Regardless, it is worthwhile to dwell on the fact that for the current choice of parameters a spontaneous sign-switching behavior of the DE density phenomenologically emerges, which is a familiar concept from the the gDE except that it lacked wiggles required by the Galaxy BAO data [56, 112]. Then in a sense, simply assigning a sinusoidal function of the scale factor a to the inertial mass density of the usual vacuum energy of QFT can be said to "complete" the gDE or $\Lambda_{\rm s}$CDM models by introducing

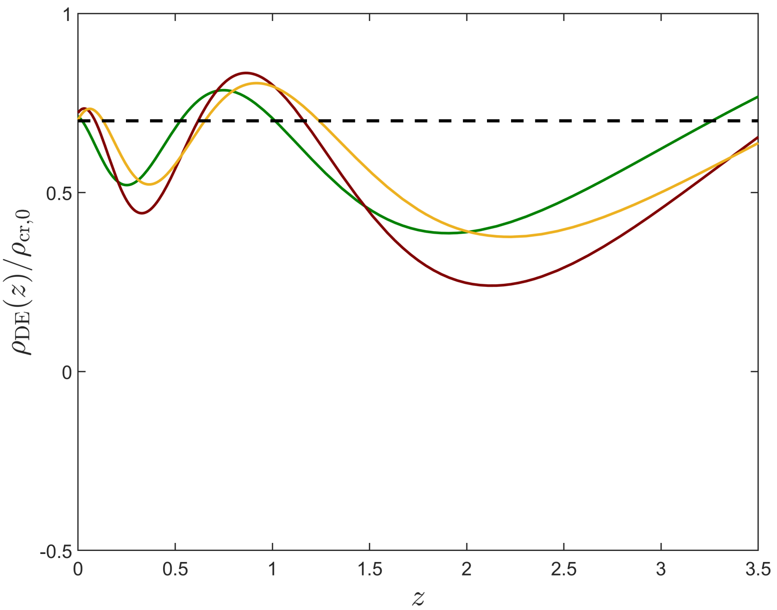

Figure 3.4 : The DE density $\rho_{\rm DE}(z)$ normalized by the present-day critical density vs z but this time plotted in linear at small redshifts. Again the dashed line intersects the vertical axis at 0.7.

wiggles that fit much better with the Galaxy BAO on top of the sign-switch conjecture, fortunately living up to our initial expectations.

Moreover, oscillations (see Fig. 3.3) in $\rho_{\rm DE}(z)$ begin at redshifts smaller than the critical redshift $z < z_{\rm c}$ but keeps on with ever-decaying amplitudes and ever-increasing frequencies and then settles into $\Omega_{\rm DE}(z \to -1) \approx 0.64$ passing through $\Omega_{\rm DE,0} \approx 0.70$ today, which is in fact what we call the damped oscillation. In this regard, the scalar field interpretation of the effective DE density appears to be tantilizing to consider as a mechanism similar to the Hubble friction effect $3H\dot{\phi} \propto \sqrt{\rho_{\rm m}(z) + \rho_{\rm DE}(z)}$ might be lying beneath the apparent damping. Though this scenario cannot be implemented by single-field models since the dark energy EoS parameter passes well below the phantom divide line $w_{\rm DE}(z) = -1$ during its evolution a couple of times as seen in Fig. 3.5.

Notice also that unlike the gDE or $\Lambda_{\rm s}$CDM models, the oscillatory $\rho_{\rm DE}(z)$ is unbounded from below as the term $\mathrm{Ci}[Q_2/(1+z)] \to -\infty$; however, it turns out that it grows in negative values much more slowly than dust and radiation energy densities grow in positive values so it does not pose a problem for the early universe. On the contrary, the presence of a negative energy source in the early universe might be a necessity at the perturbative level such that it hastens the formation of LSS. This can be shown as long as we keep our faith in the Newtonian treatment, which is a very good approximation of classical GR [133]. So the evolution of perturbations is governed by the linear density constrast equation,

$$\ddot{\delta}_{\rm m} + 2H\dot{\delta}_{\rm m} - 4\pi G\bar{\rho}_{\rm m}\delta_{\rm m} = 0 \tag{3.35}$$

where $\delta_{\rm m}$ is the matter density contrast defined as $\delta_{\rm m} = \delta\rho_{\rm m}/\bar{\rho}_{\rm m}$. Because $3H^2 \propto \sum_i \rho_i$, a negative valued DE density causes a reduction in the total energy, hence a repressed friction term $2H(t)\dot{\delta}_m$, amplifying the rate at which matter overdensities grow [8]. Interestingly enough, one of the recent observations made by the famous James Webb Space Telescope (JWST) unraveled that first galaxies formed at the dawn of the Universe were more clustered and massive than expected within the context of the ΛCDM, which lends partial support to the argument above [154–156].

One of the other key features of our oscillating dark energy model is the inertial mass density of the vacuum energy is parametrized in such a manner that on average it is identical to the usual cosmological constant/vacuum energy. This can be validated by calculating the average values of some main cosmological functions such as the Hubble parameter $\langle H_{\rm DE}(z)\rangle \approx H_{\Lambda\rm CDM}(z)$ for $0 < z < z_*$. Take for instance the EoS parameter. Despite its complicated appearance,

$$w_{\rm DE}(a) = -1 - \frac{\bar{\xi}_1\sin(Q_2 a) + \bar{\xi}_2\cos(Q_2 a)}{3[\bar{\Lambda} + \bar{\xi}_1{\rm Si}(Q_2 a) + \bar{\xi}_2{\rm Ci}(Q_2 a)]}, \tag{3.36}$$

expectedly, we see in Fig. 3.5 that the dark energy EoS parameters indeed oscillate around the pivot EoS $w_\Lambda = -1$ point of the cosmological constant Λ with the cycles spreaded along much of the history of the Universe. If the amplitude of oscillations is big enough, it is even possible for the oscillating DE to mimic dust with $w = 0$ in relatively short scale factor intervals for example at $0.65 \lesssim a \lesssim 0.69$ for the red curve in Fig. 3.5. However, when averaged over adequately long period of time, the dark energy EoS is given by the cosmological constant EoS $\langle w_{\rm DE}(a)\rangle \approx w_\Lambda = -1$ or put it another way on average what we have at hand is actually nothing but the same usual vacuum energy $\langle \varrho_{\rm DE}\rangle \approx 0$. In this sense, the act of averaging can be said to smooth out the wiggly, up-and-down but highly non-trivial details to that of the immutable Λ.

That being said, all the three cases possess poles at the scale factor values $a_{\rm green} = 0.0265$, $a_{\rm red} = 0.0262$ and $a_{\rm yellow} = 0.0212$ for which the effective DE density vanishes or equivalently its sign flips. One however should not immediately be alarmed by the existence of poles since the $\rho_{\rm DE}$(a) and its corresponding EoS $w_{\rm DE}(a)$ are effective as we just mentioned. Such a singular behavior is ubiquitous also in other models in the literature [8, 56, 57, 157, 158].

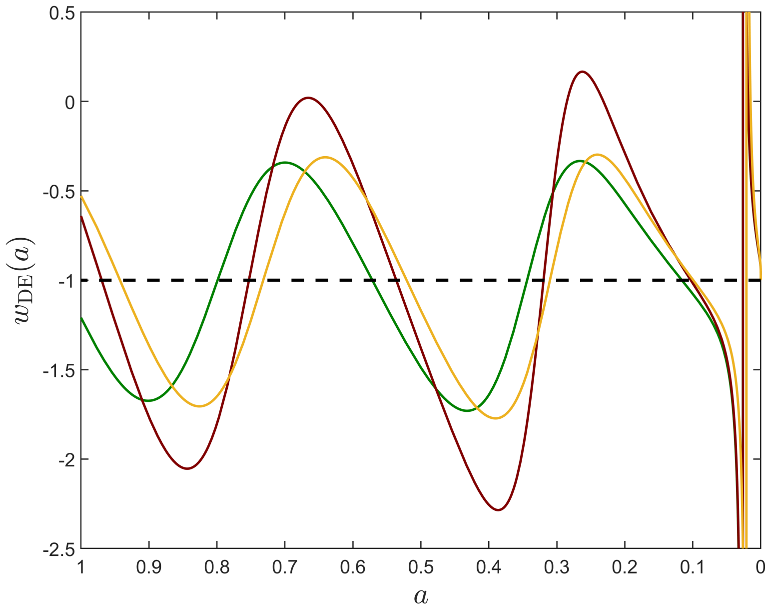

Figure 3.5 : The evolution of the dark energy EoS $w_{\rm DE}$ with the scale factor a. The curves complete about two cycles in almost the entire history of the universe and quickly converge to $w = -1$ after the pole and behave like the Λ for $a \sim 0$.

What is more, plotting the EoS parameter in the redshift space around the late-Universe gives us the chance to compare them with the model-independently reconstructed redshift evolution of dynamical dark energy EoS based on the latest observations [76, 77]. It is quite striking that the EoS parameter $w_{\rm DE}(z)$ curves in Fig. 3.6, especially the yellow one, resulted from our preliminary investigation, demonstrate a very similar pattern to that of the reconstructed one in Ref. [76] in Fig. 3.7 obtained from the observational data. The dips and bumps overlap roughly for $0.2 \lesssim z \lesssim 2$. To detail, the curve constructed from the data oscillates, albeit a little bit displaced or phase-shifted to larger redshifts with a varying amplitude, about $w = -1$ just like the case for the yellow curve in Fig. 3.6. It favors a dip for $0.2 \lesssim z \lesssim 0.5$ and very distinctive bump $0.5 \lesssim z \lesssim 1$ followed by a clear preference for the phantom region beyond $z \sim 1.2$ Whereas for larger redshifts $z > 2$, where the error in the measurement is possibly greater, the coherence between the two curves disappears.

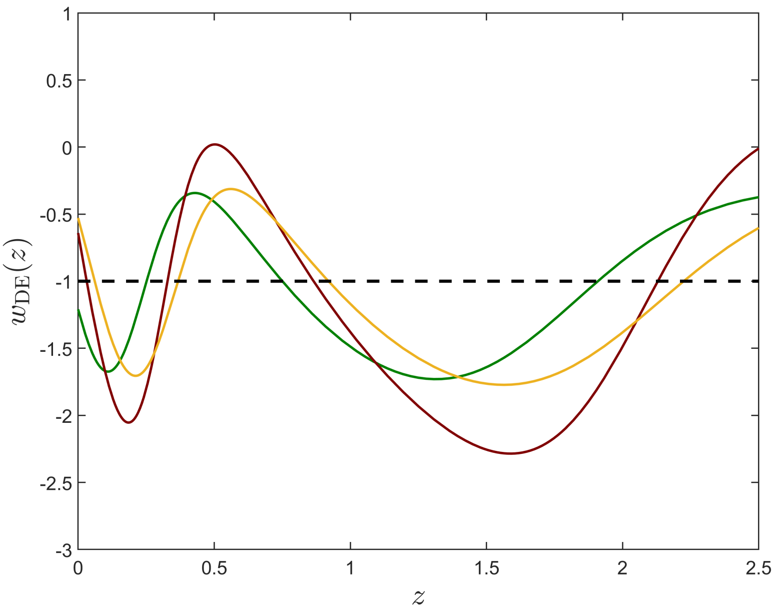

Figure 3.6 : $w_{\rm DE}(z)$ vs z plotted between $z = 0 - 2.5$ for comparison with the reconstructed DE EoS parameter.

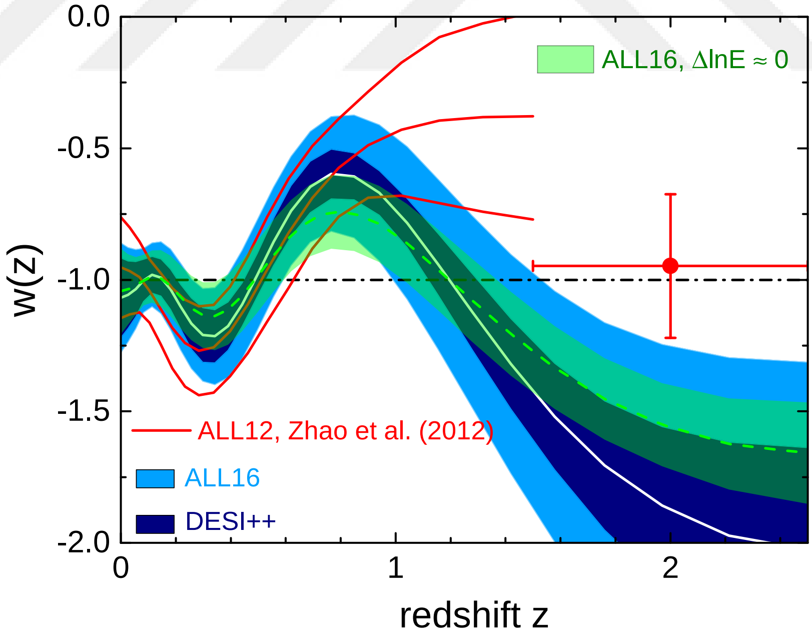

Figure 3.7 : The reconstructed dark energy EoS $w_{\rm DE}(z)$ based on the CMB, SNIa, and BAO data. Light blue band (ALL16) is the 68% confidence level region favored by the data. The dark blue band (DESI++) within ALL16 represents the forecasted 68% CL uncertainty from DESI++ The red error bars with 68% CL is $w(z)$ preferred by the ALL12 reconstruction at $z = 2$. (The fig. is retrieved from Ref. [76].)

We proceed with computing another commonly used function that will assist us in comparing our model against the data. The deceleration parameter $q(z)$ is a measure of whether or not the Universe is in a state of accelerated expansion. To calculate it we use its definition $q \equiv -\ddot{a}a/\dot{a}^2$. Nonetheless, our expansion dynamics is quite difficult to analyze in terms of the cosmic time t.

So it is possible to change variables through the following transformation

$$H(z) = -\frac{1}{(1+z)}\frac{\mathrm{d}z}{\mathrm{d}t} \tag{3.37}$$

and re-express $q(t)$ in terms of the redshift z as

$$q(z) = -1 + (1+z)\frac{H'(z)}{H(z)}, \tag{3.38}$$

where the prime $'$ denotes differentiation with respect to the redshift z. Then plugging in the Hubble functional of our model we obtain it in a slightly more complicated form,

$$q(z) = -1 + \frac{3\,\omega_{\mathrm{m}}(1+z)^3 + 4\,\omega_{\mathrm{r}}(1+z)^4 + (h^2 - \omega_{\mathrm{m}} - \omega_{\mathrm{r}})(1+z)f'_{\mathrm{DE}}(z)}{2\left[\omega_{\mathrm{m}}(1+z)^3 + \omega_{\mathrm{r}}(1+z)^4 + (h^2 - \omega_{\mathrm{m}} - \omega_{\mathrm{r}})f_{\mathrm{DE}}(z)\right]} \tag{3.39}$$

with $f'_{\mathrm{DE}}(z)$ being

$$f'_{\mathrm{DE}}(z) = -\frac{1}{(1+z)}\left[\bar{\xi}_1 \sin\left(\frac{Q_2}{1+z}\right) + \bar{\xi}_2 \cos\left(\frac{Q_2}{1+z}\right)\right]. \tag{3.40}$$

Fig. 3.8 shows that the inherited oscillations in $q(z)$ exhibit similar bumps and dips around the best fit ΛCDM value as was the case with other functions. Superimposing Fig. 3.8 and the evidence-weighted reconstruction of $q(z)$ in Fig. 3.9 retrieved from Ref. [77], we likewise notice a similar wiggly pattern oscillating about the ΛCDM in both.

In the left panel (C), the dip with $q(z) > 0$ for $1 \lesssim z \lesssim 1.5$, the successive bump with $q(z) > 0$ for $0.35 \lesssim z \lesssim 0.70$ and another dip with $q(z) < 0$ for $0.20 \lesssim z \lesssim 0.35$ coincides quite well with the prediction of the model. On the other hand, the data pefer a larger bump for $z \sim 0.1$, which is not included in the plot. The larger bump appears to be displaced a bit into the future $z < 0$.

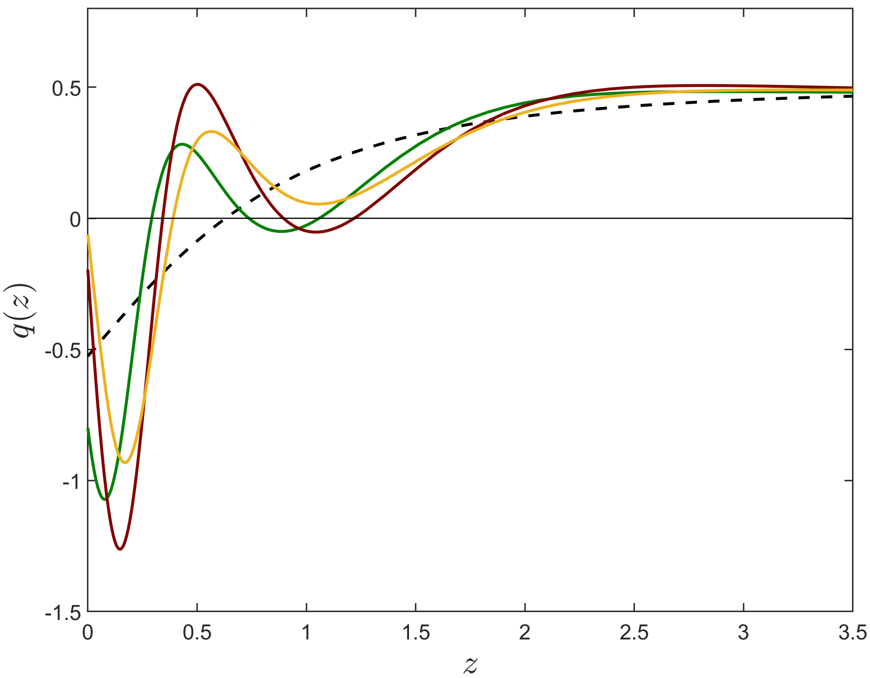

Figure 3.8 : $q(z)$ vs z. For comparison see the Fig. 3.9.

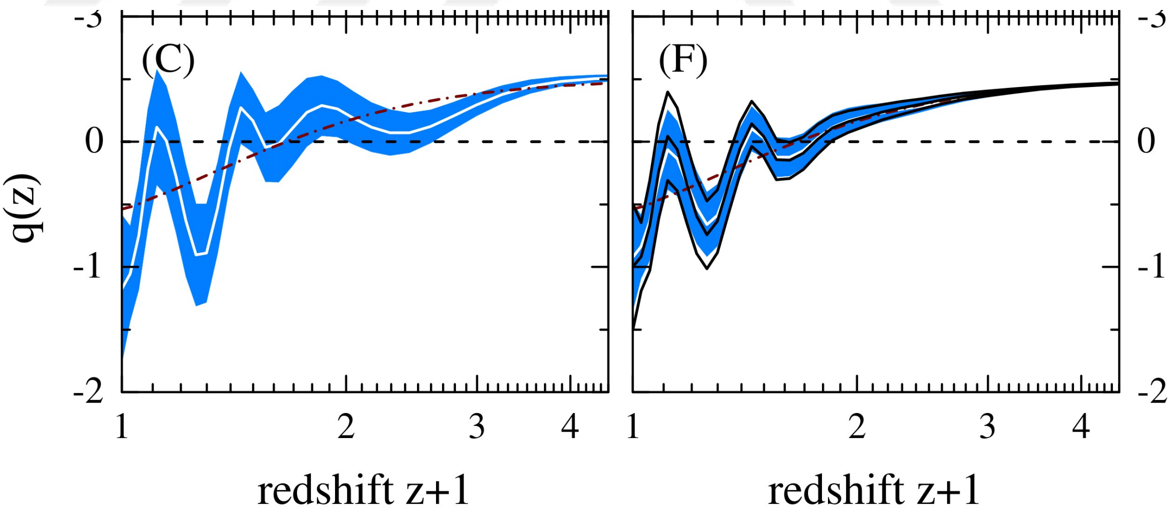

Figure 3.9 : The reconstructed deceleration parameter $q(z)$ vs z. The blue bands show the best fit with 68% CL uncertainty in both panels. On the left panel the reconstruction is performed for a range of variation of X in each bin set by $\Delta_X = 4$ where $X_i = X(a_i)$, $i = 1, \ldots, N$, is the binned evolution function given by $X(a) \equiv \rho_{\rm DE}^{\rm eff}(a)/\rho_{\rm DE,0}^{\rm eff}$. On the right panel, generated with $\Delta_X = 0.09$ (black solid curve) and the evidence-weighted reconstruction. The figure is retrieved from [77].

Lastly, we see that although on average the oscillating DE is the same as the usual cosmological constant/vacuum energy of the ΛCDM model, i.e., $\langle q(z)\rangle \approx q_{\Lambda\mathrm{CDM}}(z)$ as expected, it suggests something dramatically different. In the ΛCDM model, when the cosmological constant dominates the material content, the Universe embarks on an accelerated expansion and gradually evolves to the de-Sitter phase with the Hubble parameter converging to a constant. This implies that as the vacuum energy density ρ_Λ associated with the Λ does not get diluted away by the expansion unlike any other source, the Universe eventually enters an ever-accelerating stage. Whereas in the case where the vacuum energy of the standard model is replaced by the oscillating DE, the Universe swings back and forth between consecutive periods of acceleration and deceleration forever in the DE dominated epoch because the Fig. 3.5 shows for the the red curve that the dark energy EoS periodically passes above and below $-1/3$. In an alternative case (the green curve for example), the Universe may undergo a couple of cycles of deceleration and acceleration before shifting into an ever-accelerating stage. This then provokes the idea that currently observed acceleration might be merely one of the many others that could happen during the long history and future of the Universe thus there is nothing special about today. However, on the other hand note that it does not completely resolve the coincidence problem. As the model tracks the ΛCDM on average, why the present day densities of matter and DE are comparable still remains a mystery just as in the standard model.

3.3 Consistency With the Inevitable Manifestation of Wiggles

In the 2nd chapter, we have outlined why the deformations $\psi(z)$ imposed on the Hubble radius of a universe consistent with the early and late-time description of the ΛCDM cannot be of the arbitrary kind but be of the wiggly kind coming in the form of wavelets [105]. It meant that their integrals over the boundaries $[0, z_*]$ must vanish to fulfil the admissibility condition [130, 131],

$$\Psi(z_*) \equiv \int_0^{z_*} \psi(z)\mathrm{d}z = 0. \tag{3.41}$$

Besides, we remind that these wavelets in the late Universe could be attributed to various origins such as the dark energy density. That is to say, periodic or not, an oscillation in the DE density passing on to the Hubble radius of the model under consideration in actual qualifies to describe the required wiggly behavior, provided the so-called conditions are satisfied. Then coupled with the fact that our method of parameter estimation in the 3rd chapter involved fixing the comoving angular diameter distance $D_M(z_*)$ to last scattering surface to that of the ΛCDM, oscillations displayed for $z < z_\mathrm{c}$ by the DE density $\rho_\mathrm{DE}(z)$ that is resulted from our choice of updating the null inertial mass density of the usual vacuum to a sinusoidal function are anticipated to be in accordance with the inevitable manifestation of wiggles in the late Universe. We can verify this assertion numerically for our deformations $\psi_i(z)$. If the Hubble radii for each case are given by,

$$\frac{1}{H_{\mathrm{DE},i}(z)} = \frac{1}{\sqrt{\Omega_{\mathrm{m},0}(1+z)^3 + \Omega_{\mathrm{r},0}(1+z)^4 + \Omega_{\mathrm{DE},0} f_{\mathrm{DE},i}(z)}} \tag{3.42}$$

where $f_{\mathrm{DE},i}(z)$ gives the DE dynamics for i = green, red, yellow curves in Fig. 3.1,

$$f_{\mathrm{DE},i}(z) = \left[\bar{\Lambda}_i + \bar{\xi}_{1,i}\mathrm{Si}\left(\frac{Q_{2,i}}{1+z}\right) + \bar{\xi}_{2,i}\mathrm{Ci}\left(\frac{Q_{2,i}}{1+z}\right)\right] \tag{3.43}$$

then we can define,

$$\psi_i(z) = \frac{1}{H_{\mathrm{DE},i}(z)} - \frac{1}{H_{\Lambda\mathrm{CDM}}(z)}. \tag{3.44}$$

In chapter 2 we presented the exact or perfect version of the conditions and the theorem but in all honesty they are too stringent for our purposes, so in our physical calculations we demand that they approximately hold and expect that,

$$\Psi_i(z_*) \approx 0, \tag{3.45}$$

in particular,

$$\Psi_{\text{green}}(z_*) = \int_0^{z_*=1089.92} \psi_{\text{green}}(z)\mathrm{d}z = 4.9\times10^{-7}\ [\mathrm{km}^{-1}\,\mathrm{s}\,\mathrm{Mpc}], \tag{3.46}$$

$$\Psi_{\text{red}}(z_*) = \int_0^{z_*=1089.92} \psi_{\text{red}}(z)\mathrm{d}z = -2.6\times10^{-7}\ [\mathrm{km}^{-1}\,\mathrm{s}\,\mathrm{Mpc}], \tag{3.47}$$

$$\Psi_{\text{yellow}}(z_*) = \int_0^{z_*=1089.92} \psi_{\text{yellow}}(z)\mathrm{d}z = -5.5\times10^{-7}\ [\mathrm{km}^{-1}\,\mathrm{s}\,\mathrm{Mpc}]. \tag{3.48}$$

And, as expected, all $\Psi(z_*)$'s are very close to zero, i.e., $\Psi_i(z_*) \sim \mathcal{O}(10^{-7})$ $[\mathrm{km}^{-1}\,\mathrm{s}\,\mathrm{Mpc}]$, validating Equation (3.45). They deviate from the ΛCDM's Hubble radius 4.63×10^{-2} $[\mathrm{km}^{-1}\,\mathrm{s}\,\mathrm{Mpc}]$ by a few parts in a hundred thousand, or equivalently from the ΛCDM's corresponding $D_M(z_*) = 13872.83 \pm 25.31$ Mpc (Planck 2018) [5] by $c\Psi_{\text{yellow}}(z_*) = 0.0165$ Mpc, which is vanishingly small, that is in line with Equation (2.15) such that,

$$\int_0^{z_*=1089.92} \frac{\mathrm{d}z}{H_{\Lambda\mathrm{CDM}}(z)} \approx \int_0^{z_*=1089.92} \frac{\mathrm{d}z}{H_{\mathrm{DE},,i}(z)} \approx 4.63\times10^{-2}\ \mathrm{km}^{-1}\,\mathrm{s}\,\mathrm{Mpc}. \tag{3.49}$$

This numerical calculation clearly demonstrates that our parametrization indeed satisfies that admissibility condition (the 2nd condition) Equation (2.17) in fact almost exactly.

As for the other conditions, the 1st condition that $\psi_i(z > z_*) = 0$ was already implicitly dictated by fixing $D_M(z_*)$ to the ΛCDM's prediction. Even in the otherwise situation, around $z = z_*$, $\rho_{\mathrm{DE}}(z)$ is negligible so the model converges to the ΛCDM anyway; therefore, we expect the deformations due to the DE density to disappear as we go to the past. And to see whether or not the last condition (3rd one) $\psi_i(z=0) = 0$ is also met, we should first remind that if this condition is exactly satisfied, then addressing the Hubble tension is not possible since for $\psi_i(z=0) = 0$ to hold, we must have $H_{\mathrm{DE},0,i} = H_{\Lambda\mathrm{CDM},0}$ as can be seen from,

$$\psi_i(z=0) = \frac{1}{H_{0,i}} - \frac{1}{H_{\Lambda\mathrm{CDM},0}}. \tag{3.50}$$

For this reason, $1/H_0$ of a feasible model that promises to resolve the H_0 tension should slightly deviate from the one inferred assuming the ΛCDM. Taking $H_{\Lambda\mathrm{CDM},0} = 67.36\ \mathrm{km}\,\mathrm{s}^{-1}\,\mathrm{Mpc}^{-1}$ as well as $H_{0,\text{green}} = 70.57\ \mathrm{km}\,\mathrm{s}^{-1}\,\mathrm{Mpc}^{-1}$, $H_{0,\text{red}} = 71.78\ \mathrm{km}\,\mathrm{s}^{-1}\,\mathrm{Mpc}^{-1}$ and $H_{0,\text{yellow}} = 69.41\ \mathrm{km}\,\mathrm{s}^{-1}\,\mathrm{Mpc}^{-1}$ according to our preliminary investigation, doing the calculations yields

$$\psi_{\text{green}}(z=0) = -0.000693\ \mathrm{km}^{-1}\,\mathrm{s}\,\mathrm{Mpc}, \tag{3.51}$$

$$\psi_{\text{red}}(z=0) = -0.000932 \ \text{km}^{-1}\,\text{s}\,\text{Mpc}, \tag{3.52}$$

$$\psi_{\text{yellow}}(z=0) = -0.000456 \ \text{km}^{-1}\,\text{s}\,\text{Mpc}, \tag{3.53}$$

which are all small enough $\psi_i(z=0) \sim \mathcal{O}(10^{-4})\ \text{km}^{-1}\,\text{s}\,\text{Mpc}$ to satisfy the condition $\psi_i(z=0) \approx 0$ approximately but big enough to yield H_0 values in agreement with the $H_0 = 73.04 \pm 1.04\ \text{km}\,\text{s}^{-1}\,\text{Mpc}^{-1}$ of the SH0ES [36] and $H_0 = 69.8 \pm 0.8\ \text{km}\,\text{s}^{-1}\,\text{Mpc}^{-1}$ of the TRGB measurements [118]. We have thus shown that the numerical calculations above ascertains the legitimacy of our oscillating DE model as a late-time modification on top of the ΛCDM according to the criteria given in Ref. [105].

$$\psi(z) \propto \Delta\rho_{\text{DE}}(z) = \rho_{\text{DE},0}\left[\bar{\Lambda} + \bar{\xi}_1 \text{Si}\left(\frac{Q_2}{1+z}\right) + \bar{\xi}_2 \text{Ci}\left(\frac{Q_2}{1+z}\right)\right] - \rho_\Lambda \tag{3.54}$$

Finally, in Fig. 3.10, we see the evolution of deformations $\psi_i(z)$

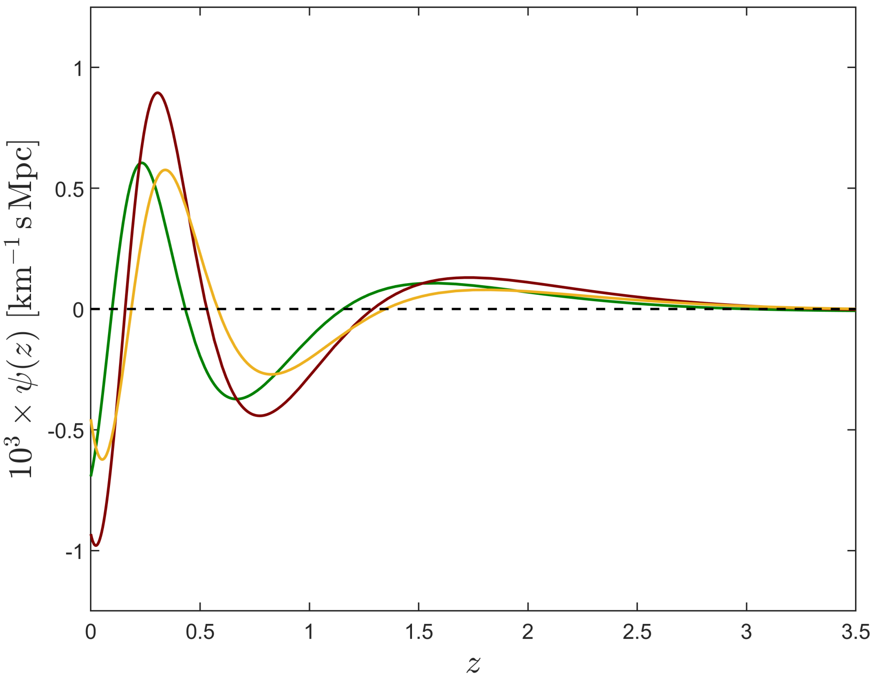

Figure 3.10 : $\psi(z) = 1/H(z) - 1/H_{\Lambda\text{CDM}}(z)$ vs z. Oscillations begin with small amplitudes and frequency then they grow over time. The distance from the dashed line represents departure from the ΛCDM. A visual demonstration that the areas below and above the dashed line roughly cancel eachother out. Accordingly, it can be said that ΛCDM is the averaged-out version of the oscillating DE.

pervading all the other functions with respect to the redshift z. It shows how much the model is off the ΛCDM, which is in fact given by the fractional deviation of the Hubble parameter in dimensionless quantities,

$$\delta(z) = \left(\frac{H_{\mathrm{DE},i} - H_{\Lambda\mathrm{CDM}}}{H_{\Lambda\mathrm{CDM}}} \right) \propto \psi(z). \tag{3.55}$$

The generic feature observed in these deviations is that, as the future unfolds, the frequency of the oscillatory deformations goes up, which is simply owing to the fact that we parametrized the argument of sin in terms of the scale factor. So $a \to \infty$ implies that the number of cycles in these functions tends towards infinity (recall our choice of parametrization in the Introduction). Nevertheless, on average they keep tracking the ΛCDM while imparting some non-trivial influences on the expansion and its related dynamics of the Universe. Therefore, substituting the Λ back for our dynamical DE gives the same evolution in a coarse-grained fashion and misses the little details that might be constituting rather non-trivial parts/reasons of/for today's significant tensions and problems prevailing in the standard cosmological model.

4. CONCLUSIONS

In this dissertation, we have first discussed the significant challenges the standard cosmological model has recently been facing [23–29, 31]. The major ones include the H_0 tension [32–35], Ly-α [54, 55] and Galaxy BAO tension [112, 114], growth tension (S_8) [122–127,155,159] and M_B tension [119–121] as well as the long-standing coincidence problem [90–93]. We have then made mention of several attempts aimed at tackling these discrepancies in and out of context of GR and elaborated some dynamical dark energy models and EoS parametrizations within GR [60–73,137–144]. One well-studied and unique example of this kind involves the parametrization of the inertial mass density ϱ being a very fundamental physical quantity with regard to the nature of matter [56–59]. In the case of dark energy, even the simplest deviations from the null inertial mass density of the usual vacuum energy lead to interesting cosmological consequences. We have presented in the light of observational analyses that as the simplest possible deviation, the simple-gDE model with negative constant inertial mass density, with or without the assistance of the spatial curvature, can not resolve the discrepancies [58]. However, once it is permitted to be minimally dynamical as in the gDE, then it begins displaying interesting properties that are promising and worthy of closer attention such as sign-switch of energy density [56]. It turns out that observational data very strongly and persistently favor a scenario in which the gDE energy density attains negative values in the past and turns positive recently around $z = 2.32$ to accelerate the expansion. When the gDE is taken to the limit where its parameter λ tends to arbitrarily large negative values, it gives rise to what is called the sign-switching cosmological constant, which leads to the Λ_sCDM model that is capable of alleviating numerous leading tensions simultaneously [57,59]. It yields an excellent fit to the Ly-α BAO data [54, 114, 115] thanks to its negative effective energy density in the past which in turn results in a boosted H_0 values today in remarkable consistency with the local H_0 measurements. Since the Λ_sCDM is essentially identical to the ΛCDM for $z < z_\dagger$, the amelioration of the H_0 tension can then be mapped into supernova absolute magnitude M_B via the luminosity-distance and can be utilized to mitigate the relevant M_B tension as well. The model also predicts smaller matter density $\Omega_{\mathrm{m},0}$ than the ΛCDM corresponding to a reduced S_8 in better agreement with the independent cosmological probes [128]. However, the data analyses indicate that all of these achievements of the Λ_{s}CDM are held back by the Galaxy BAO data which set the lower limit on the values switching-redshift $z_\dagger$ can assume [57, 59]. In other words, the Galaxy BAO dataset does not allow for small $z_\dagger$ that can realize greater enhancements in H_0 and the associated M_B tension for the model to be in accordance with the SH0ES measurements without getting into tension with the rest of the datasets. Accordingly, if a type of behavior that somehow conforms to the Galaxy BAO better can be incorporated into the picture on the top of Λ_{s}CDM and its sign-switch conjecture, there might appear more rooms for possible improvements in the fits with no compromise. This calls for a particular wiggly behavior in the expansion rate of the late-Universe, which is also underpinned by the inevitable manifestation of wiggles given in Chapter 3 [105].

In the hope of accomplishing this, we have then parametrized the inertial mass density of the QFT vacuum energy $\varrho_{\mathrm{DE}} = Q_1 \sin[Q_2(a-1)+\varphi]$ as a first order Fourier expansion, whereby we have made sure that the parametrization recovers the ΛCDM model on average, i.e., $\langle \varrho_{\mathrm{DE}} \rangle \approx \rho_\Lambda + p_\Lambda = 0$. The basic properties characterizing the oscillations in ϱ_{DE} hence ρ_{DE} are as usual the amplitude $\bar{\Lambda}$, frequency Q_2 and phase φ that come up as free parameters of the model. In the preliminary investigation of the parameters, we have fixed the pre-recombination physics of the model to that of the ΛCDM model by means of the acoustic angular scale $100\theta_* = 1.04110 \pm 0.00031$, physical matter $\omega_{\mathrm{m}} = 0.1430 \pm 0.0011$ and radiation $\omega_{\mathrm{r}} = 2.469\times10^{-5}(1+0.2271N_{\mathrm{eff}})$ densities [5] in order to establish a background-level consistency with the CMB data. We have observed that in parameter ranges $0.7 \lesssim \bar{\Lambda} \lesssim 1.3$, $13 \lesssim Q_2 \lesssim 15$ and for various phase values, it is possible to obtain fits in good agreement with the BAO Ly-α-Ly-α (correlation) data at $z_{\mathrm{eff}} = 2.34$, Ly-α-Quasar (cross-correlation) data at $z_{\mathrm{eff}} = 2.35$), Galaxy/BAO consensus at $z_{\mathrm{eff}} = 0.38, 0.51, 0.61$ [112,114,115], TRGB and SH0ES measurements of H_0 [36, 118] given in $H(z)/(1+z)$ and $c\ln(1+z)/D_M$ at the same time. Besides, when the combined parameter $\bar{\xi}_2 > 0$, the oscillating DE generates a similar sign-switch behavior prior to the beginning of oscillations to those of the simple-gDE and gDE as well as the Λ_sCDM except that in contrast to the gDE and Λ_sCDM, the energy density of the oscillating DE is unbounded from below and the sign-switching redshift z_c ($z_\dagger$ in the case of Λ_sCDM) is much greater $z_c > 36$ ($z_\dagger \sim 2.3$) due to the relatively high frequency $Q_2 \sim 14$ of the term $\mathrm{Ci}(Q_2 a)$. Though, conceivably, a negative-crossing energy density $\rho_{\rm DE}$ in the low redshift range $1.5 \lesssim z \lesssim 2.5$ might be actualized due possibly to an oscillation with increased amplitude, which would play nicely with the negative DE density suggestion of the BOSS DR11 findings in that range [54].

We have carried on with comparing the results of preliminary investigation with the model-independent reconstructions of the dark energy EoS parameter $w_{\rm DE}(z)$ and the deceleration parameter $q(z)$. We have figured out that the oscillating dark energy EoS and the reconstructed EoS (ALL16 and DESI++) [76] exhibit a very similar wiggly pattern and agree well for $0.2 < z < 2$. Likewise the prediction of the oscillating DE is in line with the reconstructed deceleration parameter [77] for $0.20 < z < 1.50$, albeit slightly worse than the EoS. One implication of the high-amplitude oscillations (as is the case with the red curve) in $q(z)$ is that the Universe suffers from an acceleration followed by deceleration periodically when the oscillating DE dominates, which arguably makes the question of “why now?” a trivial one.

In the last chapter, we have done a consistency-check in reference to the manifestation of wiggles. It has turned out that the smooth deformations $\psi_i(z)$ induced by the promotion of $\varrho_\Lambda = 0$ to $\varrho_{\rm DE} \propto \sin(a)$ on the Hubble radius $H^{-1}(z)$ of the ΛCDM cause deviations of few parts in hundred thousand from the ΛCDM’s comoving angular diameter distance $D_M(z_*)$ to last scattering surface, i.e., they have vanishing integral $\Psi(z_*) \approx 0$ over $[0, z_*]$, satisfying the so-called admissibility condition. This is practically consistent with wavelet description of the deviations from the ΛCDM’s Hubble radius such that they must be oscillatory not arbitrary, given the conditions $\psi_i(z > z_*) \approx 0$ and $\psi_i(z = 0) \approx 0$.

Ultimately, the sinusoidal parametrization of the inertial mass density of vacuum energy with respect to the scale factor seems to have promising implications that require further studies according to the results of the preliminary investigation done in this dissertation. It yields better fits to the Galaxy BAO [112] than the other inertial mass density parametrizations on top of the sign-switch phenomenon while simulatenously remaining in concert with other datasets [36, 114, 115, 118]. Therefore, it is quite possible that the oscillating DE will further improve the Λ_sCDM model, thanks to its novel wiggly behavior. Indeed a robust observational analysis is needed for a much better exploration of the parameter space and more conclusive resolutions to the existing tensions, which unfortunately we were unable to carry out for computationally demanding reasons (since it would take the computer to calculate a number of numerical integrations for every single prior value due to $\mathrm{Ci}(a)$ and $\mathrm{Si}(a)$ so as to implement the MC algorithm) before the completion of this dissertation. Our very next step will be to extend the scope of this work by performing observational data analysis.

REFERENCES

[1] **Riess, A.G.**, **Filippenko, A.V.**, **Challis, P.**, **Clocchiatti, A.**, **Diercks, A.**, **Garnavich, P.M.**, **Gilliland, R.L.**, **Hogan, C.J.**, **Jha, S.**, **Kirshner, R.P.** *et al.* (1998). Observational Evidence from Supernovae for an Accelerating Universe and a Cosmological Constant, *The Astronomical Journal*, *116*(3), 1009–1038, `http://dx.doi.org/10.1086/300499`.

[2] **Perlmutter, S.**, **Aldering, G.**, **Goldhaber, G.**, **Knop, R.A.**, **Nugent, P.**, **Castro, P.G.**, **Deustua, S.**, **Fabbro, S.**, **Goobar, A.** *et al.* (1999). Measurements of Ω and Λ from 42 High-Redshift Supernovae, *The Astrophysical Journal*, *517*(2), 565–586, `https://doi.org/10.1086%2F307221`.

[3] **Komatsu, E.**, **Dunkley, J.**, **Nolta, M.R.**, **Bennett, C.L.**, **Gold, B.**, **Hinshaw, G.**, **Jarosik, N.**, **Larson, D.**, **Limon, M.**, **Page, L.**, **Spergel, D.N.** *et al.* (2009). Five-Year Wilkinson Microwave Anisotropy Probe (WMAP) Observations: Cosmological Interpretation, *The Astrophysical Journal Supplement Series*, *180*(2), 330–376, `https://doi.org/10.1088%2F0067-0049%2F180%2F2%2F330`.

[4] **Ade, P.A.**, **Aghanim, N.**, **Arnaud, M.**, **Ashdown, M.**, **Aumont, J.**, **Baccigalupi, C.**, **Banday, A.**, **Barreiro, R.**, **Bartlett, J.**, **Bartolo, N.** *et al.* (2016). Planck 2015 results-xiii. cosmological parameters, *Astronomy & Astrophysics*, *594*, A13.

[5] **Aghanim, N.**, **Akrami, Y.**, **Ashdown, M.**, **Aumont, J.**, **Baccigalupi, C.**, **Ballardini, M.**, **Banday, A.J.**, **Barreiro, R.B.**, **Bartolo, N.**, **Basak, S.**, **Battye, R.** *et al.* (2020). Planck 2018 results. VI. Cosmological Parameters, *Astronomy & Astrophysics*, *641*, A6, `https://doi.org/10.1051%2F0004-6361%2F201833910`.

[6] **Tegmark, M.**, **Strauss, M.A.**, **Blanton, M.R.**, **Abazajian, K.**, **Dodelson, S.**, **Sandvik, H.**, **Wang, X.**, **Weinberg, D.H.**, **Zehavi, I.**, **Bahcall, N.A.** *et al.* (2004). Cosmological parameters from SDSS and WMAP, *Phys. Rev. D*, *69*, 103501, `https://link.aps.org/doi/10.1103/PhysRevD.69.103501`.

[7] **Eisenstein, D.J.**, **Zehavi, I.**, **Hogg, D.W.**, **Scoccimarro, R.**, **Blanton, M.R.**, **Nichol, R.C.**, **Scranton, R.**, **Seo, H.J.**, **Tegmark, M.** *et al.* (2005). Detection of the Baryon Acoustic Peak in the Large-Scale Correlation Function of SDSS Luminous Red Galaxies, *The Astrophysical Journal*, *633*(2), 560–574, `https://doi.org/10.1086%2F466512`.

[8] **Sahni, V., Shafieloo, A. and Starobinsky, A.A.** (2014). Model-Independent Evidence for Dark Energy Evolution from Baryon Acoustic Oscillations, *The Astrophysical Journal*, *793*(2), L40, `https://doi.org/10.1088%2F2041-8205%2F793%2F2%2Fl40`.

[9] **Aiola, S., Calabrese, E., Maurin, L., Naess, S., Schmitt, B.L., Abitbol, M.H., Addison, G.E., Ade, P.A.R., Alonso, D., Amiri, M., Amodeo, S., Angile, E., Austermann, J.E., Baildon, T., Battaglia, N., Beall, J.A., Bean, R.** *et al.* (2020). The Atacama Cosmology Telescope: DR4 maps and cosmological parameters, *Journal of Cosmology and Astroparticle Physics*, *2020*(12), 047–047, `https://doi.org/10.1088%2F1475-7516%2F2020%2F12%2F047`.

[10] **Sahni, V. and Starobinsky, A.A.** (2000). The Case for a positive cosmological Lambda term, *Int. J. Mod. Phys. D*, *9*, 373–444, `astro-ph/9904398`.

[11] **Carroll, S.M.** (2001). The Cosmological Constant, *Living Reviews in Relativity*, *4*(1), `https://doi.org/10.12942%2Flrr-2001-1`.

[12] **Copeland, E.J., Sami, M. and Tsujikawa, S.** (2006). Dynamics of Dark Energy, *International Journal of Modern Physics D*, *15*(11), 1753–1935, `https://doi.org/10.1142%2Fs021827180600942x`.

[13] **Peebles, P.J.E.** (1984). Tests of Cosmological Models Constrained by Inflation, *Astrophys. J.*, *284*, 439–444.

[14] **Peebles, P.J.E. and Ratra, B.** (2003). The cosmological constant and dark energy, *Reviews of Modern Physics*, *75*(2), 559–606, `https://doi.org/10.1103%2Frevmodphys.75.559`.

[15] **Dodelson, S. and Schmidt, F.** (2021). *Modern Cosmology*, Academic Press, second edition, `https://www.sciencedirect.com/science/article/pii/B9780128159484000061`.

[16] **Walker, T.P., Steigman, G., Schramm, D.N., Olive, K.A. and Kang, H.S.** (1991). Primordial Nucleosynthesis Redux, *APJ*, *376*, 51.

[17] **Olive, K.A., Steigman, G. and Walker, T.P.** (2000). Primordial nucleosynthesis: Theory and observations, *Phys. Rept.*, *333*, 389–407, `astro-ph/9905320`.

[18] **Steigman, G.** (2007). Primordial Nucleosynthesis in the Precision Cosmology Era, *Annual Review of Nuclear and Particle Science*, *57*(1), 463–491, `https://doi.org/10.1146%2Fannurev.nucl.56.080805.140437`.

[19] **Iocco, F., Mangano, G., Miele, G., Pisanti, O. and Serpico, P.D.** (2009). Primordial nucleosynthesis: From precision cosmology to fundamental physics, *Physics Reports*, *472*(1-6), 1–76, `https://doi.org/10.1016%2Fj.physrep.2009.02.002`.

[20] **Cyburt, R.H., Fields, B.D., Olive, K.A. and Yeh, T.H.** (2016). Big bang nucleosynthesis: Present status, *Rev. Mod. Phys.*, *88*, 015004, `https://link.aps.org/doi/10.1103/RevModPhys.88.015004`.

[21] **Pitrou, C., Coc, A., Uzan, J.P. and Vangioni, E.** (2018). Precision big bang nucleosynthesis with improved Helium-4 predictions, *Physics Reports*, *754*, 1–66, `https://doi.org/10.1016%2Fj.physrep.2018.04.005`.

[22] **Bernardeau, F., Colombi, S., Gaztañaga, E. and Scoccimarro, R.** (2002). Large-scale structure of the Universe and cosmological perturbation theory, *Physics Reports*, *367*(1-3), 1–248, `https://doi.org/10.1016%2Fs0370-1573%2802%2900135-7`.

[23] **Bull, P., Akrami, Y., Adamek, J., Baker, T., Bellini, E., Jiménez, J.B., Bentivegna, E., Camera, S., Clesse, S., Davis, J.H., Dio, E.D., Enander, J., Heavens, A.** *et al.* (2016). Beyond ΛCDM: Problems, solutions, and the road ahead, *Physics of the Dark Universe*, *12*, 56–99, `https://doi.org/10.1016%2Fj.dark.2016.02.001`.

[24] **Bullock, J.S. and Boylan-Kolchin, M.** (2017). Small-Scale Challenges to the ΛCDM Paradigm, *Annual Review of Astronomy and Astrophysics*, *55*(1), 343–387, `https://doi.org/10.1146%2Fannurev-astro-091916-055313`.

[25] **Di Valentino, E.** (2017). Crack in the cosmological paradigm, *Nature Astron.*, *1*(9), 569–570, `1709.04046`.

[26] **Valentino, E.D., Anchordoqui, L.A., Özgür Akarsu, Ali-Haimoud, Y., Amendola, L., Arendse, N., Asgari, M., Ballardini, M., Basilakos, S., Battistelli, E., Benetti, M., Birrer, S., Bouchet, F.R., Bruni, M., Calabrese, E.** *et al.* (2021). Snowmass2021 - Letter of interest cosmology intertwined I: Perspectives for the next decade, *Astroparticle Physics*, *131*, 102606, `https://doi.org/10.1016%2Fj.astropartphys.2021.102606`.

[27] **Valentino, E.D., Anchordoqui, L.A., Özgür Akarsu, Ali-Haimoud, Y., Amendola, L., Arendse, N., Asgari, M., Ballardini, M., Basilakos, S., Battistelli, E., Benetti, M., Birrer, S., Bouchet, F.R., Bruni, M., Calabrese, E.** *et al.* (2021). Snowmass2021 - Letter of interest cosmology intertwined II: The hubble constant tension, *Astroparticle Physics*, *131*, 102605, `https://doi.org/10.1016%2Fj.astropartphys.2021.102605`.

[28] **Valentino, E.D., Anchordoqui, L.A., Özgür Akarsu, Ali-Haimoud, Y., Amendola, L., Arendse, N., Asgari, M., Ballardini, M., Basilakos, S., Battistelli, E., Benetti, M., Birrer, S., Bouchet, F.R., Bruni, M.** *et al.* (2021). Cosmology intertwined III: $f\sigma_8$ and S_8, *Astroparticle Physics*, *131*, 102604, `https://doi.org/10.1016%2Fj.astropartphys.2021.102604`.

[29] **Valentino, E.D.**, **Anchordoqui, L.A.**, **Özgür Akarsu**, **Ali-Haimoud, Y.**, **Amendola, L.**, **Arendse, N.**, **Asgari, M.**, **Ballardini, M.**, **Basilakos, S.**, **Battistelli, E.**, **Benetti, M.**, **Birrer, S.**, **Bouchet, F.R.**, **Bruni, M.** *et al.* (2021). Snowmass2021 - Letter of interest cosmology intertwined IV: The age of the universe and its curvature, *Astroparticle Physics*, *131*, 102607, `https://doi.org/10.1016%2Fj.astropartphys.2021.102607`.

[30] **Abdalla, E.** *et al.* (2022). Cosmology intertwined: A review of the particle physics, astrophysics, and cosmology associated with the cosmological tensions and anomalies, *JHEAp*, *34*, 49–211, `2203.06142`.

[31] **Perivolaropoulos, L. and Skara, F.** (2022). Challenges for ΛCDM: An update, *New Astronomy Reviews*, *95*, 101659, `https://doi.org/10.1016%2Fj.newar.2022.101659`.

[32] **Freedman, W.L.** (2017). Cosmology at a Crossroads, *Nature Astron.*, *1*, 0121, `1706.02739`.

[33] **Wong, K.C.**, **Suyu, S.H.**, **Chen, G.C.F.**, **Rusu, C.E.**, **Millon, M.**, **Sluse, D.**, **Bonvin, V.**, **Fassnacht, C.D.** *et al.* (2019). H0LiCOW – XIII. A 2.4 per cent measurement of H0 from lensed quasars: 5.3σ tension between early- and late-Universe probes, *Monthly Notices of the Royal Astronomical Society*, *498*(1), 1420–1439, `https://doi.org/10.1093%2Fmnras%2Fstz3094`.

[34] **Riess, A.G.** (2019). The expansion of the Universe is faster than expected, *Nature Reviews Physics*, *2*(1), 10–12, `https://doi.org/10.1038%2Fs42254-019-0137-0`.

[35] **Valentino, E.D.**, **Mena, O.**, **Pan, S.**, **Visinelli, L.**, **Yang, W.**, **Melchiorri, A.**, **Mota, D.F.**, **Riess, A.G. and Silk, J.** (2021). In the realm of the Hubble tension—a review of solutions, *Classical and Quantum Gravity*, *38*(15), 153001, `https://doi.org/10.1088%2F1361-6382%2Fac086d`.

[36] **Riess, A.G.**, **Yuan, W.**, **Macri, L.M.**, **Scolnic, D.**, **Brout, D.**, **Casertano, S.**, **Jones, D.O.**, **Murakami, Y.**, **Anand, G.S.**, **Breuval, L.**, **Brink, T.G.** *et al.* (2022). A Comprehensive Measurement of the Local Value of the Hubble Constant with 1 km/s/Mpc Uncertainty from the Hubble Space Telescope and the SH0ES Team, *The Astrophysical Journal Letters*, *934*(1), L7, `https://doi.org/10.3847%2F2041-8213%2Fac5c5b`.

[37] **Riess, A.G.**, **Casertano, S.**, **Yuan, W.**, **Macri, L.**, **Bucciarelli, B.**, **Lattanzi, M.G.**, **MacKenty, J.W.**, **Bowers, J.B.**, **Zheng, W.**, **Filippenko, A.V.**, **Huang, C. and Anderson, R.I.** (2018). Milky Way Cepheid Standards for Measuring Cosmic Distances and Application to Gaia DR2: Implications for the Hubble Constant, *The Astrophysical Journal*, *861*(2), 126, `https://doi.org/10.3847%2F1538-4357%2Faac82e`.

[38] **Riess, A.G.**, **Casertano, S.**, **Yuan, W.**, **Macri, L.M. and Scolnic, D.** (2019). Large Magellanic Cloud Cepheid Standards Provide a 1% Foundation for the Determination of the Hubble Constant and Stronger Evidence for Physics beyond ΛCDM, *The Astrophysical Journal*, *876*(1), 85, https://doi.org/10.3847%2F1538-4357%2Fab1422.

[39] **Riess, A.G.**, **Casertano, S.**, **Yuan, W.**, **Bowers, J.B.**, **Macri, L.**, **Zinn, J.C. and Scolnic, D.** (2021). Cosmic Distances Calibrated to 1% Precision with Gaia EDR3 Parallaxes and Hubble Space Telescope Photometry of 75 Milky Way Cepheids Confirm Tension with ΛCDM, *The Astrophysical Journal Letters*, *908*(1), L6, https://doi.org/10.3847%2F2041-8213%2Fabdbaf.

[40] **Weinberg, S.** (1989). The cosmological constant problem, *Rev. Mod. Phys.*, *61*, 1–23, https://link.aps.org/doi/10.1103/RevModPhys.61.1.

[41] **Zlatev, I.**, **Wang, L. and Steinhardt, P.J.** (1999). Quintessence, Cosmic Coincidence, and the Cosmological Constant, *Phys. Rev. Lett.*, *82*, 896–899, https://link.aps.org/doi/10.1103/PhysRevLett.82.896.

[42] **Weinberg, S.** (2000). The Cosmological Constant Problems (Talk given at Dark Matter 2000, February, 2000), https://arxiv.org/abs/astro-ph/0005265.

[43] **Velten, H.E.S.**, **vom Marttens, R.F. and Zimdahl, W.** (2014). Aspects of the cosmological "coincidence problem", *The European Physical Journal C*, *74*(11), https://doi.org/10.1140%2Fepjc%2Fs10052-014-3160-4.

[44] **Nojiri, S. and Odintsov, S.D.** (2007). Introduction to Modified Gravity And Gravitational Alternative for Dark Energy, *International Journal of Geometric Methods in Modern Physics*, *04*(01), 115–145, https://doi.org/10.1142%2Fs0219887807001928.

[45] **Amendola, L. and Tsujikawa, S.** (2010). *Dark Energy: Theory and Observations*, Cambridge University Press.

[46] **Capozziello, S. and Laurentis, M.D.** (2011). Extended Theories of Gravity, *Physics Reports*, *509*(4-5), 167–321, https://doi.org/10.1016%2Fj.physrep.2011.09.003.

[47] **Ratra, B. and Peebles, P.J.E.** (1988). Cosmological consequences of a rolling homogeneous scalar field, *Phys. Rev. D*, *37*, 3406–3427, https://link.aps.org/doi/10.1103/PhysRevD.37.3406.

[48] **Caldwell, R.R.**, **Dave, R. and Steinhardt, P.J.** (1998). Cosmological Imprint of an Energy Component with General Equation of State, *Physical Review Letters*, *80*(8), 1582–1585, https://doi.org/10.1103%2Fphysrevlett.80.1582.

[49] **Vagnozzi, S.**, **Dhawan, S.**, **Gerbino, M.**, **Freese, K.**, **Goobar, A. and Mena, O.** (2018). Constraints on the sum of the neutrino masses in dynamical dark energy models with $w \geq -1$ are tighter than those obtained in ΛCDM, *Physical Review D*, *98*(8), `https://doi.org/10.1103%2Fphysrevd.98.083501`.

[50] **Valentino, E.D.**, **Ferreira, R.Z.**, **Visinelli, L. and Danielsson, U.** (2019). Late time transitions in the quintessence field and the H_0 tension, *Physics of the Dark Universe*, *26*, 100385, `https://doi.org/10.1016%2Fj.dark.2019.100385`.

[51] **Valentino, E.D.**, **Melchiorri, A. and Silk, J.** (2020). Cosmological constraints in extended parameter space from the Planck 2018 Legacy release, *Journal of Cosmology and Astroparticle Physics*, *2020*(01), 013–013, `https://doi.org/10.1088%2F1475-7516%2F2020%2F01%2F013`.

[52] **Banerjee, A.**, **Cai, H.**, **Heisenberg, L.**, **Colgáin, E.Ó .**, **Sheikh-Jabbari, M. and Yang, T.** (2021). Hubble sinks in the low-redshift swampland, *Physical Review D*, *103*(8), `https://doi.org/10.1103%2Fphysrevd.103.l081305`.

[53] **Vázquez, J.A.**, **Tamayo, D.**, **Sen, A.A. and Quiros, I.** (2021). Bayesian model selection on scalar ε-field dark energy, *Physical Review D*, *103*(4), `https://doi.org/10.1103%2Fphysrevd.103.043506`.

[54] **Delubac, T.**, **Bautista, J.E.**, **Busca, N.G.**, **Rich, J.**, **Kirkby, D.**, **Bailey, S.**, **Font-Ribera, A.**, **Slosar, A.**, **Lee, K.G.**, **Pieri, M.M.**, **Hamilton, J.C.**, **Aubourg, É.**, **Blomqvist, M.**, **Bovy, J.** *et al.* (2015). Baryon acoustic oscillations in the Lyα forest of BOSS DR11 quasars, *Astronomy & Astrophysics*, *574*, A59, `https://doi.org/10.1051%2F0004-6361%2F201423969`.

[55] **Aubourg, É .**, **Bailey, S.**, **Bautista, J.E.**, **Beutler, F.**, **Bhardwaj, V.**, **Bizyaev, D.**, **Blanton, M.**, **Blomqvist, M.**, **Bolton, A.S.**, **Bovy, J.**, **Brewington, H.**, **Brinkmann, J.**, **Brownstein, J.R.**, **Burden, A.**, **Busca, N.G.** *et al.* (2015). Cosmological implications of baryon acoustic oscillation measurements, *Physical Review D*, *92*(12), `https://doi.org/10.1103%2Fphysrevd.92.123516`.

[56] **Özgür Akarsu**, **Barrow, J.D.**, **Escamilla, L.A. and Vazquez, J.A.** (2020). Graduated dark energy: Observational hints of a spontaneous sign switch in the cosmological constant, *Physical Review D*, *101*(6), `https://doi.org/10.1103%2Fphysrevd.101.063528`.

[57] **Özgür Akarsu**, **Kumar, S.**, **Özülker, E. and Vazquez, J.A.** (2021). Relaxing cosmological tensions with a sign switching cosmological constant, *Physical Review D*, *104*(12), `https://doi.org/10.1103%2Fphysrevd.104.123512`.

[58] **Acquaviva, G.**, **Özgür Akarsu**, **Katırcı, N. and Vazquez, J.A.** (2021). Simple-graduated dark energy and spatial curvature, *Physical Review*

D, *104*(2), https://doi.org/10.1103%2Fphysrevd.104.023505.

[59] **Akarsu, O.**, **Kumar, S.**, **Ozulker, E.**, **Vazquez, J.A. and Yadav, A.** (2022). Relaxing cosmological tensions with a sign switching cosmological constant: Improved results with Planck, BAO and Pantheon data, https://arxiv.org/abs/2211.05742.

[60] **Johri, V.B.** (2004). Parametrization of Dark Energy Equation of State, https://arxiv.org/abs/astro-ph/0409161.

[61] **Linder, E.V. and Huterer, D.** (2005). How many dark energy parameters?, *Physical Review D*, *72*(4), https://doi.org/10.1103%2Fphysrevd.72.043509.

[62] **Liberato, L. and Rosenfeld, R.** (2006). Dark energy parametrizations and their effect on dark halos, *Journal of Cosmology and Astroparticle Physics*, *2006*(07), 009–009, https://doi.org/10.1088%2F1475-7516%2F2006%2F07%2F009.

[63] **Johri, V.B. and Rath, P.K.** (2006). Dynamical age of the universe as a constraint on the parametrization of the dark energy equation of state, *Physical Review D*, *74*(12), https://doi.org/10.1103%2Fphysrevd.74.123516.

[64] **Ichikawa, K. and Takahashi, T.** (2007). Dark energy parametrizations and the curvature of the universe, *Journal of Cosmology and Astroparticle Physics*, *2007*(02), 001–001, https://doi.org/10.1088%2F1475-7516%2F2007%2F02%2F001.

[65] **Usmani, A.A.**, **Ghosh, P.P.**, **Mukhopadhyay, U.**, **Ray, P.C. and Ray, S.** (2008). The dark energy equation of state, *Monthly Notices of the Royal Astronomical Society: Letters*, *386*(1), L92–L95, https://doi.org/10.1111%2Fj.1745-3933.2008.00468.x.

[66] **Liu, D.J.**, **Li, X.Z.**, **Hao, J. and Jin, X.H.** (2008). Revisiting the parametrization of equation of state of dark energy via SNIa data, *Monthly Notices of the Royal Astronomical Society*, *388*(1), 275–281, https://doi.org/10.1111%2Fj.1365-2966.2008.13380.x.

[67] **Linden, S. and Virey, J.M.** (2008). Test of the Chevallier-Polarski-Linder parametrization for rapid dark energy equation of state transitions, *Physical Review D*, *78*(2), https://doi.org/10.1103%2Fphysrevd.78.023526.

[68] **Barboza, E.M.**, **Alcaniz, J.S.**, **Zhu, Z.H. and Silva, R.** (2009). Generalized equation of state for dark energy, *Physical Review D*, *80*(4), https://doi.org/10.1103%2Fphysrevd.80.043521.

[69] **Ke, S.**, **Yong-Feng, H. and Tan, L.** (2011). The effects of parametrization of the dark energy equation of state, *Research in Astronomy and Astrophysics*, *11*(12), 1403, https://dx.doi.org/10.1088/1674-4527/11/12/003.

[70] **Tripathi, A.**, **Sangwan, A. and Jassal, H.** (2017). Dark energy equation of state parameter and its evolution at low redshift, *Journal of Cosmology and Astroparticle Physics*, *2017*(06), 012–012, `https://doi.org/10.1088%2F1475-7516%2F2017%2F06%2F012`.

[71] **Davari, Z.**, **Malekjani, M. and Artymowski, M.** (2018). New parametrization for unified dark matter and dark energy, *Physical Review D*, *97*(12), `https://doi.org/10.1103%2Fphysrevd.97.123525`.

[72] **Tamayo, D. and Vá zquez, J.A.** (2019). Fourier-series expansion of the dark-energy equation of state, *Monthly Notices of the Royal Astronomical Society*, *487*(1), 729–736, `https://doi.org/10.1093%2Fmnras%2Fstz1229`.

[73] **Pan, S.**, **Yang, W. and Paliathanasis, A.** (2020). Imprints of an extended Chevallier–Polarski–Linder parametrization on the large scale of our universe, *The European Physical Journal C*, *80*(3), `https://doi.org/10.1140%2Fepjc%2Fs10052-020-7832-y`.

[74] **Shafieloo, A.**, **Alam, U.**, **Sahni, V. and Starobinsky, A.A.** (2006). Smoothing supernova data to reconstruct the expansion history of the Universe and its age, *Monthly Notices of the Royal Astronomical Society*, *366*(3), 1081–1095, `https://doi.org/10.1111%2Fj.1365-2966.2005.09911.x`.

[75] **Mukherjee, A.** (2016). Acceleration of the universe: a reconstruction of the effective equation of state, *Monthly Notices of the Royal Astronomical Society*, *460*(1), 273–282, `https://doi.org/10.1093%2Fmnras%2Fstw964`.

[76] **Zhao, G.B.**, **Raveri, M.**, **Pogosian, L.**, **Wang, Y.**, **Crittenden, R.G.**, **Handley, W.J.**, **Percival, W.J.**, **Beutler, F.**, **Brinkmann, J.**, **Chuang, C.H.**, **Cuesta, A.J.**, **Eisenstein, D.J.** *et al.* (2017). Dynamical dark energy in light of the latest observations, *Nature Astronomy*, *1*(9), 627–632, `https://doi.org/10.1038%2Fs41550-017-0216-z`.

[77] **Wang, Y.**, **Pogosian, L.**, **Zhao, G.B. and Zucca, A.** (2018). Evolution of Dark Energy Reconstructed from the Latest Observations, *The Astrophysical Journal*, *869*(1), L8, `https://doi.org/10.3847%2F2041-8213%2Faaf238`.

[78] **Zhang, Y.C.**, **Zhang, H.Y.**, **Wang, D.D.**, **Qi, Y.H.**, **Wang, Y.T. and Zhao, G.B.** (2017). Probing dynamics of dark energy with latest observations, *Research in Astronomy and Astrophysics*, *17*(6), 050, `https://doi.org/10.1088%2F1674-4527%2F17%2F6%2F50`.

[79] **Chevallier, M. and Polarski, D.** (2001). Accelerating Universe with Scaling Dark Matter, *International Journal of Modern Physics D*, *10*(02), 213–223, `https://doi.org/10.1142%2Fs0218271801000822`.

[80] **Linder, E.V.** (2003). Exploring the Expansion History of the Universe, *Physical Review Letters*, *90*(9), `https://doi.org/10.1103%2Fphysrevlett.90.091301`.

[81] **Alestas, G. and Perivolaropoulos, L.** (2021). Late-time approaches to the Hubble tension deforming $H(z)$, worsen the growth tension, *Monthly Notices of the Royal Astronomical Society*, *504*(3), 3956–3962, `https://doi.org/10.1093%2Fmnras%2Fstab1070`.

[82] **Linder, E.V.** (2002). Probing dark energy with SNAP, *4th International Workshop on the Identification of Dark Matter*, pp.52–57, `astro-ph/0210217`.

[83] **Feng, C.J.**, **Shen, X.Y.**, **Li, P. and Li, X.Z.** (2012). A new class of parametrization for dark energy without divergence, *Journal of Cosmology and Astroparticle Physics*, *2012*(09), 023–023, `https://doi.org/10.1088%2F1475-7516%2F2012%2F09%2F023`.

[84] **Akarsu, O.**, **Dereli, T. and Vazquez, J.A.** (2015). A divergence-free parametrization for dynamical dark energy, *JCAP*, *06*, 049, `1501.07598`.

[85] **Mehrabi, A.** (2018). Growth of perturbations in dark energy parametrization scenarios, *Physical Review D*, *97*(8), `https://doi.org/10.1103%2Fphysrevd.97.083522`.

[86] **Bassett, B.A.**, **Corasaniti, P.S. and Kunz, M.** (2004). The Essence of Quintessence and the Cost of Compression, *The Astrophysical Journal*, *617*(1), L1–L4, `https://doi.org/10.1086%2F427023`.

[87] **Guo, Z.K.**, **Piao, Y.S.**, **Zhang, X. and Zhang, Y.Z.** (2005). Cosmological evolution of a quintom model of dark energy, *Physics Letters B*, *608*(3-4), 177–182, `https://doi.org/10.1016%2Fj.physletb.2005.01.017`.

[88] **Feng, B.**, **Li, M.**, **Piao, Y.S. and Zhang, X.** (2006). Oscillating quintom and the recurrent universe, *Physics Letters B*, *634*(2-3), 101–105, `https://doi.org/10.1016%2Fj.physletb.2006.01.066`.

[89] **Román-Garza, J.**, **Verdugo, T.**, **Magaña, J. and Motta, V.** (2019). Constraints on barotropic dark energy models by a new phenomenological q(z) parameterization, *The European Physical Journal C*, *79*(11), `https://doi.org/10.1140%2Fepjc%2Fs10052-019-7390-3`.

[90] **Dodelson, S.**, **Kaplinghat, M. and Stewart, E.** (2000). Solving the Coincidence Problem: Tracking Oscillating Energy, *Physical Review Letters*, *85*(25), 5276–5279, `https://doi.org/10.1103%2Fphysrevlett.85.5276`.

[91] **Linder, E.V.** (2006). On oscillating dark energy, *Astropart. Phys.*, *25*, 167–171, `astro-ph/0511415`.

[92] **Nojiri, S. and Odintsov, S.D.** (2006). The oscillating dark energy: future singularity and coincidence problem, *Physics Letters B*, *637*(3), 139–148, https://doi.org/10.1016%2Fj.physletb.2006.04.026.

[93] **Barenboim, G.**, **Requejo, O.M. and Quigg, C.** (2006). Observational constraints on undulant cosmologies, *Journal of Cosmology and Astroparticle Physics*, *2006*(04), 008–008, https://doi.org/10.1088%2F1475-7516%2F2006%2F04%2F008.

[94] **Frieman, J.A.**, **Hill, C.T.**, **Stebbins, A. and Waga, I.** (1995). Cosmology with Ultralight Pseudo Nambu-Goldstone Bosons, *Physical Review Letters*, *75*(11), 2077–2080, https://doi.org/10.1103%2Fphysrevlett.75.2077.

[95] **Abrahamse, A.**, **Albrecht, A.**, **Barnard, M. and Bozek, B.** (2008). Exploring parameter constraints on quintessential dark energy: The pseudo-Nambu-Goldstone-boson model, *Physical Review D*, *77*(10), https://doi.org/10.1103%2Fphysrevd.77.103503.

[96] **Cheon, K. and Lee, J.** (2021). N = 2 PNGB quintessence dark energy, *Journal of the Korean Physical Society*, *79*(3), 336–342, https://doi.org/10.1007%2Fs40042-021-00235-7.

[97] **Wang, Y. and Garnavich, P.M.** (2001). Measuring Time Dependence of Dark Energy Density from Type Ia Supernova Data, *The Astrophysical Journal*, *552*(2), 445–451, https://doi.org/10.1086%2F320552.

[98] **Maor, I.**, **Brustein, R.**, **McMahon, J. and Steinhardt, P.J.** (2002). Measuring the equation of state of the universe: Pitfalls and prospects, *Phys. Rev. D*, *65*, 123003, https://link.aps.org/doi/10.1103/PhysRevD.65.123003.

[99] **Mamon, A.**, **K.Bamba and S.Das** (2017). Constraints on reconstructed dark energy model from SN Ia and BAO/CMB observations, *Eur. Phys. J. C*, *77*(29).

[100] **Wang, D. and Meng, X.H.** (2017). No evidence for dynamical dark energy in two models, *Physical Review D*, *96*(10), https://doi.org/10.1103%2Fphysrevd.96.103516.

[101] **Mamon, A.A.** (2018). A new parametrization for dark energy density and future deceleration, *Modern Physics Letters A*, *33*(20), 1850113, https://doi.org/10.1142%2Fs0217732318501134.

[102] **Valentino, E.D.**, **Mukherjee, A. and Sen, A.A.** (2021). Dark Energy with Phantom Crossing and the H0 Tension, *Entropy*, *23*(4), 404, https://doi.org/10.3390%2Fe23040404.

[103] **Ellis, G.F.R. and van Elst, H.** (1999). Cosmological models: Cargese lectures 1998, *NATO Sci. Ser. C*, *541*, 1–116, gr-qc/9812046.

[104] **Ellis, G.F.R.**, **Maartens, R. and MacCallum, M.A.H.** (2012). *Relativistic Cosmology*, Cambridge University Press.

[105] **Akarsu, O.**, **Colgain, E.O.**, **Ozulker, E.**, **Thakur, S. and Yin, L.**, (2022), The inevitable manifestation of wiggles in the expansion of the late universe, `https://arxiv.org/abs/2207.10609`.

[106] **Alam, S.**, **Aubert, M.**, **Avila, S.**, **Balland, C.**, **Bautista, J.E.**, **Bershady, M.A.**, **Bizyaev, D.**, **Blanton, M.R.**, **Bolton, A.S.**, **Bovy, J.**, **Brinkmann, J.**, **Brownstein, J.R.**, **Burtin, E. and OTHERS** (2021). Completed SDSS-IV extended Baryon Oscillation Spectroscopic Survey: Cosmological implications from two decades of spectroscopic surveys at the Apache Point Observatory, *Physical Review D*, *103*(8), `https://doi.org/10.1103%2Fphysrevd.103.083533`.

[107] **Efstathiou, G. and Gratton, S.** (2020). The evidence for a spatially flat Universe, *Monthly Notices of the Royal Astronomical Society: Letters*, *496*(1), L91–L95, `https://doi.org/10.1093%2Fmnrasl%2Fslaa093`.

[108] **Vagnozzi, S.**, **Valentino, E.D.**, **Gariazzo, S.**, **Melchiorri, A.**, **Mena, O. and Silk, J.** (2021). The galaxy power spectrum take on spatial curvature and cosmic concordance, *Physics of the Dark Universe*, *33*, 100851, `https://doi.org/10.1016%2Fj.dark.2021.100851`.

[109] **Vagnozzi, S.**, **Loeb, A. and Moresco, M.** (2021). Eppur è piatto? The Cosmic Chronometers Take on Spatial Curvature and Cosmic Concordance, *The Astrophysical Journal*, *908*(1), 84, `https://doi.org/10.3847%2F1538-4357%2Fabd4df`.

[110] **Anderson, L.**, **Aubourg, É .**, **Bailey, S.**, **Beutler, F.**, **Bhardwaj, V.**, **Blanton, M.**, **Bolton, A.S.**, **Brinkmann, J.**, **Brownstein, J.R.**, **Burden, A.**, **Chuang, C.H.**, **Cuesta, A.J.**, **Dawson, K.S.**, **Eisenstein, D.J.** *et al.* (2014). The clustering of galaxies in the SDSS-III Baryon Oscillation Spectroscopic Survey: baryon acoustic oscillations in the Data Releases 10 and 11 Galaxy samples, *Monthly Notices of the Royal Astronomical Society*, *441*(1), 24–62, `https://doi.org/10.1093%2Fmnras%2Fstu523`.

[111] **Beutler, F.**, **Blake, C.**, **Colless, M.**, **Jones, D.H.**, **Staveley-Smith, L.**, **Campbell, L.**, **Parker, Q.**, **Saunders, W. and Watson, F.** (2011). The 6dF Galaxy Survey: baryon acoustic oscillations and the local Hubble constant, *Monthly Notices of the Royal Astronomical Society*, *416*(4), 3017–3032, `https://doi.org/10.1111%2Fj.1365-2966.2011.19250.x`.

[112] **Alam, S.**, **Ata, M.**, **Bailey, S.**, **Beutler, F.**, **Bizyaev, D.**, **Blazek, J.A.**, **Bolton, A.S.**, **Brownstein, J.R.**, **Burden, A.**, **Chuang, C.H.**, **Comparat, J.**, **Cuesta, A.J.**, **Dawson, K.S.**, **Eisenstein, D.J.** *et al.* (2017). The clustering of galaxies in the completed SDSS-III Baryon Oscillation Spectroscopic Survey: cosmological

analysis of the DR12 galaxy sample, *Monthly Notices of the Royal Astronomical Society*, *470*(3), 2617–2652, `https://doi.org/10.1093%2Fmnras%2Fstx721`.

[113] **Ata, M.**, **Baumgarten, F.**, **Bautista, J.**, **Beutler, F.**, **Bizyaev, D.**, **Blanton, M.R.**, **Blazek, J.A.**, **Bolton, A.S.**, **Brinkmann, J.**, **Brownstein, J.R.**, **Burtin, E.**, **Chuang, C.H.**, **Comparat, J.**, **Dawson, K.S.**, **de la Macorra, A.**, **Du, W.**, **du Mas des Bourboux, H.**, **Eisenstein, D.J.** *et al.* (2017). The clustering of the SDSS-IV extended Baryon Oscillation Spectroscopic Survey DR14 quasar sample: first measurement of baryon acoustic oscillations between redshift 0.8 and 2.2, *Monthly Notices of the Royal Astronomical Society*, *473*(4), 4773–4794, `https://doi.org/10.1093%2Fmnras%2Fstx2630`.

[114] **de Sainte Agathe, V.**, **Balland, C.**, **du Mas des Bourboux, H.**, **Busca, N.G.**, **Blomqvist, M.**, **Guy, J.**, **Rich, J.**, **Font-Ribera, A.**, **Pieri, M.M.**, **Bautista, J.E.** *et al.* (2019). Baryon acoustic oscillations at $z = 2.34$ from the correlations of Lyα absorption in eBOSS DR14, *Astronomy & Astrophysics*, *629*, A85, `https://doi.org/10.1051%2F0004-6361%2F201935638`.

[115] **Blomqvist, M.**, **du Mas des Bourboux, H.**, **Busca, N.G.**, **de Sainte Agathe, V.**, **Rich, J.**, **Balland, C.**, **Bautista, J.E.**, **Dawson, K.**, **Font-Ribera, A.**, **Guy, J.**, **Goff, J.M.L.**, **Palanque-Delabrouille, N.**, **Percival, W.J.**, **Pérez-Ràfols, I.**, **Pieri, M.M.**, **Schneider, D.P.**, **Slosar, A. and Yèche, C.** (2019). Baryon acoustic oscillations from the cross-correlation of Lyα absorption and quasars in eBOSS DR14, *Astronomy & Astrophysics*, *629*, A86, `https://doi.org/10.1051%2F0004-6361%2F201935641`.

[116] **Gómez-Valent, A. and Amendola, L.** (2018). H_0 from cosmic chronometers and Type Ia supernovae, with Gaussian Processes and the novel Weighted Polynomial Regression method, *Journal of Cosmology and Astroparticle Physics*, *2018*(04), 051–051, `https://doi.org/10.1088%2F1475-7516%2F2018%2F04%2F051`.

[117] **Cooke, R.J.**, **Pettini, M.**, **Jorgenson, R.A.**, **Murphy, M.T. and Steidel, C.C.** (2014). Precision Measures of the Primordial Abundance of Deuterium, *The Astrophysical Journal*, *781*(1), 31, `https://doi.org/10.1088%2F0004-637x%2F781%2F1%2F31`.

[118] **Freedman, W.L.**, **Madore, B.F.**, **Hatt, D.**, **Hoyt, T.J.**, **Jang, I.S.**, **Beaton, R.L.**, **Burns, C.R.**, **Lee, M.G.** *et al.* (2019). The Carnegie-Chicago Hubble Program. VIII. An Independent Determination of the Hubble Constant Based on the Tip of the Red Giant Branch, *The Astrophysical Journal*, *882*(1), 34, `https://doi.org/10.3847%2F1538-4357%2Fab2f73`.

[119] **Scolnic, D.M.**, **Jones, D.O.**, **Rest, A.**, **Pan, Y.C.**, **Chornock, R.**, **Foley, R.J.**, **Huber, M.E.**, **Kessler, R.**, **Narayan, G.**, **Riess, A.G.**, **Rodney, S.**, **Berger, E.**, **Brout, D.J.**, **Challis, P.J.** *et al.* (2018). The Complete

Light-curve Sample of Spectroscopically Confirmed SNe Ia from Pan-STARRS1 and Cosmological Constraints from the Combined Pantheon Sample, *The Astrophysical Journal*, *859*(2), 101, https://doi.org/10.3847%2F1538-4357%2Faab9bb.

[120] **Camarena, D. and Marra, V.** (2021). On the use of the local prior on the absolute magnitude of Type Ia supernovae in cosmological inference, *Monthly Notices of the Royal Astronomical Society*, *504*(4), 5164–5171, https://doi.org/10.1093%2Fmnras%2Fstab1200.

[121] **Camarena, D. and Marra, V.** (2020). A new method to build the (inverse) distance ladder, *Monthly Notices of the Royal Astronomical Society*, *495*(3), 2630–2644, https://doi.org/10.1093%2Fmnras%2Fstaa770.

[122] **Asgari, M.**, **Tröster, T.**, **Heymans, C.**, **Hildebrandt, H.**, **van den Busch, J.L.**, **Wright, A.H.**, **Choi, A.**, **Erben, T.**, **Joachimi, B.**, **Joudaki, S.** *et al.* (2020). KiDS+VIKING-450 and DES-Y1 combined: Mitigating baryon feedback uncertainty with COSEBIs, *Astronomy & Astrophysics*, *634*, A127, https://doi.org/10.1051%2F0004-6361%2F201936512.

[123] **Abbott, T.**, **Aguena, M.**, **Alarcon, A.**, **Allam, S.**, **Allen, S.**, **Annis, J.**, **Avila, S.**, **Bacon, D.**, **Bechtol, K.**, **Bermeo, A.**, **Bernstein, G.**, **Bertin, E.**, **Bhargava, S.**, **Bocquet, S.**, **Brooks, D.**, **Brout, D.**, **Buckley-Geer, E.**, **Burke, D.** *et al.* (2020). Dark Energy Survey Year 1 Results: Cosmological constraints from cluster abundances and weak lensing, *Physical Review D*, *102*(2), https://doi.org/10.1103%2Fphysrevd.102.023509.

[124] **Ade, P.A.R.**, **Aghanim, N.**, **Arnaud, M.**, **Ashdown, M.**, **Aumont, J.**, **Baccigalupi, C.**, **Banday, A.J.**, **Barreiro, R.B.**, **Bartlett, J.G.**, **Bartolo, N.**, **Battaner, E.**, **Battye, R.**, **Benabed, K.** *et al.* (2016). Planck 2015 results, *Astronomy & Astrophysics*, *594*, A24, https://doi.org/10.1051%2F0004-6361%2F201525833.

[125] **Costanzi, M.**, **Rozo, E.**, **Simet, M.**, **Zhang, Y.**, **Evrard, A.E.**, **Mantz, A.**, **Rykoff, E.S.**, **Jeltema, T.**, **Gruen, D.**, **Allen, S.**, **McClintock, T.**, **Romer, A.K.**, **von der Linden, A.**, **Farahi, A.**, **DeRose, J.**, **Varga, T.N.**, **Weller, J.**, **Giles, P.**, **Hollowood, D.L.** *et al.* (2019). Methods for cluster cosmology and application to the SDSS in preparation for DES Year 1 release, *Monthly Notices of the Royal Astronomical Society*, *488*(4), 4779–4800, https://doi.org/10.1093%2Fmnras%2Fstz1949.

[126] **Kazantzidis, L. and Perivolaropoulos, L.** (2018). Evolution of the $f\sigma_8$ tension with the Planck15/ΛCDM determination and implications for modified gravity theories, *Physical Review D*, *97*(10), https://doi.org/10.1103%2Fphysrevd.97.103503.

[127] **Arjona, R., García-Bellido, J. and Nesseris, S.** (2020). Cosmological constraints on nonadiabatic dark energy perturbations, *Physical Review D*, *102*(10), https://doi.org/10.1103%2Fphysrevd.102.103526.

[128] **Heymans, C., Tröster, T., Asgari, M., Blake, C., Hildebrandt, H., Joachimi, B., Kuijken, K., Lin, C.A.** *et al.* (2021). KiDS-1000 Cosmology: Multi-probe weak gravitational lensing and spectroscopic galaxy clustering constraints, *Astronomy & Astrophysics*, *646*, A140, https://doi.org/10.1051%2F0004-6361%2F202039063.

[129] **du Mas des Bourboux, H., Rich, J., Font-Ribera, A., de Sainte Agathe, V., Farr, J., Etourneau, T., Goff, J.M.L., Cuceu, A., Balland, C., Bautista, J.E., Blomqvist, M.** *et al.* (2020). The Completed SDSS-IV Extended Baryon Oscillation Spectroscopic Survey: Baryon Acoustic Oscillations with Lyα Forests, *The Astrophysical Journal*, *901*(2), 153, https://doi.org/10.3847%2F1538-4357%2Fabb085.

[130] **Chui, C.K.** (1992). *Wavelet Analysis and Its Applications*, Academic Press, San Diego.

[131] **Burrus, C.S., Gopinath, R. and Guo, H.** (2013). *Wavelets and Wavelet Transforms*, OpenStax-CNX.

[132] **Carroll, S.** (2003). *Spacetime and Geometry: An Introduction to General Relativity*, Benjamin Cummings.

[133] **Baumann, D.** (2022). *Cosmology*, Cambridge University Press.

[134] **Guth, A.H.** (1981). Inflationary universe: A possible solution to the horizon and flatness problems, *Phys. Rev. D*, *23*, 347–356, https://link.aps.org/doi/10.1103/PhysRevD.23.347.

[135] **Linde, A.D.** (1982). A New Inflationary Universe Scenario: A Possible Solution of the Horizon, Flatness, Homogeneity, Isotropy and Primordial Monopole Problems, *Phys. Lett. B*, *108*, 389–393.

[136] **Albrecht, A. and Steinhardt, P.J.** (1982). Cosmology for Grand Unified Theories with Radiatively Induced Symmetry Breaking, *Phys. Rev. Lett.*, *48*, 1220–1223, https://link.aps.org/doi/10.1103/PhysRevLett.48.1220.

[137] **Karwal, T. and Kamionkowski, M.** (2016). Dark energy at early times, the Hubble parameter, and the string axiverse, *Physical Review D*, *94*(10), https://doi.org/10.1103%2Fphysrevd.94.103523.

[138] **Mörtsell, E. and Dhawan, S.** (2018). Does the Hubble constant tension call for new physics?, *Journal of Cosmology and Astroparticle Physics*, *2018*(09), 025–025, https://doi.org/10.1088%2F1475-7516%2F2018%2F09%2F025.

[139] **Poulin, V.**, **Smith, T.L.**, **Karwal, T. and Kamionkowski, M.** (2019). Early Dark Energy can Resolve the Hubble Tension, *Physical Review Letters*, *122*(22), https://doi.org/10.1103%2Fphysrevlett.122.221301.

[140] **Abenza, M.E.** (2020). Precision early universe thermodynamics made simple:$N_{\text{eff}}$and neutrino decoupling in the Standard Model and beyond, *Journal of Cosmology and Astroparticle Physics*, *2020*(05), 048–048, https://doi.org/10.1088%2F1475-7516%2F2020%2F05%2F048.

[141] **Nojiri, S.**, **Odintsov, S.D.**, **Gómez, D.S.C. and Sharov, G.S.** (2021). Modeling and testing the equation of state for (Early) dark energy, *Physics of the Dark Universe*, *32*, 100837, https://doi.org/10.1016%2Fj.dark.2021.100837.

[142] **Kamionkowski, M. and Riess, A.G.**, (2022), The Hubble Tension and Early Dark Energy, https://arxiv.org/abs/2211.04492.

[143] **Akita, K. and Yamaguchi, M.** (2020). A precision calculation of relic neutrino decoupling, *Journal of Cosmology and Astroparticle Physics*, *2020*(08), 012–012, https://doi.org/10.1088%2F1475-7516%2F2020%2F08%2F012.

[144] **Bennett, J.J.**, **Buldgen, G.**, **de Salas, P.F.**, **Drewes, M.**, **Gariazzo, S.**, **Pastor, S. and Wong, Y.Y.** (2021). Towards a precision calculation of the effective number of neutrinos N_{eff} in the Standard Model. Part II. Neutrino decoupling in the presence of flavour oscillations and finite-temperature QED, *Journal of Cosmology and Astroparticle Physics*, *2021*(04), 073, https://doi.org/10.1088%2F1475-7516%2F2021%2F04%2F073.

[145] **Poulin, V.**, **Smith, T.L.**, **Grin, D.**, **Karwal, T. and Kamionkowski, M.** (2018). Cosmological implications of ultralight axionlike fields, *Phys. Rev. D*, *98*, 083525, https://link.aps.org/doi/10.1103/PhysRevD.98.083525.

[146] **Capparelli, L.M.**, **Caldwell, R.R. and Melchiorri, A.** (2020). Cosmic birefringence test of the Hubble tension, *Physical Review D*, *101*(12), https://doi.org/10.1103%2Fphysrevd.101.123529.

[147] **Murai, K.**, **Naokawa, F.**, **Namikawa, T. and Komatsu, E.**, (2022), Isotropic cosmic birefringence from early dark energy, https://arxiv.org/abs/2209.07804.

[148] **Hill, J.C.**, **McDonough, E.**, **Toomey, M.W. and Alexander, S.** (2020). Early dark energy does not restore cosmological concordance, *Phys. Rev. D*, *102*, 043507, https://link.aps.org/doi/10.1103/PhysRevD.102.043507.

[149] **D'Amico, G.**, **Senatore, L.**, **Zhang, P. and Zheng, H.** (2021). The Hubble tension in light of the Full-Shape analysis of Large-Scale

Structure data, *Journal of Cosmology and Astroparticle Physics*, *2021*(05), 072, https://doi.org/10.1088%2F1475-7516%2F2021%2F05%2F072.

[150] **Wang, H. and Piao, Y.S.**, (2022), A fraction of dark matter faded with early dark energy ?, https://arxiv.org/abs/2209.09685.

[151] **Jedamzik, K.**, **Pogosian, L. and Zhao, G.B.** (2021). Why reducing the cosmic sound horizon alone can not fully resolve the Hubble tension, *Communications Physics*, *4*(1), https://doi.org/10.1038%2Fs42005-021-00628-x.

[152] **Seto, O. and Toda, Y.** (2021). Comparing early dark energy and extra radiation solutions to the Hubble tension with BBN, *Physical Review D*, *103*(12), https://doi.org/10.1103%2Fphysrevd.103.123501.

[153] **Fixsen, D.J.** (2009). The Temperature of the Cosmic Microwave Background, *The Astrophysical Journal*, *707*(2), 916–920, https://doi.org/10.1088%2F0004-637x%2F707%2F2%2F916.

[154] **Boylan-Kolchin, M.**, (2022), Stress Testing ΛCDM with High-redshift Galaxy Candidates, https://arxiv.org/abs/2208.01611.

[155] **Haslbauer, M.**, **Kroupa, P.**, **Zonoozi, A.H. and Haghi, H.** (2022). Has JWST Already Falsified Dark-matter-driven Galaxy Formation?, *The Astrophysical Journal Letters*, *939*(2), L31, https://doi.org/10.3847%2F2041-8213%2Fac9a50.

[156] **Lovell, C.C.**, **Harrison, I.**, **Harikane, Y.**, **Tacchella, S. and Wilkins, S.M.** (2022). Extreme value statistics of the halo and stellar mass distributions at high redshift: are JWST results in tension with ΛCDM?, *Monthly Notices of the Royal Astronomical Society*, *518*(2), 2511–2520, https://doi.org/10.1093%2Fmnras%2Fstac3224.

[157] **Bauer, F.**, **Sola, J. and Stefancic, H.** (2010). Dynamically avoiding fine-tuning the cosmological constant: The 'Relaxed Universe', *JCAP*, *12*, 029, 1006.3944.

[158] **Ozulker, E.** (2022). Is the dark energy equation of state parameter singular?, *Phys. Rev. D*, *106*(6), 063509, 2203.04167.

[159] **Abbott, T.**, **Abdalla, F.**, **Alarcon, A.**, **Aleksić, J.**, **Allam, S.**, **Allen, S.**, **Amara, A.**, **Annis, J.**, **Asorey, J.**, **Avila, S.**, **Bacon, D.**, **Balbinot, E.**, **Banerji, M.**, **Banik, N.**, **Barkhouse, W.**, **Baumer, M.**, **Baxter, E.**, **Bechtol, K.** *et al.* (2018). Dark Energy Survey year 1 results: Cosmological constraints from galaxy clustering and weak lensing, *Physical Review D*, *98*(4), https://doi.org/10.1103%2Fphysrevd.98.043526.

APPENDICES

APPENDIX A : 1+3 COVARIANT DECOMPOSITION

APPENDIX A

In local enough regions, spacetime can be decomposed into its temporal and spatial components relative to a congruence of timelike geodesics, which is naturally defined by the fluid flow $u^\alpha = \mathrm{d}x^\alpha/\mathrm{d}\tau$. This affinely parametrized family of congruence satisfies that $u^\alpha \nabla_\alpha u^\beta = 0$ and $u^\alpha u_\alpha = -1$. One can define the tensor field $T_{\alpha\beta} = \nabla_\beta u_\alpha$ satisfying

$$T_{\alpha\beta} u^\beta = u^\alpha T_{\alpha\beta} = 0.$$

This means that only non-zero components of $T_{\alpha\beta}$ are in the directions that are transverse to u^α. One can calculate its trace,

$$\begin{aligned}\Theta = T^\alpha_{\ \alpha} &= g^{\alpha\beta}(\nabla_\beta u_\alpha)\\ &= \nabla_\beta (g^{\alpha\beta} u_\alpha)\\ \Theta &= \nabla_\beta u^\beta,\end{aligned}$$

which gives the expansion of this timelike congruence. If we also define the new tensor

$$h_{\alpha\beta} = g_{\alpha\beta} + u_\alpha u_\beta,$$

where $h_{\alpha\beta}$ is orthogonal to u^α, that is $u^\alpha h_{\alpha\beta} = h_{\alpha\beta} u^\beta = 0$, it is straighforward to show that $h_{\alpha\beta}$ acts to project the metric tensor in spatial directions orthogonal to u^α through

$$\begin{aligned}h_{\lambda\beta} g^{\lambda\alpha} &= g_{\lambda\beta} g^{\lambda\alpha} + u_\lambda u_\beta g^{\lambda\alpha}\\ h^\alpha_{\ \beta} &= \delta^\alpha_\beta + u^\alpha u_\beta h^\alpha_{\ \beta}\\ h^\alpha_{\ \beta} h^\beta_{\ \rho} &= \delta^\alpha_\beta h^\beta_{\ \rho} + u^\alpha u_\beta h^\beta_{\ \rho}\\ h^\alpha_{\ \beta} h^\beta_{\ \rho} &= h^\alpha_{\ \rho}.\end{aligned}$$

Therefore along the directions of u^α, $h^\alpha_{\ \beta}$ yields

$$h^\alpha_{\ \beta} u^\beta = 0,$$

and on vectors ζ^α that are directed orthogonal to u^α, that is $u_\alpha \zeta^\alpha = 0$, it acts to give

$$h^\alpha_{\ \beta} \zeta^\beta = \zeta^\alpha.$$

We then call $h^\alpha_{\ \beta}$ the projection tensor that projects any arbitrary tensor field onto a 3D spatial hypersurface or plane orthogonal to the timelike vector field u^α, i.e., spatial orthogonal projection. Thus $h^\alpha_{\ \beta}$ can be interpreted as the metric of this 3D such that $h^\alpha_{\ \alpha} = 3$. Likewise we can introduce temporal orthogonal projection by defining another projection tensor $U^\alpha_{\ \beta}$,

$$U^\alpha_{\ \beta} U^\beta_{\ \gamma} = U^\alpha_{\ \gamma},$$

into the 1D tangent line $U^{\alpha}_{\alpha} = 1$ parallel to u^{α}, meaning $U^{\alpha}_{\beta}u^{\beta} = u^{\alpha}$ so that $U^{\alpha}_{\beta} = -u^{\alpha}u_{\beta}$. Then altogether, component of a vector X^{α} parallel to u^{α} is given by

$$X^{\alpha}_{\parallel} = U^{\alpha}_{\beta}X^{\beta}$$

while the orthogonal component is given by

$$X^{\alpha}_{\perp} = h^{\alpha}_{\beta}X^{\beta}.$$

We can for example split the metric tensor $g_{\alpha\beta}$ into its parallel and perpendicular parts $g_{\alpha\beta} = g_{\parallel\alpha\beta} + g_{\perp\alpha\beta}$ [104];

$$\begin{aligned} g_{\parallel\alpha\beta} &= U_{\alpha}{}^{\sigma}U_{\beta}{}^{\rho}g_{\sigma\rho} = U_{\alpha\beta}, \\ g_{\perp\alpha\beta} &= h_{\alpha}^{\sigma}h_{\beta}^{\rho}g_{\sigma\rho} = h_{\alpha\beta}, \end{aligned}$$

so we have

$$g_{\alpha\beta} = h_{\alpha\beta} + U_{\alpha\beta} = h_{\alpha\beta} - u_{\alpha}u_{\beta}$$

in line with the way $h_{\alpha\beta}$ was introduced above. Additionally, based on this approach we can also split the covariant derivative into its space and time components;

$$\nabla_{\alpha}u_{\beta} = -u_{\alpha}\dot{u}_{\beta} + \mathrm{D}_{\alpha}u_{\beta},$$

where D_{α} is the fully orthogonally projected covariant derivative, which for any tensorial quantity is given by [103],

$$\mathrm{D}_{\lambda}X^{\alpha\beta}{}_{\sigma\rho} = h_{\sigma}{}^{\sigma'}h_{\rho}{}^{\rho'}h^{\alpha}_{\alpha'}h^{\beta}_{\beta'}h_{\lambda}{}^{\lambda'}\nabla_{\lambda'}X^{\alpha'\beta'}{}_{\sigma'\rho'}.$$

The same procedure elaborated above can be applied to the divergence of the EMT to obtain the energy (3.4) and momentum conservation (3.5) equations . First we project $\nabla_{\mu}T^{\mu\nu} = 0$ parallel to u^{μ}, where for a perfect fluid $T_{\mu\nu}$ is given by

$$T_{\mu\nu} = \rho u_{\mu}u_{\nu} + ph_{\mu\nu}.$$

Projecting temporally,

$$\begin{aligned} u^{\nu}\nabla^{\mu}T_{\mu\nu} &= u_{\mu}u_{\nu}(\nabla^{\mu}\rho)u^{\nu} + \rho u^{\nu}(\nabla^{\mu}u_{\mu})u_{\nu} + \rho u_{\mu}u^{\nu}\nabla^{\mu}u_{\nu} + h_{\mu\nu}u^{\nu}\nabla^{\mu}p + pu^{\nu}\nabla^{\mu}h_{\mu\nu} \\ &= -u_{\mu}\nabla^{\mu}\rho - \rho\nabla^{\mu}u_{\mu} + pu^{\nu}\nabla^{\mu}h_{\mu\nu} = 0, \end{aligned}$$

and using

$$\nabla^{\mu}h_{\mu\nu} = u_{\nu}\nabla^{\mu}u_{\mu} + u_{\mu}\nabla^{\mu}u_{\nu}$$

we get

$$\begin{aligned} u^{\nu}\nabla^{\mu}T_{\mu\nu} &= -u_{\mu}\nabla^{\mu}\rho - \rho\nabla^{\mu}u_{\mu} - p\nabla^{\mu}u_{\mu} \\ &= -u_{\mu}\nabla^{\mu}\rho - (\rho + p)g_{\mu\nu}\nabla^{\mu}u^{\nu} \\ &= -u_{\mu}\nabla^{\mu}\rho - (\rho + p)(h_{\mu\nu}\nabla^{\mu}u^{\nu} - u_{\mu}u_{\nu}\nabla^{\mu}u^{\nu}), \end{aligned}$$

so we have

$$u^\nu \nabla^\mu T_{\mu\nu} = -u_\mu \nabla^\mu \rho - (\rho + p)(h_{\mu\nu} \nabla^\mu u^\nu).$$

We now project the covariant derivative $\mathrm{D}_\mu = h_\mu{}^\nu \nabla_\nu$ and define the expansion of the timelike congruence or alternatively the scalar of volume expansion rate as $\Theta = \mathrm{D}^\mu u_\mu = h^{\mu\nu} \nabla_\nu u_\mu$;

$$\begin{aligned} u^\nu \nabla^\mu T_{\mu\nu} &= -u_\mu \nabla^\mu \rho - (\rho + p)(h_{\mu\nu} \nabla^\mu u^\nu) \\ &= -u_\mu \nabla^\mu \rho - \Theta(\rho + p) \\ &= -\partial_t \rho - \nabla^i \rho u_i - \Theta(\rho + p). \end{aligned}$$

Finally we arrive at the continuity equation in the comoving frame as our first conservation equation (3.4),

$$\dot{\rho} + \Theta(\rho + p) = 0.$$

Now we can perform spatial orthogonal projection to obtain the other conservation equation. To do that we first raise index of the projection tensor $h^\nu{}_\sigma = g^{\nu\rho} h_{\rho\sigma}$, where $h^\nu{}_\sigma$ is

$$h^\nu{}_\sigma = \delta^\nu_\sigma + u^\nu u_\sigma,$$

and calculate $h^\nu{}_\sigma \nabla^\mu T_{\mu\nu} = 0$

$$h^\nu{}_\sigma \nabla^\mu T_{\mu\nu} = h^\nu{}_\sigma u_\mu u_\nu \nabla^\mu \rho + \rho h^\nu{}_\sigma u_\nu \nabla^\mu u_\mu + h^\nu{}_\sigma h_{\mu\nu} \nabla^\mu p + \rho u_\mu h^\nu{}_\sigma \nabla^\mu u_\nu + p h^\nu{}_\sigma \nabla^\mu h_{\mu\nu}.$$

It is better to work it out term by term. The first two terms vanish due to $u_\nu h^\nu{}_\sigma = 0$. And, the 3rd term $h^\nu{}_\sigma h_{\mu\nu} \nabla^\mu p = h_{\mu\sigma} \nabla^\mu p = \mathrm{D}_\sigma p$ and for the rest the 4th term reads

$$\begin{aligned} \rho u_\mu h^\nu{}_\sigma \nabla^\mu u_\nu &= \rho(\delta^\nu_\sigma + u^\nu u_\sigma) u_\mu \nabla^\mu u_\nu \\ &= \rho u_\mu \nabla^\mu u_\sigma + \rho u_\sigma u_\mu u^\nu \nabla^\mu u_\nu \\ &= \rho \dot{u}_\sigma, \end{aligned}$$

and for the last term we have

$$\begin{aligned} p h^\nu{}_\sigma \nabla^\mu h_{\mu\nu} &= p h^\nu{}_\sigma [\nabla^\mu (g_{\mu\nu} + u_\mu u_\nu)] \\ &= p h^\nu{}_\sigma (u_\nu \nabla^\mu u_\mu + u_\mu \nabla^\mu u_\nu) \\ &= p h^\nu{}_\sigma u_\nu \nabla^\mu u_\mu + p \delta^\nu_\sigma u_\mu \nabla^\mu u_\nu + p u^\nu u_\sigma u_\mu \nabla^\mu u_\nu \\ &= p u_\mu \nabla^\mu u_\sigma \\ &= p \dot{u}_\sigma, \end{aligned}$$

where we in the first line used the metric compatibility $\nabla^\mu g_{\mu\nu} = 0$. Overall we end up with the momentum conservation equation,

$$h^\nu{}_\sigma \nabla^\mu T_{\mu\nu} = \mathrm{D}_\sigma p + (\rho + p) \dot{u}_\sigma = 0,$$

which goes by the name of Euler equation (3.5)

$$\mathrm{D}_\mu p + (\rho + p) \dot{u}_\mu = 0.$$

CURRICULUM VITAE

Name Surname : Cihad Kıbrıs

EDUCATION :

- **B.Sc.** : 2019, Istanbul Technical University, Faculty of Electrical and Electronics, Electrical Engineering

C. Kıbrıs

A REMEDY FOR MAJOR COSMOLOGICAL TENSIONS: DARK ENERGY WITH AN OSCILLATING INERTIAL MASS DENSITY

2022